



universität
wien

DIPLOMARBEIT

Titel der Diplomarbeit

„The Role of Posttranslational Modifications in the Endocytosis
of Muscle-Specific Kinase“

Verfasserin

Marlies Schlauf

angestrebter akademischer Grad

Magistra der Naturwissenschaften (Mag.rer.nat.)

Wien, 2011

Studienkennzahl lt. Studienblatt:

A 490

Studienrichtung lt. Studienblatt:

Diplomstudium Molekulare Biologie

Betreuerin / Betreuer:

Priv. Doz. Mag. Dr. Ruth Herbst

Für Peter

Ich wünsche,
du hättest diese Arbeit noch lesen können!

“I have not failed. I’ve just found 10 000 ways that won’t work.”

Thomas A. Edison

Table of Contents

1	Introduction	1
1.1	The Neuromuscular Junction	1
1.1.1	NMJ Structure.....	1
1.1.2	NMJ Formation.....	2
1.1.3	Agrin/ LRP4/ MuSK-Signaling.....	3
1.2	Neuromuscular Diseases	4
1.3	Agrin.....	5
1.4	MuSK	5
1.4.1	The Receptor Tyrosine Kinase Superfamily	5
1.4.2	MuSK Structure and Function.....	6
1.4.3	MuSK Regulation	6
1.4.4	MuSK Downstream Signaling	7
1.5	LRP4	7
1.6	Dok7	8
1.7	Ubiquitination.....	9
1.8	Endocytosis & Ubiquitination	12
1.9	Protein Degradation.....	13
1.9.1	Endosomal-Lysosomal Degradation.....	13
1.9.2	Rab7.....	14
1.9.3	Proteasomal Degradation	14
1.9.4	Inhibitors of Protein Degradation.....	14
2	Aim of the Project	17
3	Results and Discussion.....	18
3.1	Activation of MuSK in a Heterologous Cell System	18
3.1.1	Antibody-Induced Activation of MuSK.....	18
3.1.2	Co-Expression of MuSK with Associated Muscle-Specific Proteins and Stimulation with Agrin.....	20
3.1.2.1	Generation of Single Cell Clones Stably Expressing Dok7	22
3.1.3	Constitutive Activation & Inactivation of MuSK	23
3.1.3.1	Characterization of SBP-MuSK-K608A and SBP-MuSK-LS745/746MT in COS-7 Cells	24
3.1.3.2	Internalization of SBP-MuSK-K608A and SBP-MuSK-LS745/746MT in COS-7 Cells	25
3.2	The Role of MuSK Ubiquitination in MuSK Endocytosis and Degradation.....	26
3.2.1	Characterization of HA-MuSK-Ubwt and HA-MuSK-Ubmut in COS-7 Cells	27
3.2.2	Stability of HA-MuSK-Ubwt and HA-MuSK-Ubmut in COS-7 cells.....	31
3.2.3	Internalization of HA-MuSK-Ubwt and HA-MuSK-Ubmut in COS-7 Cells	33
3.2.4	Colocalization of HA-MuSK-Ubwt and HA-MuSK-Ubmut with Rab7 during Internalization.....	34
4	Conclusion and Outlook.....	36

5	Materials and Methods	38
5.1	Materials	38
5.2	Plasmids.....	38
5.3	Chemicals and Reagents.....	39
5.4	Solutions and Buffers	41
5.5	Cell Culture	42
5.5.1	Cell Culture Conditions	42
5.5.2	Preparation of Agrin/ OptiMEM	42
5.5.3	Freezing Cells.....	43
5.5.4	Thawing Cells.....	43
5.5.5	Transient Transfection	43
5.5.5.1	CaCl ₂ / BBS–Transfection	43
5.5.5.2	Turbofect-Transfection.....	45
5.5.6	Stable Transfection	46
5.5.7	Agrin-Stimulation.....	47
5.5.8	Antibody-Mediated Stimulation of MuSK	47
5.5.9	Immunocytochemistry.....	47
5.5.9.1	Conventional Immunocytochemistry	47
5.5.9.2	Surface Protein Internalization Assay (Streptavidin)	48
5.5.9.3	Surface Protein Internalization Assay (Antibody).....	48
5.6	Molecular Biology	51
5.6.1	Cell Lysis.....	51
5.6.2	Preparation of Total Aliquots for Immunoblotting	52
5.6.3	(Co-)Immunoprecipitation	52
5.6.4	(Co-)Pull-Down	53
5.6.5	SDS-PAGE and Immunoblotting.....	53
5.6.6	Stripping of an Immunoblot after Development	55
5.6.7	Biochemical Quantification of MuSK Tyrosine Phosphorylation	55
5.6.8	Analysis of Protein Stability in COS-7 Cells.....	56
5.6.9	Cloning	56
5.6.9.1	Enzymatic Restriction	56
5.6.9.2	DNA Purification after Enzymatic Restriction.....	56
5.6.9.3	DNA Ligation	57
5.6.9.4	Cloning of SBP-MuSK-K608A and SBP-MuSK-LS745/746MT	57
5.6.9.5	Cloning of HA-MuSK-Ubwt and HA-MuSK-Ubmut.....	58
5.6.10	Transformation of Competent Bacteria	58
6	Abbreviations.....	60

7	References	63
8	Appendix.....	72
8.1	Acknowledgements.....	72
8.2	Zusammenfassung	73
8.3	Abstract	74
8.4	Lebenslauf	75
8.5	Curriculum Vitae	77

1 Introduction

1.1 The Neuromuscular Junction

The transduction of signals between neurons or from neurons to other target cells depends on structurally elaborate, asymmetric cell-cell-contacts termed synapses. The process of synapse formation, synaptogenesis, is highly complex. It involves correct guidance of neurons to their targets and the establishment of specialized structures at the synaptic membranes. Synapses are most abundant in the central nervous system (CNS). Nonetheless fundamental knowledge on synaptogenesis has been gained from studying a synapse in the peripheral nervous system: The neuromuscular junction (NMJ), which mediates signal transduction from motor neurons to muscle cells. Compared to synaptic sites in the CNS the NMJ is larger in size and more easily accessible (reviewed in (Sanes and Lichtman, 2001)) making it a particularly favorable model system.

1.1.1 NMJ Structure

Figure 1a and b depict the ultrastructure of a mature rodent neuromuscular synapse. The motor nerve terminal is completely insulated by a peripheral Schwann cell except for the area, which contacts the muscle fiber. This part of the neuronal cell membrane is termed presynaptic membrane. It opposes the postsynaptic membrane of the muscle cell that is invaginated in adult muscle forming postjunctional folds. In between the two membranes, in the so called synaptic cleft, the synaptic basal lamina is located, which is composed of extracellular matrix proteins. When a stimulus arrives at the motor nerve terminal, it induces fusion of acetylcholine (ACh)-containing vesicles with the presynaptic membrane. ACh molecules are released into the synaptic cleft and bind to acetylcholine receptors (AChRs) situated at the crests of the junctional folds (Wu et al.).

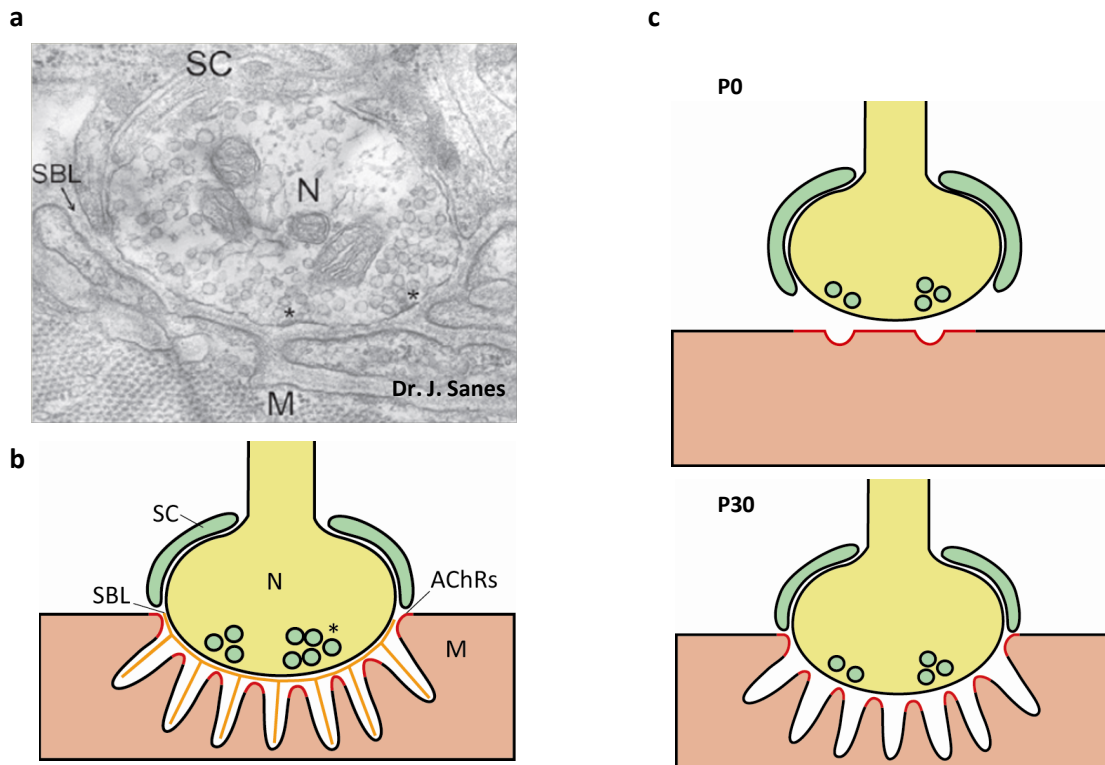


Figure 1 | **a** | **Electron Micrograph of a Mature Rodent NMJ** EM image courtesy of Dr J. Sanes, Harvard University, USA., from (Wu et al.) | **b** | **The Structure of a Mature Vertebrate NMJ** Schematic drawing adapted from (Sanes and Lichtman, 2001). N... motor neuron, SC... Schwann cell, SBL... synaptic basal lamina, M... muscle fiber, *... ACh-containing vesicles, postsynaptic membrane marked in red... AChR clusters | **c** | **Postnatal Maturation of the NMJ** Schematic drawing adapted from (Sanes and Lichtman, 2001). P0... postnatal day 0, P30... postnatal day 30

1.1.2 NMJ Formation

NMJ formation is a complex process that requires a series of coordinated interactions between motor nerves and muscle fibers. It is preceded by the differentiation of muscle precursor cells (myoblasts) into myotubes and eventually myofibers starting around embryonic day 12-14 (E12-14) (Ontell and Kozeka, 1984). As soon as myotubes have formed, they begin to express AChR subunits α , β , γ and δ , assemble fetal AChR pentamers ($\alpha 2\beta\gamma\delta$) and insert them into the membrane. The AChR pentamers aggregate in the central region of myofibers (Bevan and Steinbach, 1977). This 'prepatternning' is thought to be nerve-independent as it occurs prior to the arrival of motor nerve axons (Lin et al., 2001; Yang et al., 2001) and is also observed in mice lacking phrenic or motor nerves (Yang et al., 2000). Motor neuron growth cones subsequently contact muscle fibers around E13. It has been found that motor neurons stray from central regions of myofibers upon lack of prepatterned clusters (DeChiara et al., 1996; Jing et al., 2009; Lin et al., 2001; Yang et al., 2001; Zhang et al., 2004). This suggests that aneural AChRs clusters, probably not by themselves but by so far unknown factors, guide normal motor axon pathway finding (reviewed by (Wu et al.)).

Motor neuron attachment establishes one synaptic site per myofiber, which is often innervated by several motor axons at the beginning (reviewed by (Lichtman and Colman, 2000)). At the synaptic site AChR clusters become stabilized or new clusters are aggregated whereas other pre-existing clusters diffuse until E18.5 ((Lin et al., 2001; Vock et al., 2008; Yang et al., 2001)). During postnatal NMJ maturation the postsynaptic membrane forms invaginations and AChR clusters are concentrated at the crests of the resulting so-called postjunctional folds (Figure 1c). These folds are commonly described as structurally resembling pretzels if viewed from above (Figure 2).

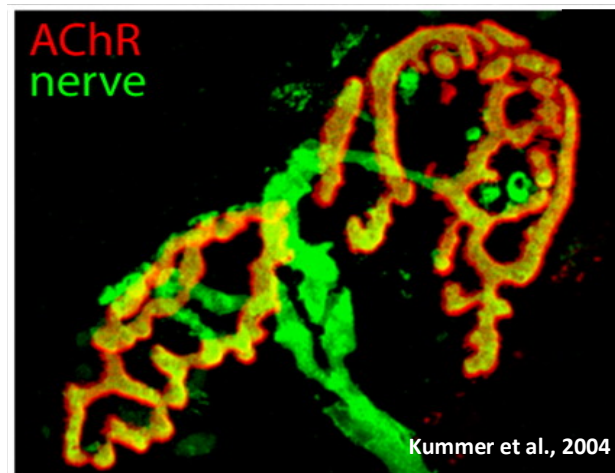


Figure 2| The NMJ of an Adult Mouse Image from (Kummer et al., 2004).

In parallel to pretzel-formation, multiple innervations are reduced to only one motor neuron contact per synapse within two weeks after birth (reviewed by (Lichtman and Colman, 2000)). ACh-induced muscle activity decreases expression of AChR subunit γ (Duclert and Changeux, 1995) in favour of AChR subunit ϵ , which replaces subunit γ in AChR pentamers. Thus the fetal form of AChR, AChR γ , is exchanged with adult AChR ϵ on the cell surface. The two AChR subtypes differ in their functional properties (Mishina et al., 1986) and both have been shown to be essential for normal synaptic development and function (Missias et al., 1997; Takahashi et al., 2002; Witzemann et al., 1996).

1.1.3 Agrin/ LRP4/ MuSK-Signaling

Elucidation of the molecular factors and signaling pathways controlling neuronal AChR clustering and NMJ formation was originally hampered by the fact that the specific activity of synaptic components, i.e. the moles per gram of tissue, is low in muscle. But investigation of the ray, *Torpedo californica*, boosted research on NMJ formation. The electric organ of this sea dweller can be considered a hypertrophied NMJ, from which the contractile components have been lost (Cartaud et al., 2000). Thus, the specific activity of AChRs is ~ 1000 times higher than in muscle (Berg et al., 1972). Many central postsynaptic components, such as AChRs but also MuSK, agrin and rapsyn, which will be discussed in the following, were first isolated from *Torpedo* electric organs (Cartaud et al., 2000).

The extracellular matrix protein agrin was identified as key activator of postsynaptic differentiation already in 1989 (McMahan, 1990; Wallace, 1989). Motor nerve terminals release agrin, which associates with the synaptic basal lamina. It binds the postsynaptic transmembrane receptor protein LRP4 that clusters and activates a receptor tyrosine kinase termed muscle-specific kinase (MuSK) on the myofiber membrane. The cytoplasmic membrane-associated muscle protein Dok7 supports this activation process. Through association with the cytoplasmic linker protein rapsyn and several not completely elucidated signaling processes, activated MuSK induces clustering of AChRs and other postsynaptic molecules and thus the formation of the NMJ (Figure 3).

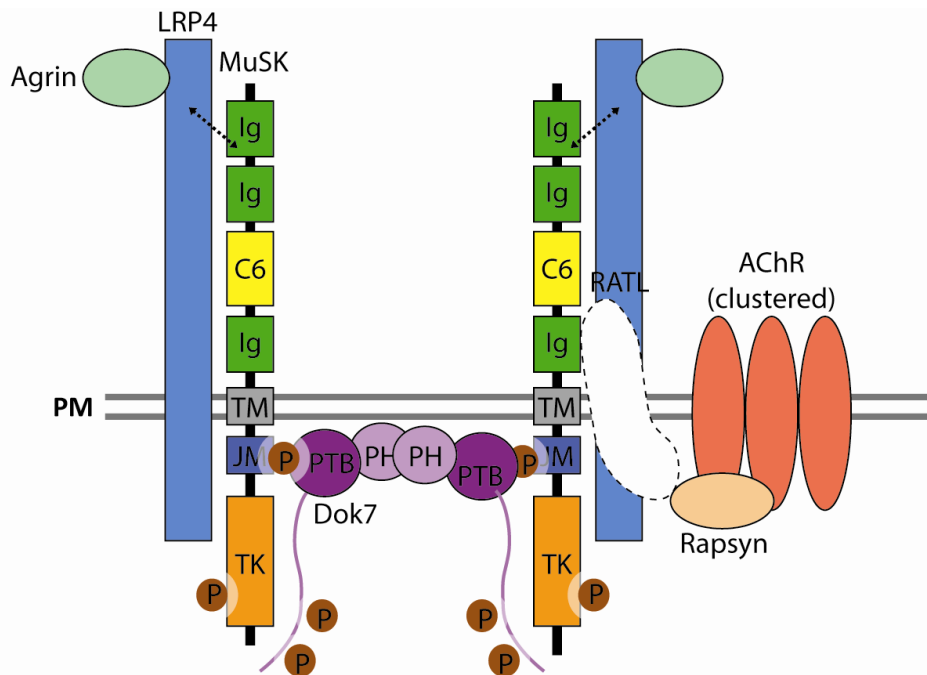


Figure 3| Agrin/ LRP4/ MuSK-Signaling Schematic drawing adapted from (Burden, ; Ghazanfari et al., ; Wu et al.). Motor neurons release agrin, which binds LRP4 and stimulates MuSK autophosphorylation and activation. (LRP4 has been shown to directly interact with MuSK. It is supposed that interaction is dependent on the most N-terminal Ig domain of MuSK as indicated by dotted arrows.) Autophosphorylation of MuSK is supported by Dok7 through binding of the Dok7 PTB-domain to MuSK and Dok7 PH-PTB dimerization. Activated MuSK induces AChR clustering through a mechanism that is not fully understood. The process is dependent on rapsyn, but it is unclear whether MuSK directly interacts with rapsyn or via a so far unknown hypothetical protein RATL (indicated by the dashed outline). Ig... Ig domain, C6... cysteine-rich domain, TM... transmembrane domain, JM... juxtamembrane domain, TK... kinase domain, P... phosphorylation, PM... plasma membrane, PH.... PH-domain, PTB... PTB-domain. For details see chapters 1.1.3 to 1.6.

1.2 Neuromuscular Diseases

Severe impairment of NMJ formation or function, resulting in muscle weakness, is causative for congenital myasthenic syndromes (CMS). Mutations leading to CMS have been identified in several NMJ components including all subunits of the AChR, MuSK, rapsyn and Dok7 (Beeson et al., 2006; Chevessier et al., 2004; Engel et al., 2003; Sine and Engel, 2006). Defects in AChR subunits commonly change the expression or the kinetic properties of the AChR pentamers. In contrast, patients with Dok7 mutations often exhibit abnormal NMJ size or structure (as reviewed in (Engel et al.)). Whereas these types of muscle weaknesses have a genetic background others constitute autoimmune diseases. In acquired myasthenia gravis (MG), patients produce antibodies against NMJ components. About 85 % of MG patients test positive for AChR antibodies (Meriggioli, 2009), which upon binding to postsynaptic AChRs lead to focal destruction of the postsynaptic membrane (Meriggioli and Sanders, 2009). Of the remaining 15 % about 70 % are positive for antibodies against MuSK (Vincent et al., 2008). The pathogenicity of MuSK antibodies is not completely understood, but injection of anti-MuSK-positive patient IgG has been shown to cause depletion of postsynaptic MuSK and disassembly of AChR clusters in mice (Cole et al.). The remaining 30% do not test positive for either of the two antibodies and are thus termed seronegative. However, they might express antibodies against other postsynaptic components.

1.3 Agrin

Agrin is a large heparin proteoglycan that is expressed in different isoforms by myotubes, Schwann cells and motor neurons at the NMJ. It was found in 1989 to be capable of inducing aggregation of AChRs as well as other components of the postsynaptic apparatus on cultured myotubes (Wallace, 1989). In 'The agrin hypothesis' McMahan suggested that agrin is the key signal in nerve-dependent postsynaptic differentiation (McMahan, 1990). This hypothesis was supported by the findings that postsynaptic differentiation is strongly impaired in agrin-deficient mice (Gautam et al., 1996) and that introduction of agrin into denervated muscle induces the formation of an almost complete postsynaptic apparatus (Bezakova and Lomo, 2001; Cohen et al., 1997; Meier et al., 1997). Agrin has three splice sites x, y and z. Alternative splicing generates isoforms containing one or more splice inserts of different lengths at the x, y and z sites. For instance, Agrin_{12,8,0} comprises a 12 amino acid (aa) insert at the x site, an 8 aa insert at the y and no insert at the z-site. Neuron specific isoforms have a 4 aa insert at the y splicing position and an 8, 11 or 19 aa insert at the z position. The insert at the x position is not biologically relevant. Inserts at the z site are characteristic for neuronal isoforms and are not found in agrin forms expressed in other tissues. Thus neuronal agrin is commonly termed z⁺ agrin (Ferns et al., 1993). That neuronal z⁺ agrin but not the muscle-derived isoform, known as z⁻ agrin, is essential for NMJ formation was demonstrated via z⁺ *agrin* knockout mice. These exhibited similarly defective NMJ formation as complete *agrin* deletion mutants (Burgess et al., 1999). Compared to muscle-derived agrin, the neuronal isoform z⁺ agrin was shown to be approximately 1000 times more potent in inducing AChR clusters (Gesemann et al., 1995). On the basis of these findings agrin was initially proposed to be required for AChR clustering. However, AChR prepatterning at E13-14 is normal in *agrin*-deficient mice implicating that the protein is dispensable for the process. But upon lack of agrin, motor neurons are unable to form stable synaptic contacts with the prepatterned clusters leading to excessive axonal branching and dispersion of primary AChR clusters (Lin et al., 2001; Yang et al., 2001). Consequently it was proposed that agrin acts (in complex with MuSK) as component of a neuronal stop signal (Dimitropoulou and Bixby, 2005) capable of stabilizing neuron-muscle interaction, inhibiting AChR dispersion (Witzemann, 2006) and regulating axonal branching (Campagna et al., 1995; Gautam et al., 1996).

1.4 MuSK

Muscle-specific kinase (MuSK), a 100 kDa transmembrane protein belonging to the RTK superfamily, was originally identified due to its selective expression in the electric organ of the ray, *Torpedo californica* (Jennings et al., 1993) and in mammalian muscle (Valenzuela et al., 1995).

1.4.1 The Receptor Tyrosine Kinase Superfamily

RTKs are a diverse family of cell surface receptors, which are involved in major signaling pathways regulating proliferation, differentiation, migration and metabolic changes (Schlessinger and Ullrich, 1992). The superfamily includes receptors for insulin, epidermal growth factor (EGF), fibroblast growth factor (FGF) and platelet-derived growth factor (PDGF). Structurally, RTKs comprise an extracellular portion, which often contains various globular domains including immunoglobulin (Ig)-like, EGF-like or cysteine-rich domains, for instance. The transmembrane helix is followed by a juxtamembrane region, a tyrosine kinase domain and a C-terminal portion. Most RTKs consist of a single polypeptide chain and are monomeric in the absence of their cognate ligand. Upon binding of a ligand to the extracellular portion the receptors oligomerize, which facilitates interaction of the

intracellular kinase domains and leads to trans-autophosphorylation. Commonly, tyrosines in the activation loop (A loop) within the kinase domain are phosphorylated first, stimulating kinase activity. As a consequence, tyrosine residues situated in the juxtamembrane region, the kinase domain and the C-terminal region become phosphorylated. This generates docking sites for downstream signaling proteins with phosphotyrosine-binding modules such as SH2 domains and phosphotyrosine-binding (PTB) domains (Kuriyan and Cowburn, 1997) (reviewed in (Hubbard and Till, 2000)).

1.4.2 MuSK Structure and Function

MuSK comprises four immunoglobulin-like domains and a cysteine-rich domain in the extracellular region. The transmembrane domain is followed by a juxtamembrane domain and a catalytic tyrosine kinase domain (Ghazanfari et al.) (Figure 4). De Chiara et al. found that although AChR expression is normal in *Musk*^{-/-} mice they are unable to form NMJs and die at birth due to respiratory failure (DeChiara et al., 1996). Consistently, Glass et al. reported that neuronal agrin can not induce AChR clustering in *Musk*^{-/-} muscle fibers (Glass et al., 1996). Both findings indicated that MuSK acts as receptor for agrin. But despite intensive studies, direct interaction of MuSK and agrin could not be demonstrated. Eventually another transmembrane muscle protein, LRP4, was reported to directly interact with agrin and MuSK and was established as agrin receptor (Kim et al., 2008; Zhang et al., 2008). MuSK was shown not only to be required for agrin-responsiveness but also for agrin-independent AChR-prepatterning. Embryos lacking MuSK form neither aneural clusters nor agrin-induced clusters (DeChiara et al., 1996; Lin et al., 2001); (Yang et al., 2001).



Figure 4| Domain structure of MuSK Schematic drawing adapted from (Ghazanfari et al.). Ig... Ig domain, C6... cysteine-rich domain, TM... transmembrane domain, JM... juxtamembrane domain, TK... kinase domain, N... N-terminus, C... C-terminus.

1.4.3 MuSK Regulation

MuSK expression is upregulated upon differentiation of muscle precursor cells and downregulated when muscle fibers become innervated (Tang et al., 2006). It is integrated into the myotube membrane where it probably forms complexes with LRP4 prior to innervation (Kim et al., 2008). Upon arrival of a neuronal outgrowth and release of agrin, which binds LRP4, MuSK undergoes autophosphorylation at tyrosine (Tyr) residues and induces AChR clustering through signaling mechanisms that haven't been completely elucidated so far. Among other proteins, Dok7 (Okada et al., 2006) and Tid1 (Linnoila et al., 2008) have been reported to interact with activated MuSK and regulate MuSK function. Moreover, activation-dependent internalization of MuSK regulated by direct interaction with the ATPase N-ethylmaleimide sensitive fusion protein (NSF) was observed to be required for AChR clustering (Zhu et al., 2008). The internalization process might further be influenced by ubiquitination of endocytosed MuSK. MuSK directly interacts with PDZ domain-containing RING finger 3 (PDZRN3), a synapse-associated E3 ubiquitin ligase, which catalyzes MuSK ubiquitination. MuSK activation enhances both interaction and ubiquitination and leads to PDZRN3-dependent downregulation of MuSK cell surface levels. Inhibitor experiments suggested that this reduction of MuSK surface expression is achieved by lysosomal degradation of MuSK (Lu et al., 2007b).

1.4.4 MuSK Downstream Signaling

As described, AChR clustering is dependent on MuSK as well as on rapsyn, a 43 kDa membrane-associated cytoplasmic protein (Sanes and Lichtman, 2001), which interacts directly with AChR subunits (Froehner et al., 1990; Gautam et al., 1995; Huebsch and Maimone, 2003; Maimone and Merlie, 1993) and shows perfect co-localization with AChRs in adult NMJs (LaRochelle and Froehner, 1986; Noakes et al., 1993). However, the mechanism of MuSK-rapsyn signaling is still a matter of debate. Studies in QT-6 fibroblasts indicated that the extracellular domain of MuSK interacts with rapsyn via a rapsyn-associated transmembrane linker protein (RATL), which is expressed in muscle cells and fibroblasts (Apel et al., 1997; Zhou et al., 1999). In contrast, Antolik et al., reported agrin-independent direct interaction of a large fragment of the cytoplasmic domain of MuSK with rapsyn upon coexpression in COS-7 cells. In addition to rapsyn, small GTPases appear to influence AChR localization. Rho-GTPases Rac and Cdc42 are known as regulators of actin cytoskeleton reorganization and have been shown to be activated by agrin and to be essential for AChR clustering (Weston et al., 2000). Consistently, it has been demonstrated that actin polymerizes at sites of AChR clustering upon agrin-stimulation and that inhibition of this polymerization blocks cluster formation (Dai et al., 2000).

1.5 LRP4

After its identification, MuSK was soon established as an essential factor in agrin-induced AChR clustering. But the molecular basis for agrin/ LRP4/ MuSK-signaling remained elusive since the two proteins do not interact directly (Glass et al., 1996). It was suggested that one or more until then unknown molecules, termed myotube-associated specificity component (MASC), bridge agrin and MuSK. In 2008 two groups reported the identification of a protein called low-density lipoprotein receptor (LDLR)-related protein 4 (LRP4) as this long-sought agrin receptor (Kim et al., 2008; Zhang et al., 2008).

LRP4 comprises a large extracellular N-terminal region with multiple EGF repeats and LDLR repeats followed by a transmembrane domain and a short intracellular domain, which lacks an identifiable catalytic motif (Johnson et al., 2005; Lu et al., 2007a; Tian et al., 2006; Yamaguchi et al., 2006).

Lrp4 mutant mice suggested that LRP4 is required for the normal development of the lung, kidney and ectodermal organs. But it was found that lack of LRP4 also causes severe defects in NMJ formation and neonatal lethality as observed for *MuSK* ^{-/-} mice (Weatherbee et al., 2006). Further analysis revealed that LRP4 is enriched at the NMJ (Zhang et al., 2008). It is barely detectable in myoblasts but expression is upregulated upon differentiation and highest in well-differentiated myotubes. LRP4 could be demonstrated to be required for agrin-stimulated MuSK activation. Agrin failed to induce MuSK phosphorylation in *lrp4* mutant myotubes although surface MuSK protein expression was normal (Kim et al., 2008). Different binding assays showed that LRP4 directly interacts with agrin via its extracellular portion (Zhang et al., 2008) and that LRP4 preferentially binds neuronal agrin and exhibits only minimal affinity for non-neural isoforms (Kim et al., 2008; Zhang et al., 2008). If expressed in *lrp4* mutant myotubes, LRP4/LDLR-chimeric molecules composed of LRP4 extracellular and transmembrane and LDLR intracellular domain but not wild-type LDLR could substitute LRP4. This indicates that the cytoplasmic domain of LRP4 is dispensable for agrin-responsiveness (Kim et al., 2008).

It was found that LRP4 self-associates (Kim et al., 2008) and forms a complex with MuSK in an agrin-independent manner (Kim et al., 2008; Zhang et al., 2008). Agrin binding to LRP4 apparently increases this LRP4-MuSK association (Zhang et al., 2008). It has also been proposed that agrin induces a conformational change in the preformed complex, which leads to reorientation of adjacent MuSK molecules and thereby facilitates trans-phosphorylation (Kim et al., 2008). In earlier studies, the most N-terminal Ig-like domain in MuSK has been reported to be essential for agrin-stimulated MuSK activation (Stiegler et al., 2006; Zhou et al., 1999). Considering the described findings, this domain might be involved in LRP4/MuSK-association and in the suggested conformational rearrangement (Kim et al., 2008). However, further structural and biochemical studies are required to completely uncover the mechanisms of agrin/ LRP4/ MuSK-signaling.

1.6 Dok7

Dok7 is a member of the Dok-family of adaptor proteins that is preferentially expressed in skeletal muscle and heart and concentrated postsynaptically at NMJs in mouse skeletal muscle (Okada et al., 2006). Beeson et al. and Müller et al. demonstrated that recessive mutations at several sites in Dok7 induce congenital myasthenic syndrome (CMS) (Beeson et al., 2006; Muller et al., 2007) indicative of a role in muscle activity or NMJ development. *Dok7* knockout mice showed that Dok7 is essential for NMJ formation (Okada et al., 2006). The mice exhibit a phenotype indistinguishable from that of *MuSK* knockout mice: They are immobile at birth and die shortly afterwards, show inability to breathe and a lack of AChR cluster formation (Okada et al., 2006). Forced expression of Dok7 in C2 myotubes was found to induce MuSK autophosphorylation as well as tyrosine phosphorylation of the β subunit of the AChR complex (AChR β 1), which is usually observed upon activation of MuSK. This effect was mediated by direct physical interaction of MuSK and Dok7 (Okada et al., 2006).

The N-terminal portion of Dok7 comprises a pleckstrin-homology (PH) and a phosphotyrosine-binding (PTB) domain (Figure 5). Multiple Src homology 2 (SH2) domain target motifs i.e. multiple tyrosine phosphorylation sites (Bergamin et al., ; Okada et al., 2006) are located in the extended C-terminal region.

Mutational studies and structural analysis revealed that Dok7 interacts with MuSK via its PTB domain dependent on MuSK autophosphorylation. When clustered, MuSK molecules autophosphorylate in trans on Tyr553 in the juxtamembrane region and on Tyr750, Tyr745 and Tyr755 in the activation loop of the kinase domain (Herbst and Burden, 2000; Watty et al., 2000). Tyr553 is located in a PTB domain target motif asparagine-proline-X-tyrosine (NPXY-) motif, the X standing for an optional amino acid. Upon phosphorylation, this motif is bound by the PTB domain of Dok7. Dok7 on the one hand serves as a substrate, being phosphorylated on Tyr395 and Tyr405 (Hamuro et al., 2008). On the other hand, it activates the catalytic activity of MuSK (Inoue et al., 2009; Okada et al., 2006) by dimerizing MuSK (Bergamin et al.). Binding of Dok7 to MuSK is followed by PH-PTB dimerization of Dok7, which leads to juxtaposition of MuSK kinase domains and facilitates MuSK trans-autophosphorylation. Inhibition of Dok7 dimerization was shown to largely abolish its activating effect on MuSK autophosphorylation (Bergamin et al.). But similar to most other PH-domains in phosphotyrosine signaling pathways, also the Dok7 PH-domain rather non-specifically interacts with membrane phosphoinositides. Thus the PH-domain of Dok7 appears to serve two roles: it supports MuSK dimerization and on the other hand mediates plasma membrane localization via phosphoinositide binding (Bergamin et al.).



Figure 5| Domain architecture of human Dok7 Schematic drawing adapted from (Bergamin et al.). The positions of the PH-domain (PH) and the PTB-domain (PTB) and of two phosphorylation sites, Tyr395 (Y395) and Tyr405 (Y405) are indicated. N... N-terminus, C... C-terminus.

1.7 Ubiquitination

Ubiquitination is an ATP-consuming process, which mediates the post-translational modification of a target protein via the covalent attachment of the 76-amino acid protein ubiquitin. The conjugation reaction is highly conserved between species, just as ubiquitin (Ub) itself (Schlesinger and Bond, 1987), and is dependent on the sequential actions of three enzymes (Hershko and Ciechanover, 1998). In the first step a thiol-ester linkage is formed between the C-terminal glycine residue of Ub and the active cysteine (Cys) residue of ubiquitin activating enzyme (E1). This activation reaction is driven by the hydrolysis of one ATP to AMP and inorganic diphosphate (PP_i). Subsequently the ubiquitin molecule is transferred to the cysteinyl group of ubiquitin-conjugating enzyme (E2). Mediated by a third enzyme termed ubiquitin ligase (E3), ubiquitin is attached to a target protein via an amide (isopeptide) bond between the C-terminal glycine and an optional amino acid residue of the target protein (Figure 6). E3 ligases confer specificity to the reaction but are a strongly inhomogeneous group of proteins.

Via the described cascade a single Ub molecule may be linked to a single amino acid residue in a target protein. However, the reaction does not only allow such monoubiquitination but can also mediate the addition of multiple Ub molecules to different target sites in one protein resulting in multi-ubiquitination. Moreover, after its addition to a protein, the ubiquitin molecule itself can be targeted by the ubiquitination machinery giving rise to polyubiquitin chains (Figure 7). So far, seven Lys residues of Ub, K6, K11, K27, K29, K33, K48 or K63, have been identified that can serve as conjugation sites (Peng et al., 2003) (Figure 8). Thus, polyubiquitin chains can not only vary in length, meaning in the number of Ub molecules, but also therein, at which lysine residue individual Ub molecules are linked together. These differences have been shown to influence polyubiquitination-associated signaling. Whilst Lys48-linked polyubiquitin chains of at least four molecules have been demonstrated to target proteins to proteasomal degradation, Lys63-linked polyubiquitination might play a role in DNA damage tolerance (Pickart and Fushman, 2004), signal transduction (Mukhopadhyay and Riezman, 2007; Sun and Chen, 2004) and intracellular trafficking of membrane proteins (Geetha et al., 2005; Hicke, 1999; Mukhopadhyay and Riezman, 2007). The results of Xu et al. suggested that in general all non-Lys63-linked polyubiquitinations induce protein degradation (Xu et al., 2009). But Seibenhener et al. and Saeki et al. found that even K63-polyubiquitin chains can target proteins to the 26S proteasome (Saeki et al., 2009; Seibenhener et al., 2004). It is thought that mono- as well as polyubiquitination possess non-proteasomal regulatory functions (Hershko and Ciechanover, 1998; Pickart, 2001), but so far it has not been possible to clearly decipher the ubiquitin code.

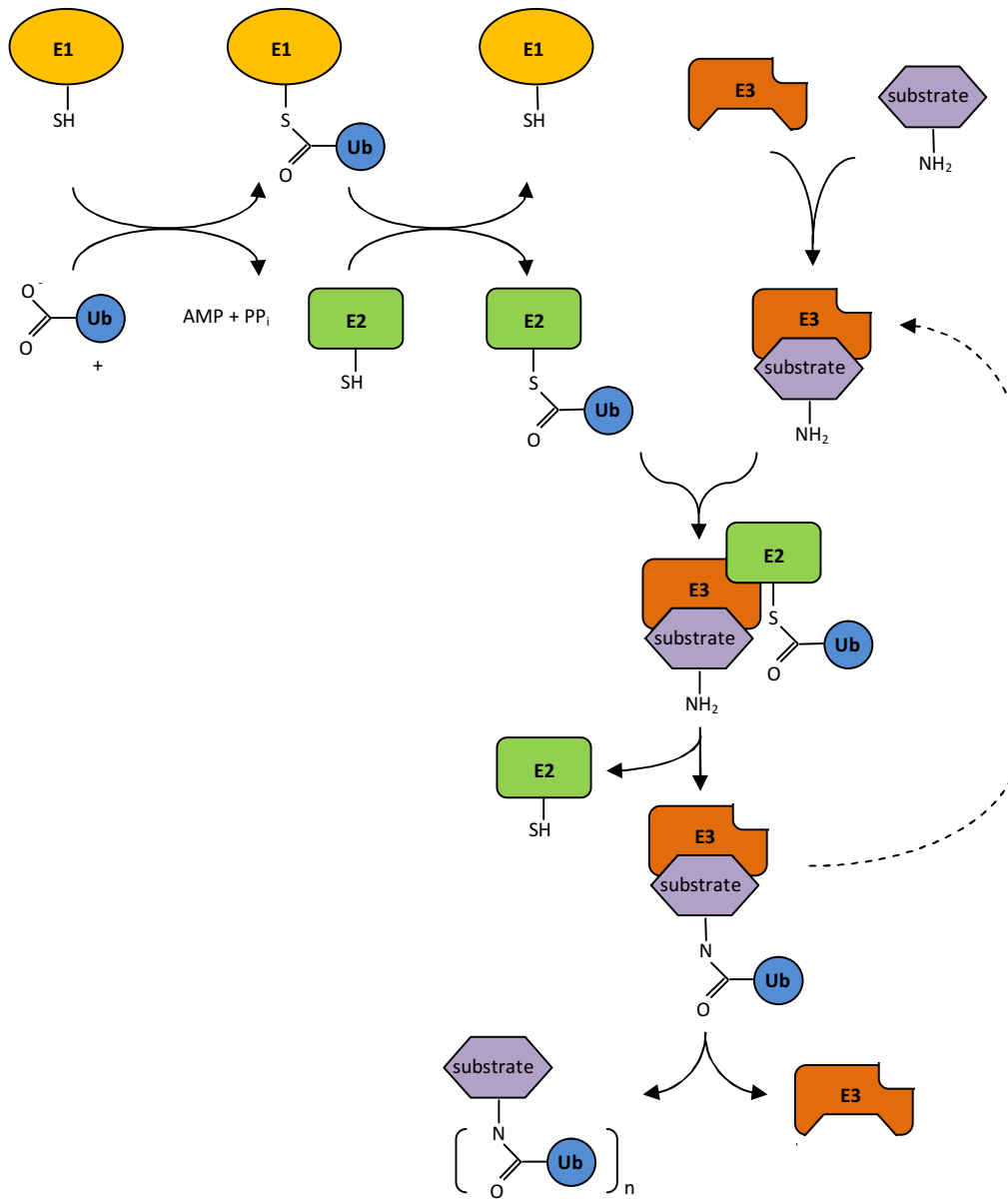


Figure 6| The Ubiquitination Cascade Schematic drawing adapted from <http://faculty.ucr.edu/~karine/research.html>, available: 2011-02-21, 4.00 p.m..

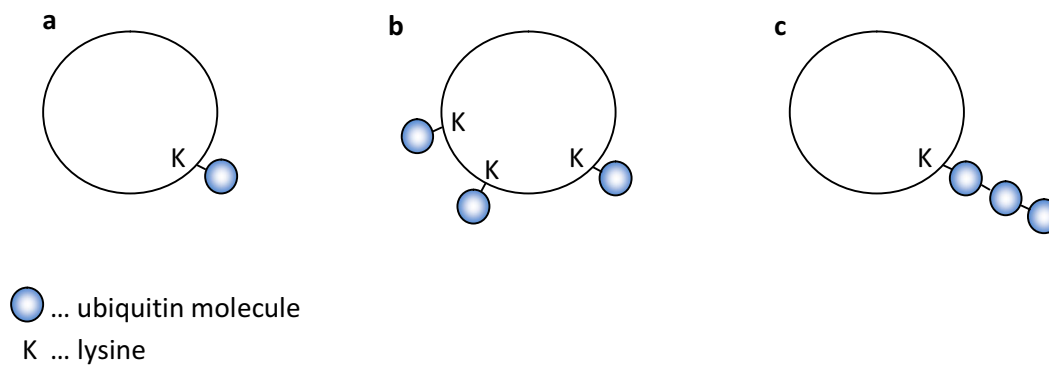


Figure 7| Types of Ubiquitination | a) Monoubiquitination | b) Multiple Monoubiquitination | c) Polyubiquitination

a

```
>gi|37571|emb|CAA44911.1| ubiquitin [Homo sapiens]
MQIFVKTTLTGKTTITLEVEPSDTIENVKAKIQDKEGIPPDQORLIFAGKQLEDGRTLSDYNIQKESTLH
LVLRLRGGAKKRKKSYTTPKKNKHKRKKVKLAVLKYKVDENGGKISRLRRECPSPDECAGVFMASHF
DRHYCGKCCLTYCFNKPEDK
```

b

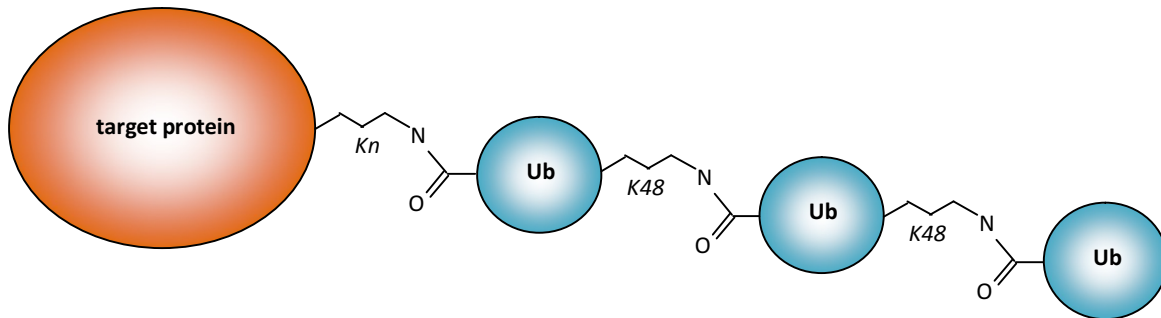


Figure 8 | a | Ubiquitin Amino Acid Sequence The amino acid sequence of human ubiquitin is depicted in the single-letter code. The seven Lys residues K6, K11, K27, K29, K33, K48 or K63 have been shown to be used for conjugating individual Ub molecules in polyubiquitin chains (shaded in gray) (Peng et al., 2003). **b | Lys48-Polyubiquitination** A target protein modified at an optional lysine residue Kn with a polyubiquitin chain. In the polyubiquitin chain each Ub molecule (but the first in the chain) is linked to a previous Ub molecule via the Lys48 residue (K48) of the previous Ub.

Considerable efforts have been undertaken to identify factors that regulate whether and at which residue a protein is ubiquitinated. It has been suggested that various structural determinants rather than a single consensus sequence direct E3 ligases to distinct lysines (reviewed in (Jadhav and Wooten, 2009)).

For instance, protein stretches that are rich in proline (P), glutamate (E), serine (S), and threonine (T) and are therefore termed PEST sequences have been described to act as proteolytic recognition signals in rapidly degraded proteins (Rogers et al., 1986). Such proteins were found to be phosphorylated at Ser and Thr residues within the PEST motif, which preceded ubiquitination and stimulated degradation via the ubiquitin-proteasome pathway (Lanker et al., 1996; Willems et al., 1996; Won and Reed, 1996; Yaglom et al., 1995). Nonetheless there also exist short sequence motifs, which mediate protein turnover. A small N-terminal motif termed “destruction box” or “D-box”, which comprises nine amino acid residues in the minimal form, regulates ubiquitination of mitotic cyclins (Glotzer et al., 1991). In the N-end rule pathway, E3 Ub ligases recognize N-degrons of proteins consisting of a destabilizing N-terminal residue and an internal lysine. Upon substrate binding, the ligase termed N-recogin catalyzes polyubiquitination of the target protein. As reviewed by Jadhav and Wooten (Jadhav and Wooten, 2009), several more such determinants for the regulation of ubiquitination have already been described, which illustrates the complexity of the process.

Like phosphorylation, ubiquitination is a reversible posttranslational modification. Whilst Ub ligases mediate conjugation of Ub, so called de-ubiquitinating enzymes (DUBs) are capable of removing Ub molecules. Longva et al. reported that inhibition of deubiquitination decreased the transport of proteins to multi-vesicular bodies, an important step in lysosomal degradation (Longva et al., 2002). In contrast J. Alwan et al. argued, that they only observed minor effects on lysosomal degradation when deubiquitination was blocked (Alwan et al., 2003). However, ubiquitination creates an

additional site for protein-protein interactions (Hicke et al., 2005; Hurley et al., 2006), which in turn could be associated with signaling pathways and might be fine-tuned by DUBs.

1.8 Endocytosis & Ubiquitination

Endocytosis enables cells to take up fluid, solutes and small particles from the extracellular environment. In the first step of this process, substrates get localized at the plasma membrane, which can be achieved by binding to cognate receptors, for instance. The membrane consequently invaginates forming a 'bud'. The bud grows until the plasma membrane at its neck is brought close enough to fuse and thereby seal off the forming vesicle.

There exist several types of endocytosis, the best studied among them being clathrin-mediated endocytosis (CME), macropinocytosis and caveolar/raft-dependent endocytosis. Less well known but currently of high scientific interest are clathrin- and caveolin/raft-independent pathways such as the Flotillin- and the Arf6-pathway (reviewed in (Mercer et al.)).

Ligand-mediated endocytosis has been described for various cell surface receptors including the Insulin receptor (Di Guglielmo et al., 1998) as an early step in the associated signaling pathways. Binding of cognate ligand was reported to stimulate targeting of receptors to clathrin-coated invaginations, which eventually form clathrin-coated vesicles. The vesicles deliver the ligand-receptor complexes to endosomal compartments where sorting processes determine the eventual fate of the cargo. The receptors can be retained in the endosome, recycled and transported back to the cell membrane or targeted to lysosomal degradation. Two functions have been attributed to ligand-mediated endocytosis. On the one hand, it is considered a mechanism to downregulate activated cell surface receptors. On the other hand, internalization might be required to position receptor at an intracellular location to enable it to interact with downstream signaling molecules (reviewed in (Ceresa and Schmid, 2000)).

In yeast, attachment of ubiquitin molecules was found to trigger internalization of transmembrane receptors (Galan and Haguener-Tsapis, 1997). This prompted researchers to uncover whether a comparable mechanism exists in mammalian cells. Studies revealed that indeed several RTKs such as EGFR, PDGFR or TrkA undergo ligand-stimulated ubiquitination (Arevalo et al., 2006; Geetha et al., 2005; Haglund et al., 2003; Huang et al., 2006; Joazeiro et al., 1999). Consistently, ubiquitination has been reported to influence the downmodulation of the majority of RTKs (reviewed in (Bache et al., 2004)). However, it is still unclear whether modification with Ub molecules directly affects endocytosis or rather regulates downstream mechanisms. Haglund et al. employed chimeric proteins composed of the extracellular and transmembrane portion of EGFR and full-length Ub to study the effect of ubiquitination on EGFR internalization (Haglund et al., 2003). The wild-type form of these bona fide monoubiquitinated EGFR-Ub chimeras was shown to become elongated by polyubiquitination at Ub, whereas an Ub mutant form could not be ubiquitinated further. It could be demonstrated that monoubiquitination was sufficient to induce receptor endocytosis, although internalization was more pronounced for the wild-type receptor. Indeed, EGFR has been shown via quantitative mass-spectrometry to be mono- as well as polyubiquitinated by Lys63-linked chains (Huang et al., 2006). Nonetheless, mutations in EGFR that inhibit ubiquitination do not significantly affect its internalization via clathrin-coated pits (Duan et al., 2003; Huang et al., 2007; Sigismund et al., 2005). This allows questioning the relevance of this modification. But, as reviewed by Acconcia et al. (Acconcia et al., 2009), receptor ubiquitination is apparently regulated by EGF concentration,

which also seems to influence targeting of the receptor to distinct internalization pathways (Sigismund et al., 2005; Woelk et al., 2006). In the respective analyses, ubiquitination was not detectable at low EGF doses and EGFR was exclusively internalized via clathrin-mediated endocytosis. At high doses, however, EGFR was ubiquitinated and targeted to clathrin-coated vesicles as well as to other, clathrin-independent pathways. As CME primarily leads to receptor recycling whereas clathrin-independent endocytosis preferentially targets EGFR to degradation (Sigismund et al., 2008), it was suggested that ubiquitination might, by determining the internalization route, regulate receptor downmodulation.

1.9 Protein Degradation

Eukaryotic cells possess two major systems for protein degradation: Lysosomes, vesicular cell organelles, represent the terminal compartment of endocytic and autophagic pathways (Luzio et al.) and account for about 10 - 20 % of total protein degradation (Gronostajski et al., 1985). 80 - 90 % of protein breakdown (Gronostajski et al., 1985) however is catalyzed by the ATP-dependent 26S proteasome, a 2000 kDa proteolytic complex (Coux et al., 1996).

1.9.1 Endosomal-Lysosomal Degradation

Lysosomes were discovered by Christian de Duve in the 1950s (De Duve et al., 1953; Gianetto and De Duve, 1955) and were originally described as vacuolar structures containing various hydrolytic enzymes that show optimal performance at an acidic pH (reviewed in (Ciechanover, 2006)). Further studies established the lysosome as the last compartment of the lysosomal degradation pathway, which accounts for the degradation of exogenous proteins (and their cognate receptors) taken up via receptor-mediated endocytosis and pinocytosis or exogenous particles engulfed during phagocytosis. Moreover, it catalyzes the breakdown of endogenous proteins and cellular organelles targeted to the lysosome via autophagy (reviewed in (Ciechanover, 2006)).

Extracellular low-density lipoprotein (LDL), for instance, is endocytosed upon binding to its receptor on the cell surface. The ligand-receptor complex is transported to the early endosome where the ligand dissociates due to the acidic pH in the endosomal lumen. This allows recycling of the receptor to the cell surface. In contrast, epidermal growth factor (EGF), another extracellular molecule also taken up via receptor-mediated endocytosis, remains bound to its receptor (reviewed in (Luzio et al., 2007)). Released ligand or the ligand-receptor complex respectively proceeds to late endosomes. These are formed from early endosomes, but the responsible mechanism is still a matter of debate. Recent live-cell imaging studies suggested that large late endosomal vesicles arise from a dynamic early endosome network and undergo a maturation process, in which they lose the small GTPase Rab5 and recruit Rab7 (Rink et al., 2005). The resulting late endosomes contain more vesicles in their lumen than early endosomes and are thus also termed multivesicular bodies (MVBs) (Luzio et al., 2007). Several theories exist on how material is subsequently transported from late endosomes to lysosomes. However, it was recently demonstrated that fusions of endosomes and lysosomes as well as kiss-and-run events, in which endosomal vesicles transiently dock to lysosomes ('kiss'), release material and dissociate again ('run'), contribute to the mixing of endosomal and lysosomal contents (Bright et al., 2005) (Figure 9b).

1.9.2 Rab7

Rab GTPases ('Ras-related in brain' (Touchot et al., 1987)) represent a diverse family of regulator proteins, which localize to the cytosolic face of intracellular membranes and are central to intracellular vesicular transport. Belonging to the Ras superfamily of small GTPases, they switch, like other regulatory GTPases, between two conformational states: the GTP-bound, 'active' conformation, which enables them to recruit and bind effector molecules (Zerial and McBride, 2001) and the GDP-bound, 'inactive' conformation.

Rab proteins obviously control distinct membrane transport pathways through localization to distinct intracellular membranes and specific binding of effector molecules (reviewed in (Stenmark and Olkkonen, 2001)). Rab4a and Rab5a have – among other Rabs - been localized to early sorting and recycling endosomal compartments (Bucci et al., 1995; Van Der Sluijs et al., 1991). In contrast, Rab7 has been described as a key regulator of membrane transport from early to late endosomes (Feng et al., 1995) and apparently plays a role in the proper aggregation and fusion of late endocytic structures, which is required for the biogenesis and maintenance of the lysosomal compartment (Bucci et al., 2000).

When tracking a protein in a cell on its way to degradation a major task is to identify the structures and organelles it is transported to. Proteins that are exclusively found in particular cellular areas, also referred to as 'markers', are helpful tools in such analysis. Due to its specific localization and function Rab7 has emerged as such a marker for late endosomal structures. Co-localization with Rab7 indicates that the protein of interest is situated in endosomal vesicles, which generally transport material to the lysosome and thus suggests degradation of the respective protein via the lysosomal pathway.

1.9.3 Proteasomal Degradation

The 26S proteasome is a proteolytic complex made up of the central 20S proteasome, which catalyzes proteolysis and two 19S complexes, which confer substrate specificity (Coux et al., 1996). The four stacked rings of the 20S proteasome surround a proteolytic chamber where proteolysis is catalyzed by multiple proteolytic sites - two chymotrypsin-like, two trypsin-like, two caspase-like sites in eukaryotes - provided by the central two β -rings (Figure 9a). Substrates enter through a small opening enclosed by the outer two α -rings. Most substrates of the proteasome are first marked by covalent modification with ubiquitin molecules by ubiquitinating enzymes (Ciechanover, 1994; Goldberg, 1995). This ensures precise and specific regulation of protein turnover. Ubiquitin chains are recognized by ubiquitin-binding sites on the 19S complexes. The chains are consequently degraded and proteins are unfolded. Both processes are catalyzed by the 19S complexes, which also facilitate entering of substrates into the 20S proteasome (reviewed in (Lee and Goldberg, 1998)). Protein degradation in the proteasome is highly processive and leads to complete digestion of substrates. Thereby it is excluded that large, potentially bioactive fragments are released into the cytosol (reviewed in (Lee and Goldberg, 1998)) (Figure 9b).

1.9.4 Inhibitors of Protein Degradation

One possibility to study degradation of a specific protein is to selectively block one of the two discussed degradative pathways and to assess the effect on turnover of the protein of interest. NH_4Cl , leupeptin and chloroquine can be used to inhibit lysosomal protein degradation (see e.g.

(Tanaka et al., 1986)). For analysis of proteasomal degradation several types of low-molecular-weight inhibitors are available. They can enter living cells and inhibit proteolysis specifically and reversibly without affecting other proteasomal functions. One such inhibitor is the peptide aldehyde Cbz-leu-leu-leucinal (also called Z-leu-leu-leu-al or MG132), which primarily targets chymotrypsin-like proteolytic activity (Lee and Goldberg, 1996; Rock et al., 1994). However, peptide aldehydes have also been reported to inhibit individual lysosomal proteases and calpains. Thus observed effects of these proteasomal inhibitors must be confirmed by use of distinct inhibitors of proteasomal activity, which do not affect other degradative pathways (Rock et al., 1994). Of course, the same is true for the use of lysosomal inhibitors.

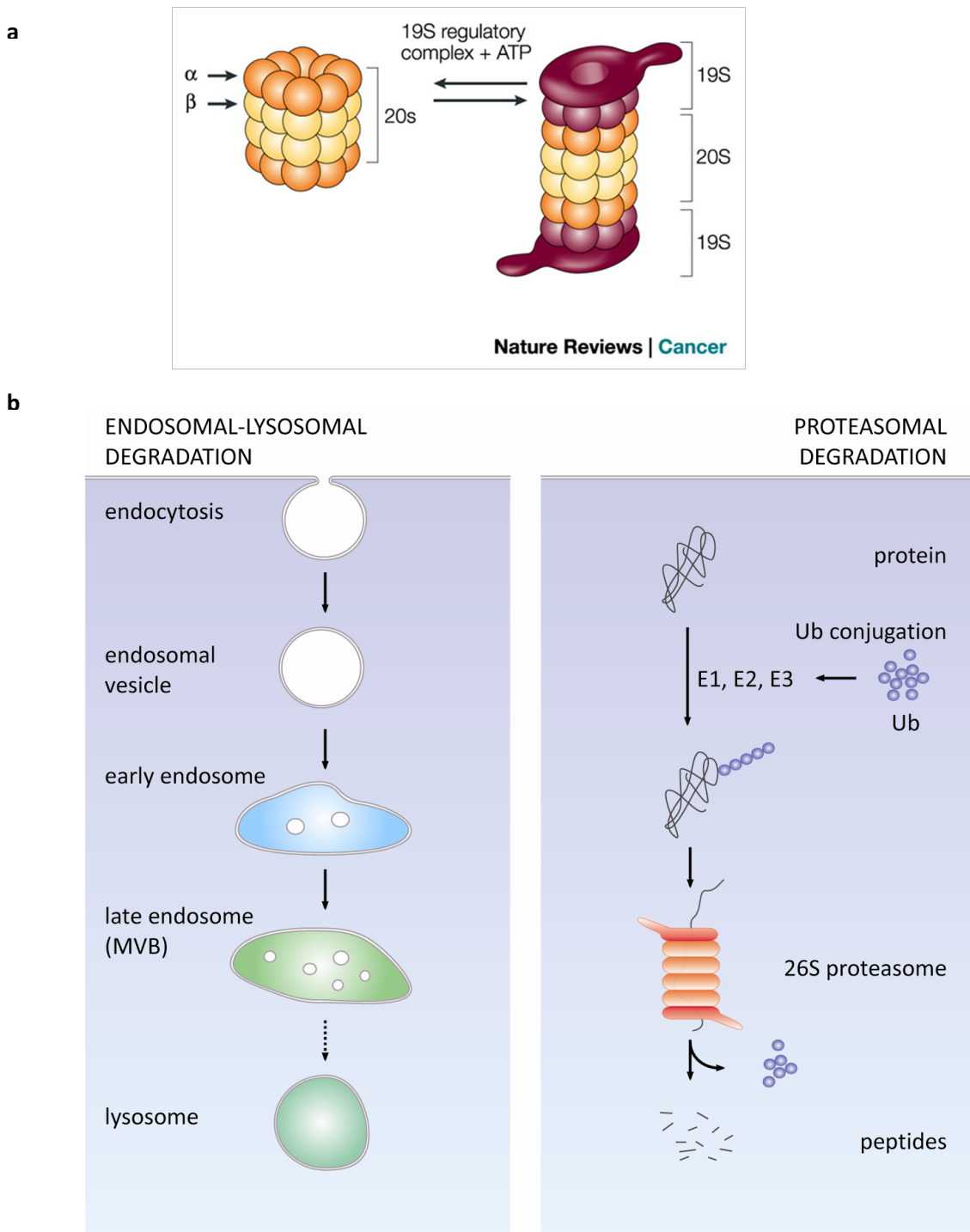


Figure 9| a| The 26S Proteasome Illustration from (Adams, 2004) The 20S Proteasome comprises two central β rings flanked by two α -rings. Together with two 19S regulatory complexes and ATP it forms the 26S proteasomal complex. | **b| Protein Degradation** Endosomal-lysosomal degradation (left side, adapted from (Luzio et al., 2007)) and proteasomal degradation (right side, adapted from (Lee and Goldberg, 1998)).

2 Aim of the Project

The aim of this diploma thesis was to further characterize the endocytosis of MuSK and the role of two posttranslational modifications, phosphorylation and ubiquitination, in this process. Of special interest were

- The effect of activation and consequent phosphorylation of MuSK on the internalization and degradation of MuSK
- The role of MuSK mono- and polyubiquitination in MuSK internalization and degradation

3 Results and Discussion

3.1 Activation of MuSK in a Heterologous Cell System

This project aimed at the establishment of a non-muscle cell system (heterologous cell system), in which MuSK can be stimulated artificially. Such a system would be useful for the investigation of MuSK endocytosis and internalization and associated processes.

Muscle-specific kinase is expressed in myotubes but not in non-muscle cell lines like COS-7, HeLa, Phoenix or HEK293T cells. To study MuSK in such heterologous cells, it was introduced via transient or stable transfection. Two methods of MuSK stimulation were subsequently tested. First of all, it was tried to artificially activate MuSK by antibody-mediated clustering (Section 3.1.1). Secondly, it was tested whether agrin could be used to stimulate heterologously expressed MuSK. Unfortunately, heterologous cells also miss the muscle intrinsic machinery required for agrin-induced MuSK activation, which comprises, among other proteins, the transmembrane agrin receptor LRP4 and the cytoplasmic protein Dok7. It was investigated whether agrin-responsiveness could be reconstituted by co-transfection of cells with MuSK and LRP4 or all three proteins (Section 3.1.2).

Both approaches would have yielded inducible experimental systems. They would have allowed activation of MuSK at a certain time point and analysis of the ensuing signaling processes. This would have been most convenient for tackling MuSK endocytosis. But in the establishment of these systems decisive obstacles were met. Thus, constitutively active and inactive MuSK mutants were used to investigate the effects of phosphorylation on MuSK internalization (Section 3.1.3.1). The mutants were transfected into the desired heterologous cells and differences in the transport processes in question were assessed. The required MuSK variants had already been created and simply had to be adapted according to experimental requirements.

3.1.1 Antibody-Induced Activation of MuSK

Heterologous cells were transiently transfected with N-terminally tagged MuSK (HA-MuSK, Myc-MuSK) and incubated for 24 h to allow protein expression. To activate MuSK, antibodies specific for the protein tag (Myc, HA) were added to the cell culture medium. Binding of antibody to the N-terminal tag of MuSK molecules should lead to clustering of RTKs and thereby induce trans-autophosphorylation and activation as shown previously (Herbst and Burden, 2000; Hopf and Hoch, 1998; Xie et al., 1997). Figure 10 depicts the principle of this approach using the example of Myc-MuSK. MuSK-transfected cells not treated with antibodies were used as reference for activation. To assess the extent of antibody-induced activation, stimulated cells and control cells were lysed and MuSK was immunoprecipitated from the lysates. The precipitates were resolved via SDS-PAGE and the immunoblots were probed for phosphotyrosine (pTyr) and Myc. The signal intensities were quantified and the ratio of corresponding pTyr and Myc signals was calculated. This ratio mirrored the phosphorylation level of MuSK in a sample i.e. the portion of total MuSK that was phosphorylated as a result of antibody-treatment.

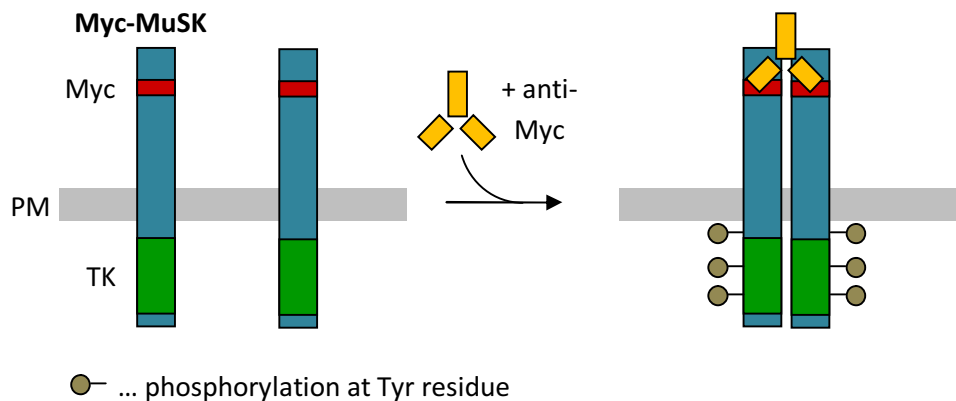


Figure 10| Antibody-mediated stimulation of N-terminally tagged MuSK Myc-MuSK comprises a Myc-tag (Myc) near the N-terminus. Upon heterologous expression of Myc-MuSK in non-muscle cells and integration of the protein into the plasma membrane (PM) this Myc-tag is exposed to the extracellular environment. Antibody specific for Myc that is added to the growth medium of Myc-MuSK expressing cells should interact with the Myc-tag and thereby cluster MuSK. MuSK aggregation should facilitate interaction of MuSK tyrosine kinase domains (TK) to induce MuSK trans-autophosphorylation.

The method was tested once with HA-MuSK and in several independent experiments with Myc-MuSK in HEK293T cells. Unfortunately, both MuSK-variants are strongly overexpressed upon transient transfection. This apparently leads to aggregation of the protein in the plasma membrane and pronounced antibody-independent activation. Of course, basal, agrin-independent auto-activation of MuSK also occurs in muscle-cells but generally at lower levels. In order to stimulate MuSK activation, cells were incubated with antibodies at a concentration of 50 nM as described in Section 5.5.8. For Myc-MuSK stimulation in HEK293T cells, also the twofold concentration of 100 nM was tested. However, it was observed that antibody treatment failed to significantly increase MuSK phosphorylation in HEK293T cells (data not shown). As HEK293T cells are known to express heterologous proteins at especially high levels, it was decided to test the experimental setting in a different cell system exhibiting less expression of transiently transfected proteins and thus probably also less basal MuSK phosphorylation. Figure 11 depicts the results of two independent experiments in COS-7 cells. In the first experiment antibody-treated cells yielded slightly increased MuSK phosphorylation compared to two untreated controls. In contrast, phosphorylation after anti- Myc-incubation was even less than in the controls in the second experiment. Moreover, phosphorylation levels in the two control samples strongly varied in both experiments.

As demonstrated, antibody treatment failed to significantly increase MuSK phosphorylation. Possibly, binding of antibody successfully induced MuSK clustering and activation but this antibody-mediated activation was not strong enough to be discriminated from basal activation via biochemical methods, as suggested above. But Myc-antibodies might also have been unable sufficiently cluster Myc-MuSK to facilitate trans-autophosphorylation. Anti-Myc binds Myc-MuSK as it has been demonstrated to label Myc-MuSK by immunocytochemistry (data not shown) and was used for immunoprecipitation. Nonetheless, it was found that this experimental setting is inapt for studying heterologous MuSK activation and endocytosis in HEK293T and COS-7 cells.

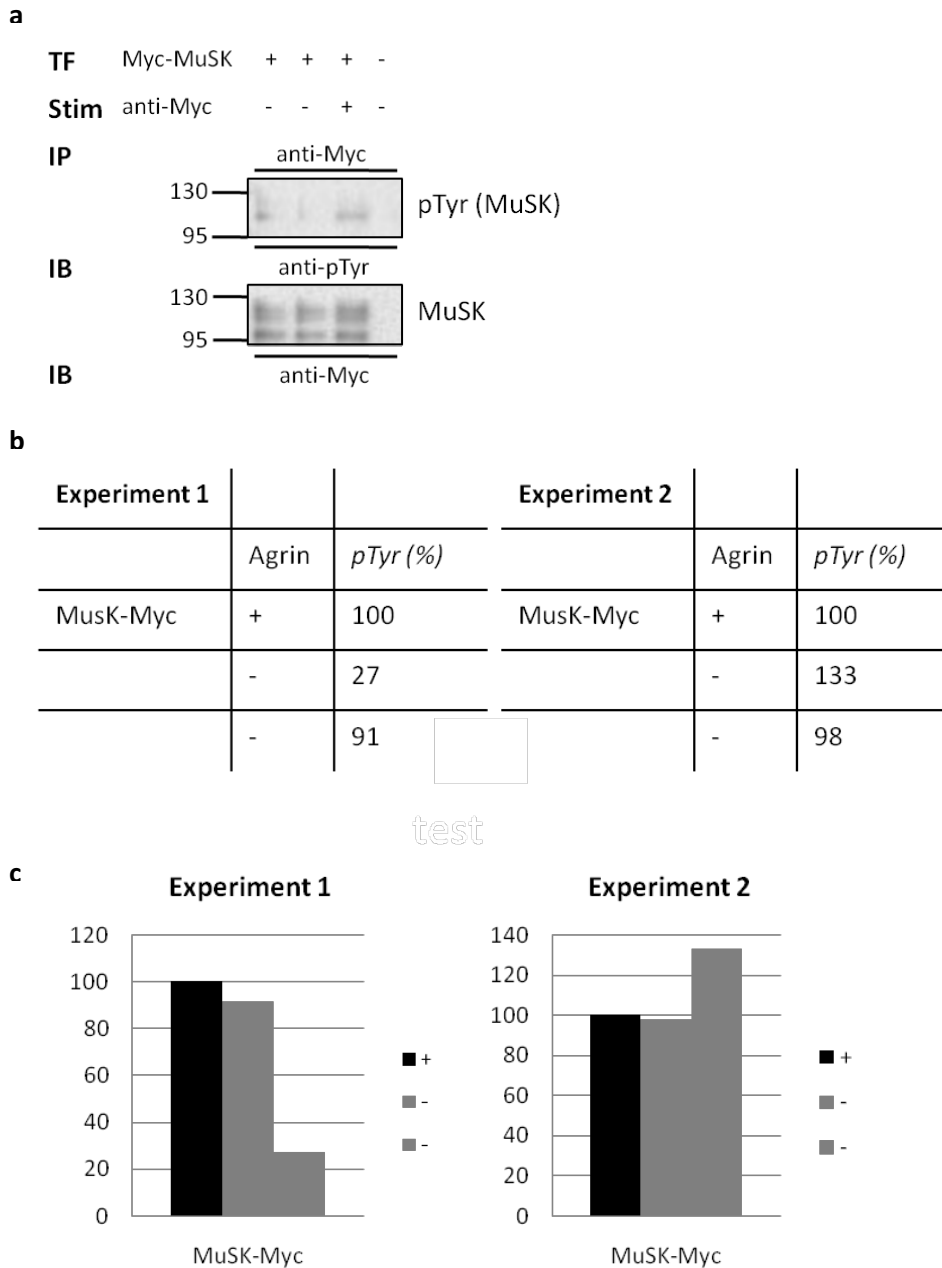


Figure 11| Quantification of Antibody-Mediated Stimulation of MuSK in COS-7 Cells COS-7 cells were transfected with Myc-MuSK and treated with 50 nM anti-Myc for 30 min or left untreated. The cells were lysed, Myc-MuSK was immunoprecipitated from the lysates with anti-Myc and resolved via SDS-PAGE. TF... transfection, Stim... stimulation, IP... immunoprecipitation, IB... immunoblot (antibody used for detection). | **a** | Immunoblots were probed for pTyr, stripped and probed for Myc (immunoblot of experiment 1). | **b, c** | The ratio of pTyr- and Myc-signals was quantified for each sample. Ratios are depicted in % of pTyr/Myc-ratio of stimulated sample.

3.1.2 Co-Expression of MuSK with Associated Muscle-Specific Proteins and Stimulation with Agrin

In this approach it was assessed whether MuSK, if co-expressed with LRP4 can be activated with agrin in heterologous cells.

To determine the efficiency of co-expression and the interaction between the expressed proteins, co-transfected HEK293T cells were lysed. MuSK or LRP4 were immunoprecipitated from the lysates and analyzed via immunoblotting Figure 12a. MuSK precipitates were probed for LRP4 showed a specific

band above 170 kDa. The band corresponded in size with the LRP4-signal detected in the lysates of co-transfected cells and in the lysates of cells transfected with LRP4 alone. In accordance, a specific MuSK signal was found when LRP4 was co-expression with MuSK and immunoprecipitated. Thus, it could be shown that MuSK and LRP4 were successfully co-expressed in HEK293T cells and interact with each other.

For agrin-stimulation experiments, cells were co-transfected with MuSK-HA and LRP4-Myc and treated with agrin or left untreated. The cells were lysed, MuSK was precipitated from the lysates and the phosphorylation levels were determined via immunoblotting as described in Section 5.6.7.

Again, it was found that MuSK strongly autophosphorylated upon heterologous expression as shown in Figure 12b and c. Moreover, no specific increase in MuSK phosphorylation was detected in MuSK precipitates derived from agrin-treated cells. Apparently, co-expression with LRP4 is not sufficient to render MuSK sensitive to agrin upon expression in HEK293T cells. The strong autophosphorylation might be the cause. But it has also been hypothesized that for stimulation of MuSK with agrin Dok7 was required in addition to LRP4. To avoid transient transfection of three different plasmids, Dok7 was stably transfected into HeLa and COS-7 cells. Both cell lines do not express heterologous proteins as highly as HEK293T cells after transient transfection. Hence, MuSK should autophosphorylate less in these cells. Dok7-positive HeLa and COS-7 cells should subsequently be transiently co-transfected with MuSK and LRP4 and used for agrin-induction experiments.

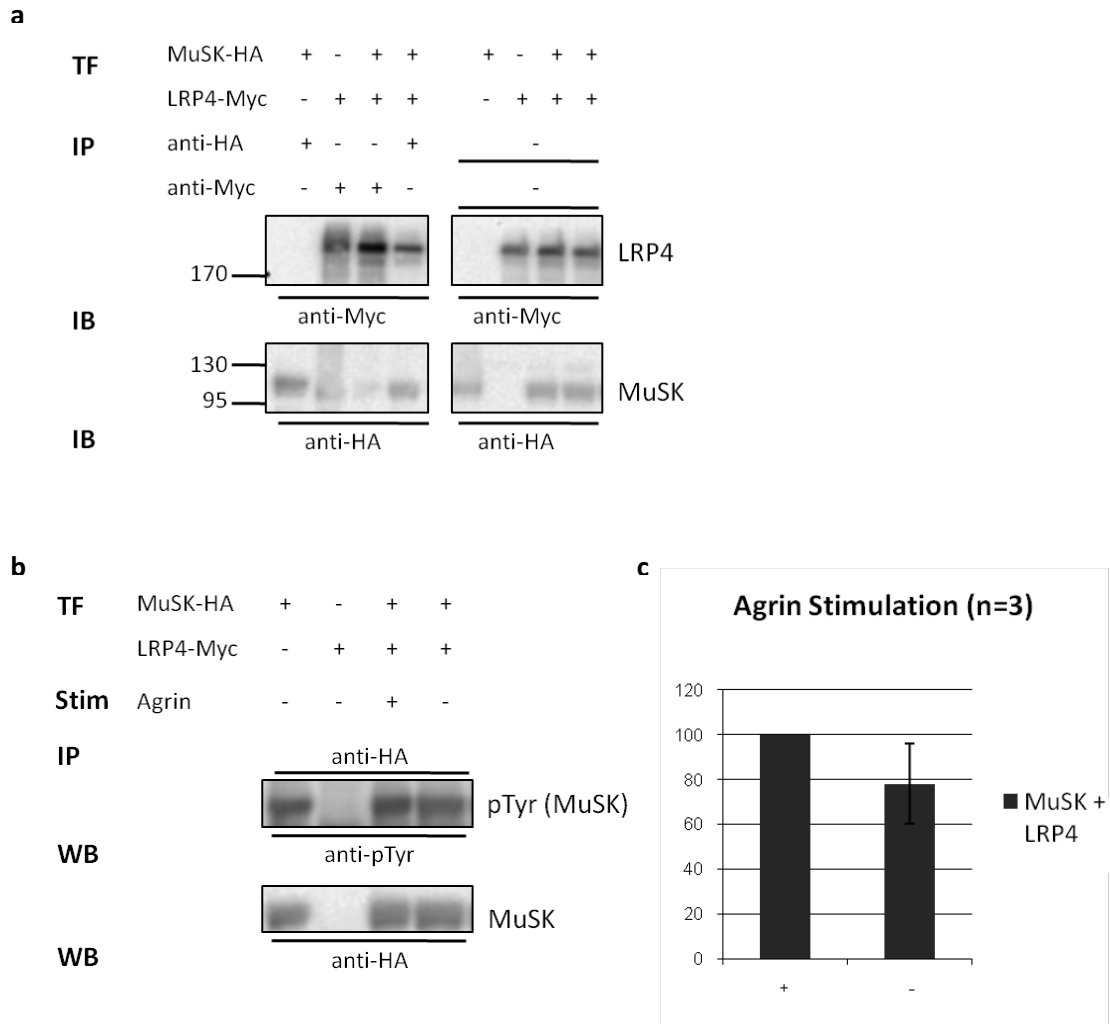


Figure 12| Co-Expression of MuSK and LRP4 in HEK293T Cells and Stimulation with Agrin| a| HEK293T cells were transfected with MuSK-HA, LRP4-Myc or both. Cells were lysed and aliquots of the lysates were taken. The rest of the lysates was subject to IP with antibodies specific for HA (anti-HA) or Myc (anti-Myc). The lysate aliquots and the precipitates were resolved via SDS-PAGE. The immunoblots were cut and the parts were probed for HA and Myc. | **b|** HEK293T cells were transfected with MuSK-HA, LRP4-Myc or both. Co-transfected cells were treated with agrin for 30min or left untreated and lysed. MuSK was precipitated from the lysates and the precipitates were resolved via SDS-PAGE. The immunoblots were probed for pTyr, stripped and probed for HA to detect MuSK. | **c|** MuSK phosphorylation in lysates of agrin stimulated and unstimulated cells co-transfected with MuSK and LRP4 was quantified (see 5.6.7) in three independent experiments.

3.1.2.1 Generation of Single Cell Clones Stably Expressing Dok7

HeLa and COS-7 cells were stably infected with retrovirus carrying C-terminally HA-tagged Dok7 controlled by a c-Fos or a TK promoter (c-Fos Dok7-HA or TK Dok7-HA) (Kim et al., 2008). The TK promoter is a stronger promoter than the c-Fos promoter. Thus, the TK promoter should lead to higher Dok7 expression whereas the c-Fos promoter should cause more physiological Dok7 expression levels. Dok7-positive cells were selected through cultivation in growth medium containing puromycin. Single-cell clones were picked and cultured and the expression level of Dok7 in the clones was determined. Dok7 expression was significantly higher in COS-7 clones than in HeLa clones. Two TK-Dok7-HA positive HeLa and two TK-Dok7-HA positive COS-7 clones exhibiting the highest and lowest Dok7-expression were used for further experiments (see Figure 13). This should allow controlling for artefacts resulting from different Dok7 expression levels.

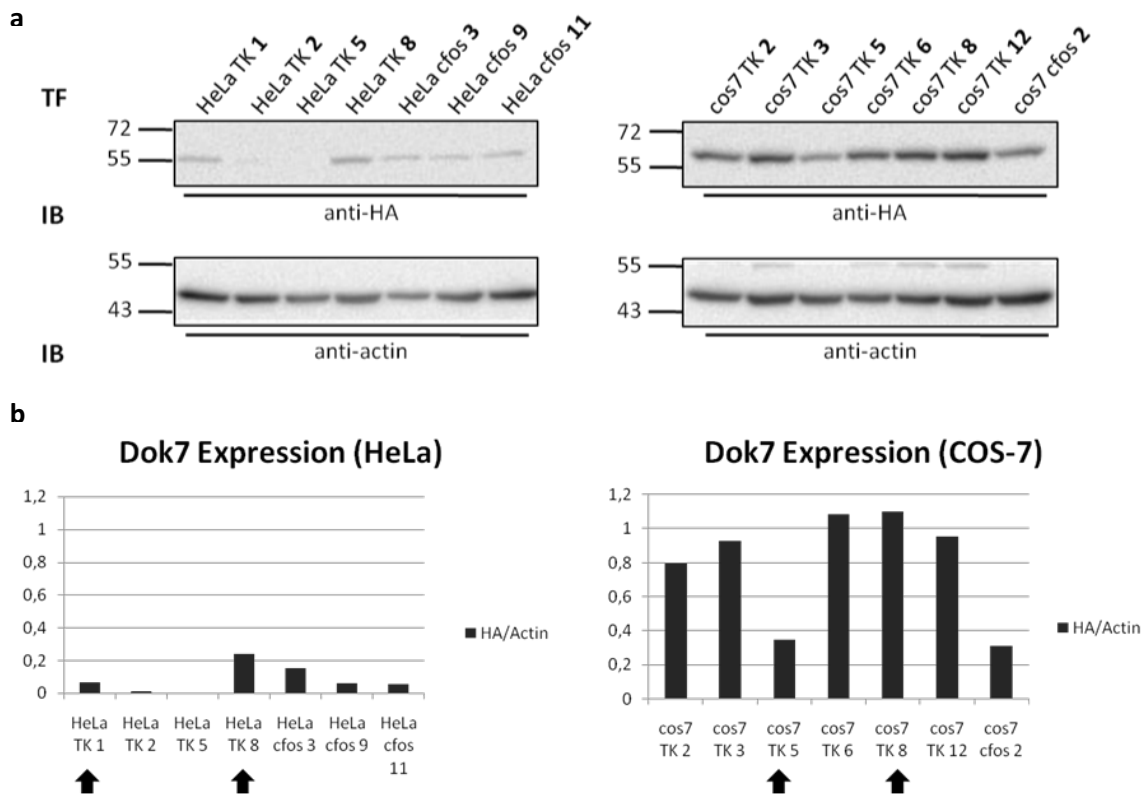


Figure 13 | Quantification of Dok7 Expression in HeLa and COS-7 Clones Stably Infected with Dok7 | a| Dok7 positive HeLa and COS-7 clones were lysed. Lysates were resolved by SDS-PAGE and immunoblots were probed for HA, to detect HA-tagged Dok7, and actin. | b| HA and actin signals were quantified and the ratio of the two signals (HA/actin) was calculated for each clone. Black arrows mark the clones that were selected for further experiments.

The selected clones were transfected with Myc-MuSK and FLAG-tagged LRP4 in several independent experiments. However, co-expression of the two proteins could never be detected biochemically. Moreover, the cells had undergone morphological changes due to repetitive passaging and long cultivation. COS-7 cells were no longer round-shaped but exhibited filopodia-like processes. HeLa cells were either rounder than usual or thinner and elongated. It was found that the selected, Dok7-positive HeLa and Dok7 clones could only poorly be transiently transfected with further proteins or were completely resistant to additional transfection. Thus, the cells were unsuitable.

3.1.3 Constitutive Activation & Inactivation of MuSK

The establishment of an inducible model system for MuSK endocytosis was found to be more difficult than expected. Therefore, kinase-inactive and kinase-active MuSK mutants MuSK-K608A and MuSK-LS745/746MT were used to study the role of phosphorylation in MuSK-endocytosis. In MuSK-K608A, arginine is expressed instead of a key lysine in the ATP binding site of MuSK, which abolishes the kinase activity of MuSK (Glass et al., 1997). MuSK-LS745/746MT comprises mutations that destabilize the conformation of the MuSK A loop. In the unphosphorylated form of MuSK, this loop sterically blocks the nucleotide and substrate binding sites. To create MuSK-LS745/746, Leu-745 and the first residue in the A loop Ser-746, which are involved in strong non-covalent interactions, were replaced by the corresponding amino acids of the insulin receptor kinase (IRK) (Till et al., 2002). The mutated amino acids do not fulfil the same functions thus weakening the inactive conformation of the A loop and rendering MuSK constitutively active. The MuSK mutants MuSK-K608A and MuSK-LS745/746MT were kindly provided by S.J. Burden. The mutants were modified by insertion of streptavidin-binding

protein (SBP)-tags near the N-terminus of MuSK (see Section 5.6.9.4 and Figure 14). SBP strongly associates with streptavidin and allows tracking the tagged proteins with fluorophore-coupled streptavidin in internalization experiments.

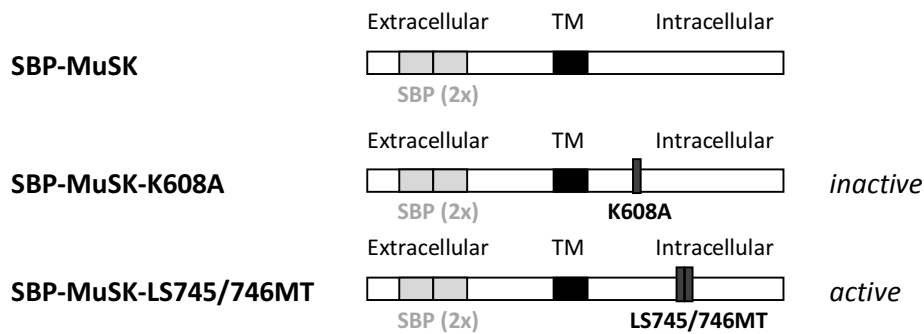


Figure 14 | Wild-type SBP-MuSK and SBP-MuSK Mutants In SBP-MuSK-K608A lysine 608 (K608) was replaced by an arginine residue rendering the protein kinase inactive. SBP-MuSK-LS745/746MT contains methionine (M) and threonine (T) instead of leucine (L) and serine (S) residues at positions 745 and 746 and thus is constitutively phosphorylated if expressed in cells.

3.1.3.1 Characterization of SBP-MuSK-K608A and SBP-MuSK-LS745/746MT in COS-7 Cells

To characterize expression and phosphorylation levels of the modified phosphorylation mutants SBP-MuSK-K608A and SBP-MuSK-LS745/746MT in comparison to wild-type SBP-MuSK, the three constructs were transiently transfected into COS-7 cells. Transfected cells were examined biochemically and via immunocytochemical stainings (Figure 15). In immunoblots, wild-type SBP-MuSK showed weak phosphorylation most probably resulting from spontaneous clustering and auto-phosphorylation. Such basal phosphorylation is, as explained previously, generally observed for MuSK wild-type variants expressed at high levels. However, phosphorylation of SBP-MuSK-LS745/746MT was significantly stronger whereas SBP-MuSK-K608A was not phosphorylated. In immunocytochemical stainings pronounced tyrosine phosphorylation was detected in the areas of the cells where SBP-MuSK-LS745/746MT was localized. In contrast, SBP-MuSK-K608A positive cells stained only weakly for pTyr and no colocalization of MuSK- and pTyr-staining was observed. Thus biochemical and immunocytochemical characterization confirmed that SBP-MuSK-K608A is kinase-inactive whereas SBP-MuSK-LS745/746MT is strongly auto-phosphorylated in a constitutive, agrin-independent manner.

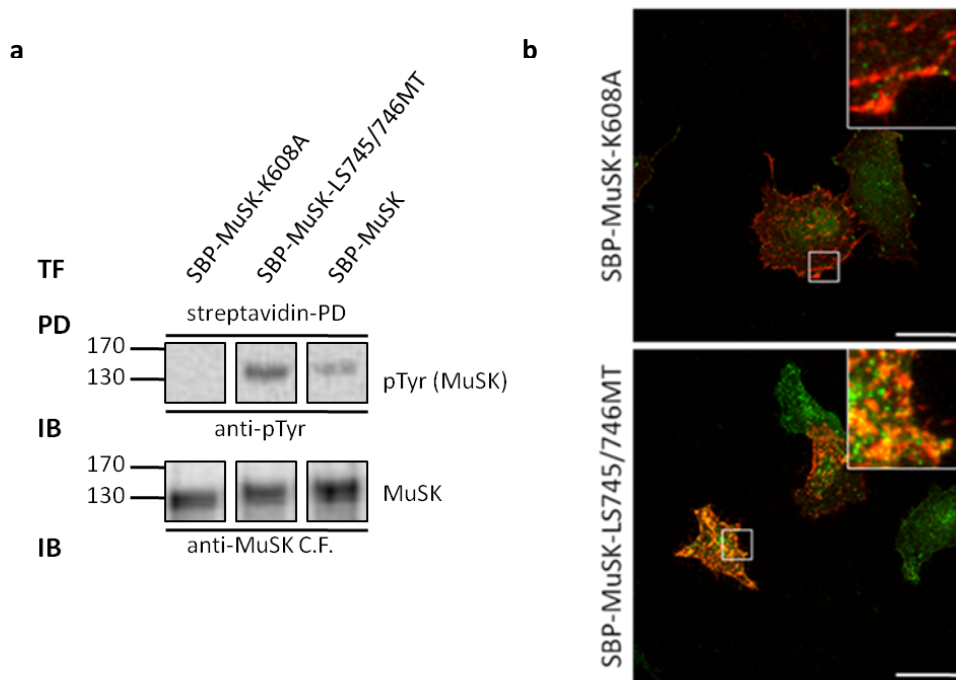


Figure 15 | Phosphorylation of SBP-MuSK wt, -K608A & -LS745/746MT | a | COS-7 cells transfected with SBP-MuSK wt, -K608A or -LS745/746MT were lysed. SBP-tagged MuSK variants were pulled down with streptavidin-coupled agarose beads (=streptavidin-PD... streptavidin-pull-down). PD-samples were resolved via SDS-PAGE and immunoblots were probed for pTyr, stripped and reprobed for MuSK. | **b |** SBP-MuSK variants K608A and LS745/746MT were transfected into COS-7 cells and the cells were immunocytochemically stained for pTyr (green) and MuSK (red). Scale bars, 25 μ m.

3.1.3.2 Internalization of SBP-MuSK-K608A and SBP-MuSK-LS745/746MT in COS-7 Cells

Next it was examined whether phosphorylation of MuSK influences its endocytosis and consecutive intracellular targeting. For this purpose SBP-tagged wild-type MuSK (SBP-MuSK) and the two phosphorylation mutants SBP-MuSK-K608A and -LS745/746MT were expressed in COS-7 cells. Living cells expressing one of the three variants were shifted to 4°C to inhibit endocytosis and incubated with fluorophore-coupled streptavidin to label MuSK on the cell surface. Unbound streptavidin was removed and endocytosis was permitted by incubating the cells at 37°C. After different incubation times, the internalization process was stopped by cooling. The cells were washed, fixed and mounted.

As demonstrated in Figure 16 wild-type MuSK was primarily localized at the cell membrane endocytosis was allowed. After 30min of incubation at 37°C SBP-MuSK was rather found in big vesicular structures near the cell nucleus and was even more concentrated in the perinuclear region after 60min. This change in localization suggests rapid internalization of the protein within 1h. A comparable redistribution process was observed for the two phosphorylation mutants K608A and LS745/746MT. No differences in the timecourse of internalization were observed. The structures to where the three MuSK variants were targeted were similar in morphology. These results suggest that the activation level of MuSK does not affect the internalization and degradation of MuSK in COS-7 cells. However, it is possible that muscle cells might express specific proteins, which change MuSK targeting in response to its activation.

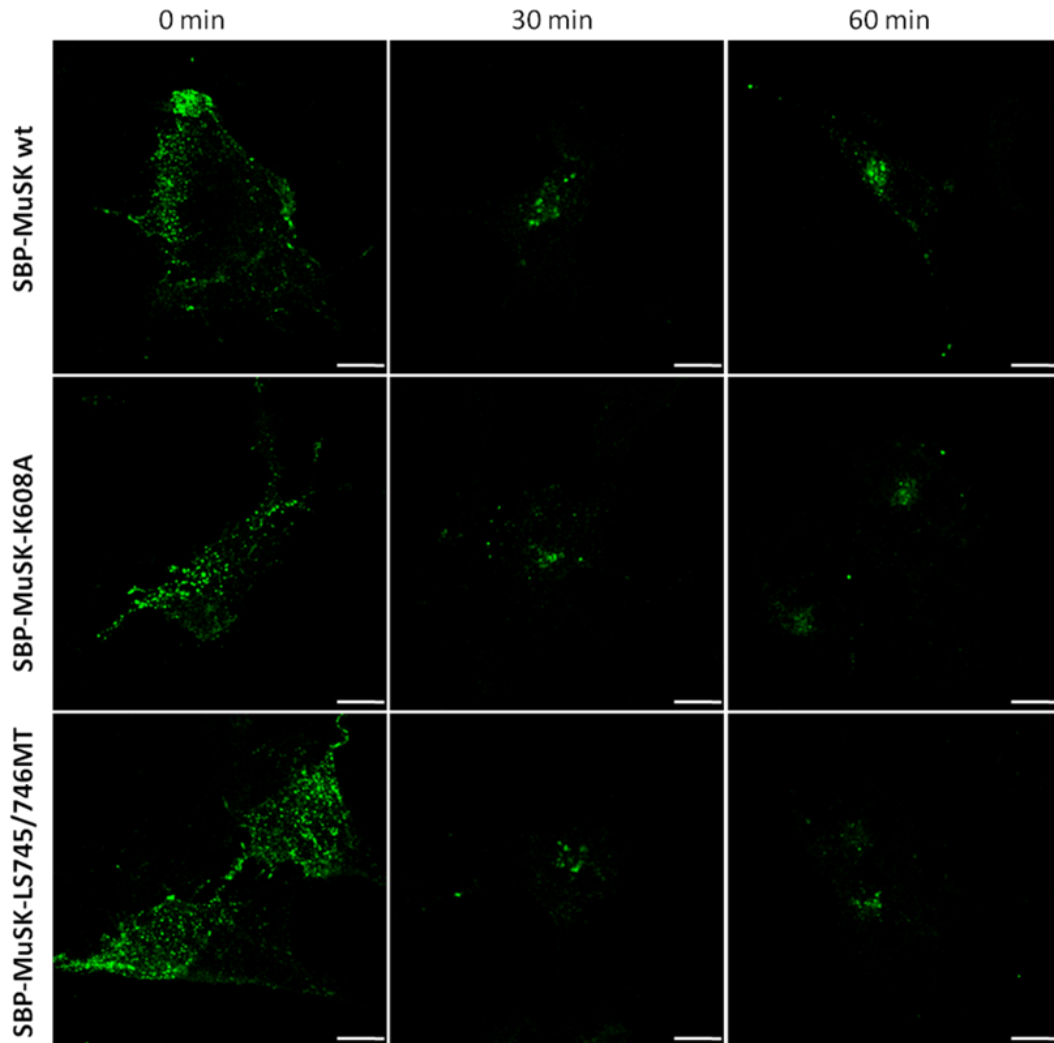


Figure 16| Internalization of wild-type SBP-MuSK, SBP-MuSK-K608A and SBP-MuSK-LS745/746MT in COS-7 Cells COS-7 cells expressing wild-type SBP-MuSK, SBP-MuSK-K608A or SBP-MuSK-LS745/746MT were labeled with fluorophore-coupled streptavidin at 4°C. After removal of unbound streptavidin, the cells were directly fixed (0 min) or incubated for 30min or 60min at 37°C before fixation. Scale bars, 10 μ m.

3.2 The Role of MuSK Ubiquitination in MuSK Endocytosis and Degradation

Like MuSK, EGFR is a receptor tyrosine kinase that has been shown to be ubiquitinated in a ligand-dependent manner (Haglund et al., 2003; Huang et al., 2006; Lu et al., 2007b). Haglund et al. analyzed the role of mono- and polyubiquitination in EGFR endocytosis and for this purpose created EGFR-Ub chimeras (Haglund et al., 2003). In these chimeras, the intracellular domain of the RTK was replaced by either wild-type ubiquitin (EGFR-Ub) or a mutated form of ubiquitin (EGFR-Ub-mut). In this mutated variant, K48 of Ub had been replaced by an arginine residue and the last two glycines had been deleted. As K48 and the C-terminal glycines of Ub are commonly involved in polyubiquitination the mutated chimera was not polyubiquitinated. Missing the intracellular portion of EGFR, EGFR-Ub and -Ub-mut were completely devoid of cytosolic signaling domains. Hence, differential ubiquitination but not additional signaling processes could influence endocytosis of these proteins.

Expression vectors encoding the two ubiquitin variants were kindly provided by S. Sigismund and P.P. Di Fiore and were used by R. Herbst to create MuSK-Ub chimeras (unpublished data). These chimeras were modified by addition of an N-terminal HA-tag (see Section 5.6.9.5 and Figure 17).

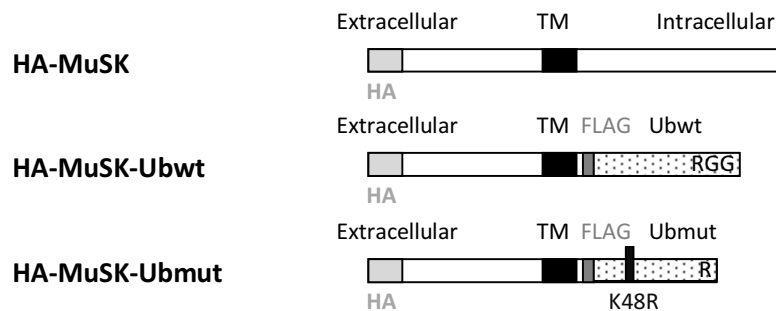


Figure 17| Wild-type HA-MuSK and HA-MuSK-Ub chimeras HA-MuSK-Ubwt & HA-MuSK-Ubmut Wild-type MuSK N-terminally fused to an HA (HA-MuSK) was used as control in internalization experiments. HA-MuSK-Ubwt is structurally similar to HA-MuSK but the intracellular portion of MuSK was replaced by a FLAG-protein tag and wild-type ubiquitin. In contrast to HA-MuSK-Ubwt, HA-MuSK-Ubmut contains two mutations in the Ub portion. Lysine 48 (K48) of Ub was replaced by arginine (R) and the last two glycines of the Ub portion were deleted.

3.2.1 Characterization of HA-MuSK-Ubwt and HA-MuSK-Ubmut in COS-7 Cells

HA-MuSK-Ubwt and HA-MuSK-Ubmut were expressed in COS-7 cells and characterized biochemically and by immunocytochemistry.

Lysates of COS-7 cells transfected with HA-MuSK-Ubwt or HA-MuSK-Ubmut were analyzed via immunoblotting as depicted in Figure 18a. In the case of HA-MuSK-Ubwt, probing with anti-HA yielded a weak band of 85 - 90 kDa and a high molecular weight smear of more than 170 kDa. This kind of blurred pattern is characteristic for polyubiquitinated proteins (see e.g. (Haglund et al., 2003)). Upon polyubiquitination, protein molecules of one type are generally modified with polyubiquitin chains of varying lengths. Consequently individual protein molecules migrate differently during SDS-PAGE and produce a protein ladder or smear rather than a single band. The weak single band and the smeary pattern were also detected in immunoprecipitates of HA-MuSK-Ubwt. In contrast, HA-MuSK-Ubmut gave two bands of less than 100 kDa. The smaller band was of the same size as the single band detected for HA-MuSK-Ubwt whereas the other band migrated 10-15kDa higher. Intriguingly, this size shift correlates with the addition of one Ub molecule (Shih et al., 2003). HA-MuSK-Ubmut also appeared as high molecular weight smear in lysates and after immunoprecipitation. But relative to the signal intensity of the smaller, ~85 kDa band the high-molecular pattern was less pronounced than in HA-MuSK-Ubwt lysates and immunoprecipitates.

Thus, biochemical analyses indicate that HA-MuSK-Ubwt is expressed primarily as polyubiquitinated protein. However, it also occurs in the unmodified form, which is bona fide monoubiquitinated as it comprises full length Ub. HA-MuSK-Ubmut occurs in two species of approximately 85 and 95 kDa. It is suggested that the 85 kDa species represents the unmodified, bona fide monoubiquitinated protein. The 95 kDa species most probably carries an additional Ub molecule and thus is di-ubiquitinated. Nonetheless also polyubiquitinated HA-MuSK-Ubmut was detected. Apparently the K48R mutation in the Ub portion and the deletion of the two C-terminal glycines of does not completely inhibit

polyubiquitination. But as explained in Section 1.7 other lysine residues of Ub such as K63 can serve as acceptor sites for Ub chains.

To confirm that both chimeras actually comprise Ub and that the 95 kDa species of HA-MuSK-Ubmut further modified with a single ubiquitin molecule the experiment depicted in Figure 18a was repeated and immunoblots were probed with P4D1. P4D1 is a monoclonal antibody specific for mono- and polyubiquitin commonly used for ubiquitin detection. It was applied by Haglund et al. to detect the EGFR-Ub chimeras and thus was expected to bind HA-MuSK-Ubwt and -Ubmut (Haglund et al., 2003). Surprisingly, the antibody failed to bind the 85 kDa species of either of the two chimeras and the 95 kDa species of HA-MuSK-Ubmut. It exclusively detected the polyubiquitin smears (data not shown). It can only be hypothesized that P4D1 binding to the small chimera species was too weak to yield a specific signal. This would also be in accordance with the results shown in Figure 19.

Expression of the two MuSK-Ub chimeras was also analysed by immunocytochemistry as demonstrated in Figure 18b. For the stainings COS-7 cells transfected with HA-MuSK-Ubwt or HA-MuSK-Ubmut were fixed and the plasma membrane was permeabilized with detergent or left intact. Antibodies cannot diffuse through intact plasma membrane. Hence, only MuSK expressed on the cell surface was stained in the case of unpermeabilized cells. For both chimeras an evenly distributed, dotted surface staining was observed, but the spots appeared to be smaller on cells expressing HA-MuSK-Ubwt. Intracellularly, HA-MuSK-Ubwt was detected throughout the cell but primarily near the nucleus. In HA-MuSK-Ubmut expressing cells the staining was much stronger and more pronounced in the peripheral areas of the cells. Apparently, HA-MuSK-Ubmut is expressed far better than HA-MuSK-Ubwt. The preferred localization of HA-MuSK-Ubwt near the cell nucleus suggests that it might be degraded to some extent right after synthesis. Nonetheless, it could be demonstrated by surface stainings that both chimeras are expressed as functional proteins that are integrated into the plasma membrane.

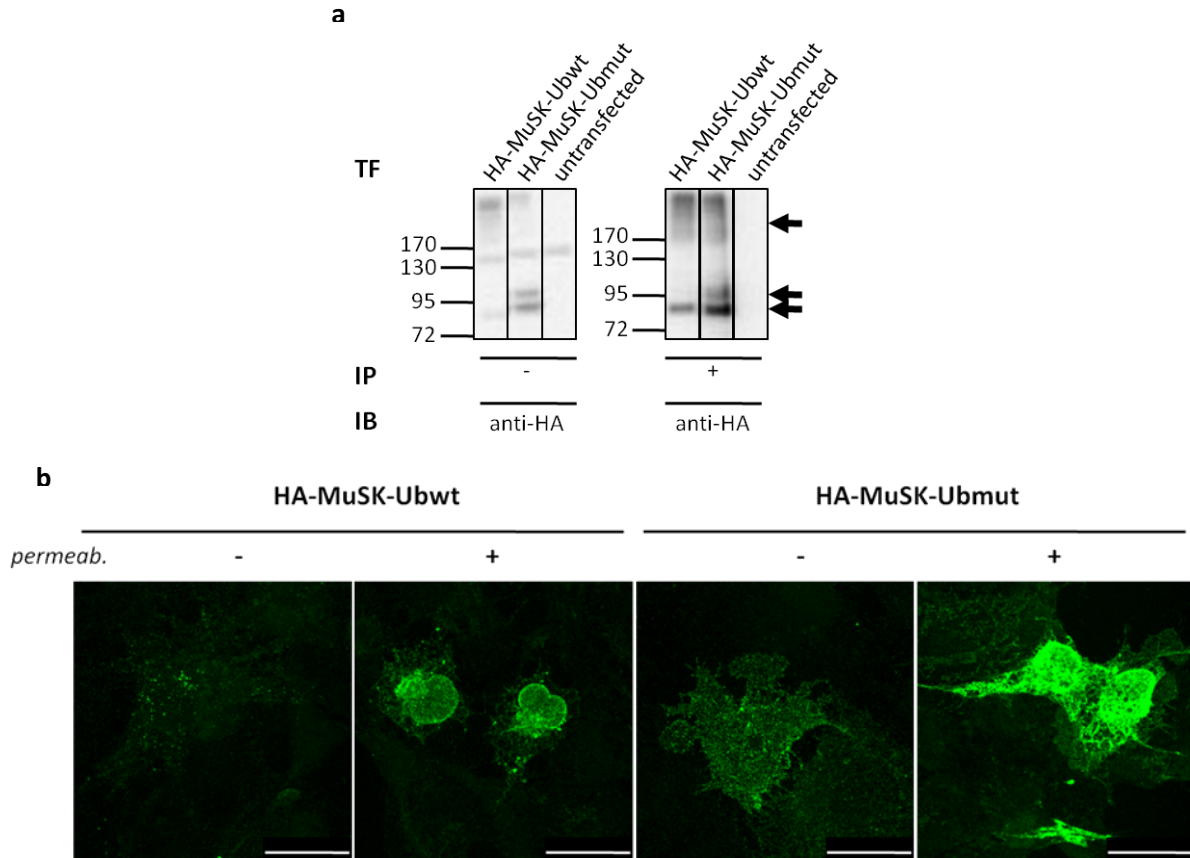


Figure 18| Expression of HA-MuSK-Ubwt and HA-MuSK-Ubmut in COS-7 cells| a| For biochemical analysis COS-7 cells transfected with HA-MuSK-Ubwt, HA-MuSK-Ubmut and untransfected cells were lysed and subjected to immunoprecipitation with antibodies against HA (anti-HA). Lysate aliquots and immunoprecipitates were resolved via SDS-PAGE and immunoblots were probed for HA. | **b|** For immunocytochemical stainings COS-7 were transfected with HA-MuSK-Ubwt or HA-MuSK-Ubmut. Cells were permeabilized and stained for HA to detect intracellular and surface MuSK. To exclusively detect surface MuSK, transfected cells were not permeabilized previous to staining. Scale bars, 25 μ m.

Figure 19 depicts an internalization experiment performed with the MuSK-Ub-chimeras, in which endocytosis and ubiquitination of HA-MuSK-Ubwt and HA-MuSK-Ubmut was studied. Internalization of the chimeras was tracked as illustrated in Figure 19a. Living COS-7 cells transfected with HA-MuSK-Ubwt or HA-MuSK-Ubmut were incubated with anti-HA antibodies at 4°C. Thereby, MuSK expressed on the cell surface was labeled while at the same time endocytosis was blocked. Unbound antibody was removed and the cells were put to 37°C, which permitted internalization, and incubated for 5 to 120min. Internalization was stopped by cooling the cells to 4°C. By incubating the intact cells in buffer of low pH, antibodies were stripped from MuSK molecules that had not been internalized until then. Subsequently, the cells were fixed, permeabilized and anti-HA bound to internalized MuSK was detected with fluorophore-coupled secondary antibodies. Ubiquitination was detected subsequently by conventional immunocytochemical staining using P4D1 antibody.

Figure 19b shows that internalization of HA-MuSK-Ubwt and HA-MuSK-Ubmut could be visualized by the described assay. But ubiquitination of the two chimeras was not clearly demonstrated. As mentioned above P4D1 antibody should bind mono- and polyubiquitin but failed to detect the bona fide monoubiquitinated species of HA-MuSK-Ubwt and HA-MuSK-Ubmut in immunoblotting. In immunocytochemical stainings, P4D1 was found to stain HA-MuSK-Ubwt positive cells in areas where HA-MuSK-Ubwt was concentrated. However, HA-MuSK-Ubmut positive cells exhibited no specific P4D1 staining. Apparently P4D1 failed to bind the Ubmut-chimera. As mentioned above, another

explanation might be that P4D1 stains monoubiquitin only weakly and thus only yields detectable signal upon overexpression of polyubiquitinated protein. Considering that all cells contain ubiquitinated proteins but were not stained with P4D1 supports this hypothesis.

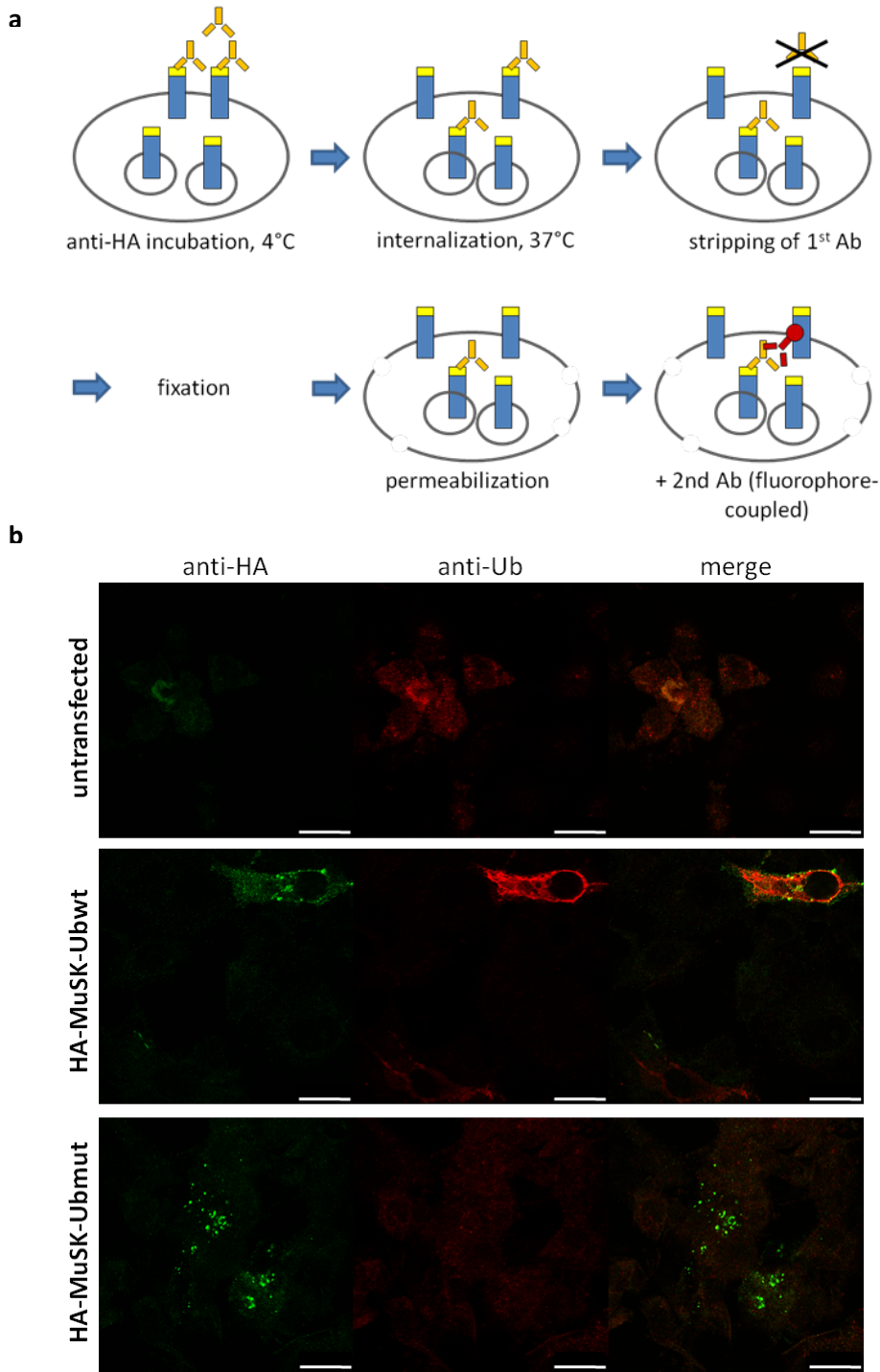


Figure 19 | Internalization of HA-MuSK-Ub chimeras and Detection of Ub | **a** | The scheme illustrates how internalization of HA-tagged MuSK molecules was tracked. | **b** | **Untransfected** COS-7 cells and cells expressing HA-MuSK-Ubwt and HA-MuSK-Ubmut were incubated with anti-HA at 4°C. Internalization was permitted by incubation at 37°C for 30min. Not internalized antibodies were removed from the surface by stripping. Cells were fixed and permeabilized. Internalized anti-HA was detected with a corresponding fluorophore-coupled secondary antibody (green). Ubiquitin was detected with antibodies specific for Ub (red). The rightmost panels represent overlays of the two stainings. For details see text. Scale bars, 25 μM.

3.2.2 Stability of HA-MuSK-Ubwt and HA-MuSK-Ubmut in COS-7 cells

The stability of wild-type HA-MuSK and the two HA-MuSK-Ub chimeras was assessed by the use of cycloheximide, a potent inhibitor of protein synthesis. The prevailing pool of proteins in the cells is degraded while no new protein is formed. Consequently, the total amount of each type of protein in a cell gradually decreases according to the half-life of the protein, which can be visualized by immunoblotting.

To determine the half-life of HA-MuSK, COS-7 cells expressing HA-MuSK were treated with cycloheximide for 5 to 120min, lysed and resolved via SDS-PAGE. The amount of intact HA-MuSK in each sample was quantified and compared to the amount of protein in untreated cells expressing HA-MuSK. The stability of the two MuSK-Ub chimeras was determined accordingly (Figure 20 and Figure 21). In the analyses EGFP was used as internal standard. It served as transfection control and as reference for quantification. COS-7 cells were always co-transfected with EGFP and the HA-MuSK variants. EGFP is highly stable with a half-life of more than 24h (Barrow et al., 2005). Thus, the total amount of EGFP should not decrease significantly after two hours of translational inhibition. Quantification of protein levels of the three HA-MuSK variants relative to EGFP therefore excluded errors resulting from inconsistent transfection efficiency and pipetting errors.

As demonstrated in Figure 20a HA-MuSK was detected as single specific band in immunoblots. In contrast, HA-MuSK-Ubwt and HA-MuSK-Ubmut occurred in distinct species, which had to be quantified individually. For the 85 kDa and the 95 kDa species of HA-MuSK-Ubmut and the weak HA-MuSK-Ubmut smear half-lives of about 70min, 90 - 100 min and 110 - 120 min were determined. Thus the 85 kDa and the 95 kDa species exhibited slightly higher stability than the wild-type form of HA-MuSK with a half-life of about 60 min whereas HA-MuSK-Ubmut smear was about twice as stable. The 85 kDa species of HA-MuSK-Ubwt was significantly less stable and had a half-life of about 15 - 20 min. In contrast, the amount of HA-MuSK-Ubwt polyubiquitin smear remained constant even after 60min of translational inhibition and only slightly decreased to around 60% after 2 h. This might suggest that the bona fide monoubiquitinated 85 kDa species of HA-MuSK-Ubwt is degraded far more quickly than the polyubiquitin variant or wild-type MuSK. However, both forms of HA-MuSK-Ubwt occur in one cell and prevalence of the two might be coupled to a chemical equilibrium, which might favor the polyubiquitinated state. Therefore, reduction of the 85 kDa species might not result from degradation but from ubiquitination of this form. It is suggested that the 85 kDa species of HA-MuSK is quickly ubiquitinated after protein synthesis. This might have also affected the determination of the half-life of polyubiquitinated HA-MuSK-Ubwt. Upon inhibition of protein synthesis, the 85 kDa species was probably ubiquitinated and moved to the pool polyubiquitinated protein during short incubation with cycloheximide. When most of the 85 kDa species was polyubiquitinated the degradation of polyubiquitinated HA-MuSK-Ubwt became apparent. This may have increased the apparent half-life of polyubiquitinated HA-MuSK-Ubwt in the analysis. Thus, the half-lives of HA-MuSK and the different species of the MuSK-Ub chimeras that were determined by cycloheximide experiments were verified by internalization experiments as reported in Section 3.2.3.

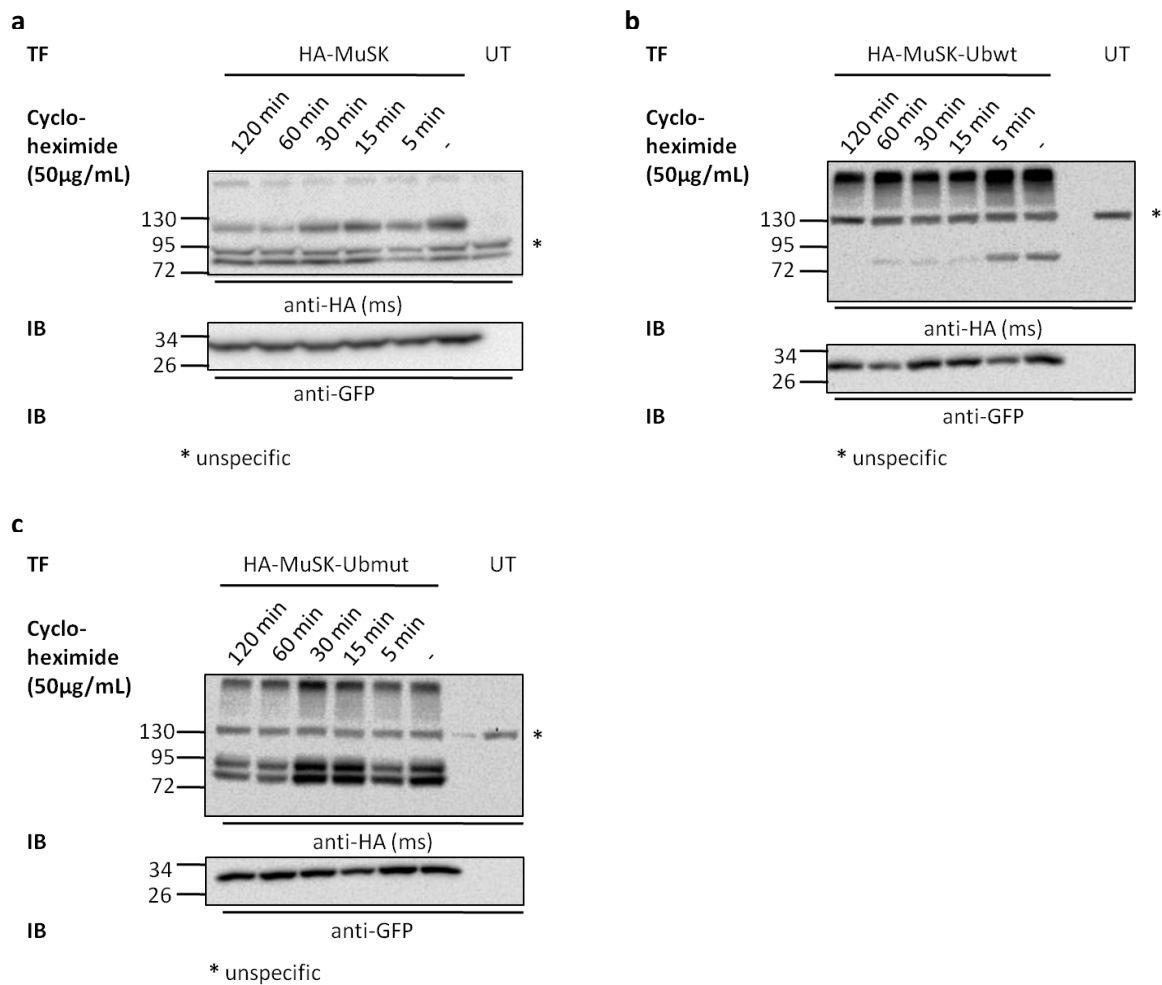


Figure 20 | Stability of HA-MuSK, HA-MuSK-Ubwt and HA-MuSK-Ubmut in COS-7 Cells | a-c | COS-7 cells expressing one of the three MuSK variants were treated with cycloheximide for 5, 15, 30, 60, 120 min or left untreated. The cells were lysed and the lysates were resolved via SDS-PAGE. Immunoblots were cut and the parts were probed for HA and GFP. Lysates of untransfected COS-7 cells (UT) resolved and blotted in parallel were used to identify unspecific bands (marked by an asterisk).

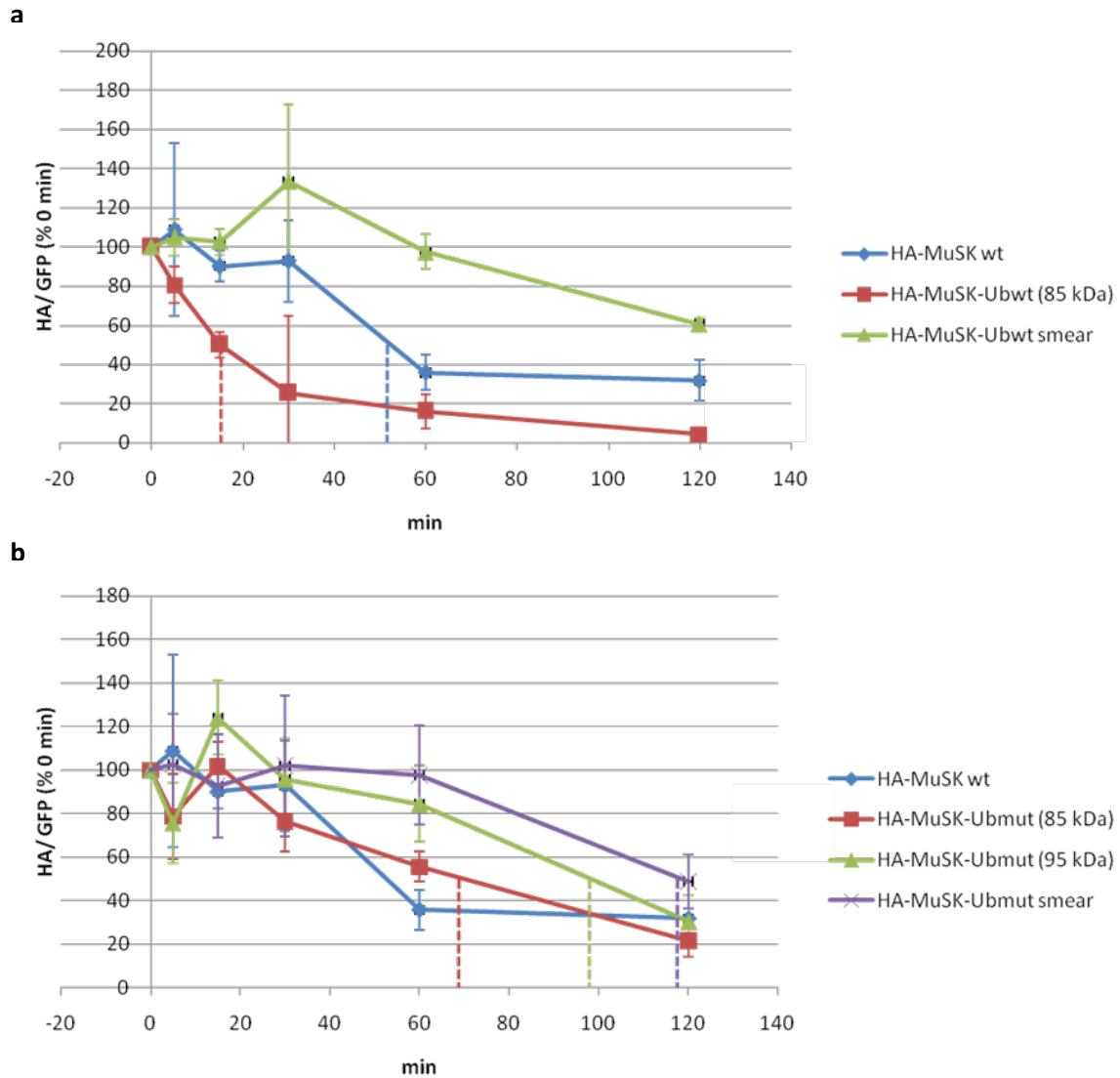


Figure 21 | Stability of HA-MuSK, HA-MuSK-Ubwt and HA-MuSK-Ubmut in COS-7 Cells HA and GFP signals were detected in immunoblots as depicted in Figure 20 and were quantified. HA/ GFP-ratios were calculated for each time point (HA-MuSK: n=3, HA-MuSK-Ubwt and HA-MuSK-Ubmut: n=4). The results of timepoints 5, 15, 30, 60 and 120 min of a timecourse were plotted in percent relative to the corresponding HA/ GFP-ratio at timepoint 0 min. The dashed lines indicate the approximate half-lives of HA-MuSK and the distinct species of HA-MuSK-Ubwt and HA-MuSK-Ubmut.

3.2.3 Internalization of HA-MuSK-Ubwt and HA-MuSK-Ubmut in COS-7 Cells

Ubiquitination has been described to influence internalization and intracellular targeting of proteins. Therefore, endocytosis and transport of HA-MuSK-Ubwt and HA-MuSK-Ubmut was further investigated via the internalization assay described in Section 3.2.1 and depicted in Figure 19a. Figure 22b illustrates internalization of HA-MuSK-Ubwt and HA-MuSK-Ubmut after 15 min and 60 min. After 15 min specific intracellular staining was observed for both chimeras. When cells expressing one of the MuSK-Ub-chimeras were fixed directly after antibody-incubation without allowing internalization (time point 0 min) only faint unspecific staining or no staining was visible. This demonstrates that antibodies bound to surface MuSK were efficiently removed by stripping. After 60 min both chimeras were found concentrated near the cell nucleus in vesicular structures. The experiment was repeated several times but significant difference in the speed of endocytosis or intracellular transport to the nucleus was not observed. This observation not consistent with the results described in Section 3.2.2 and suggests that both chimeras are comparably stable. However, it cannot be excluded that only

polyubiquitinated HA-MuSK-Ubwt was transported to the cell surface and was therefore visualized in the stainings. The 85 kDa species could have been degraded before being integrated into the plasma membrane or transformed into polyubiquitinated HA-MuSK-Ubwt. Unfortunately, it was not possible to discriminate the different species of HA-MuSK-Ubwt and HA-MuSK-Ubmut in this assay.

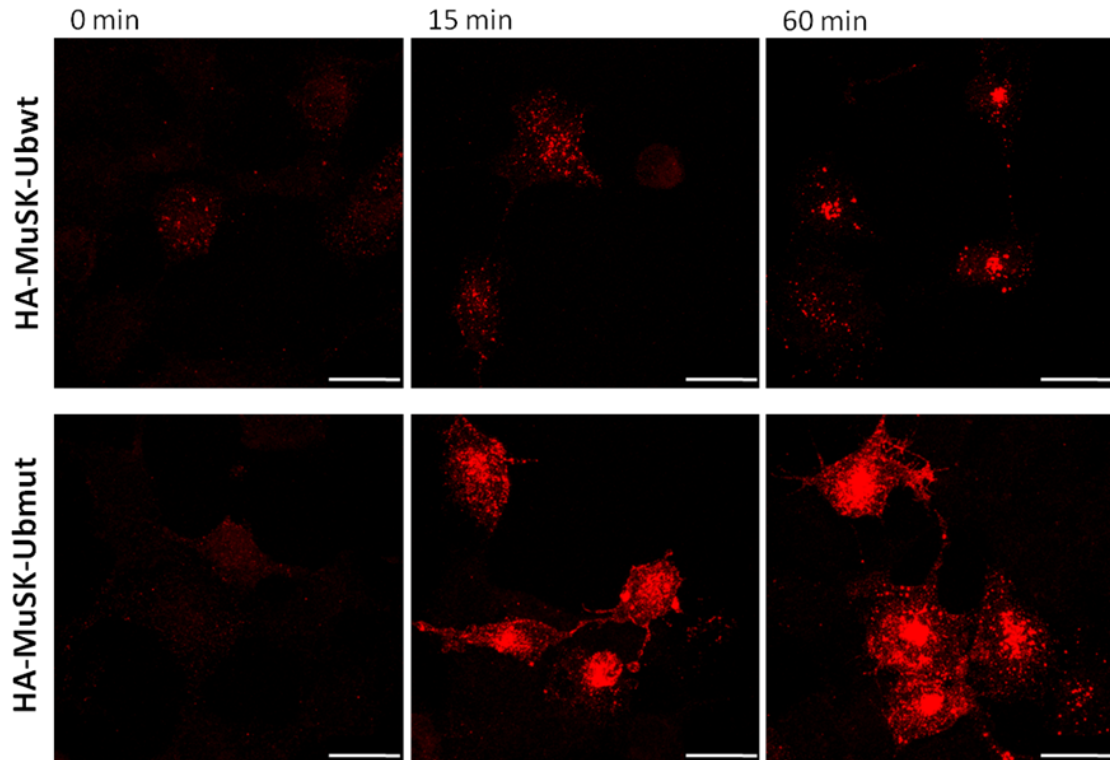


Figure 22| Internalization of HA-MuSK-Ubwt and HA-MuSK-Ubmut in COS-7 Cells COS-7 expressing HA-MuSK-Ubwt and HA-MuSK-Ubmut were incubated with anti-HA at 4°C. Then the cells were either directly stripped (0min) or MuSK internalization was permitted by incubation at 37°C for 15 min and 60 min. Scale bars, 25 µm.

3.2.4 Colocalization of HA-MuSK-Ubwt and HA-MuSK-Ubmut with Rab7 during Internalization

As the speed of internalization of HA-MuSK-Ubwt and HA-MuSK-Ubmut was comparable it was checked whether differential ubiquitination influenced which degradation pathway MuSK was targeted. For this purpose, HA-MuSK, HA-MuSK-Ubwt and HA-MuSK-Ubmut were co-transfected with Rab7, which is a marker of late endosomal vesicles. The same internalization experiment as described above was performed and localization of the three MuSK variants relative to Rab7 was examined (Figure 23). Again, no specific difference was observed between HA-MuSK and the two MuSK-Ub chimeras. After 60 min of internalization all three proteins co-localized with Rab7 in vesicular structures near the cell nucleus. HA-MuSK-Ubwt was sometimes found in smaller vesicles than the other two variants. However, this may have resulted from the lower expression level of HA-MuSK-Ubwt than from differences in internalization. Apparently, HA-MuSK, HA-MuSK-Ubwt and HA-MuSK-Ubmut are targeted to the endosomal-lysosomal degradation pathway with similar efficiency. This hypothesis needs to be verified in further experiments. HA-MuSK-Ubwt and HA-MuSK-Ubmut expressing cells were treated with the lysosomal inhibitors chloroquine and leupeptin and the proteasomal inhibitor MG132. However, breakdown of the chimeras was not successfully blocked even with a combination of lysosomal and proteasomal inhibitors (data not shown). Control

experiments with proteins for which the degradation pathway has been determined were not performed. Thus it is not certain whether the inhibitors were applied correctly.

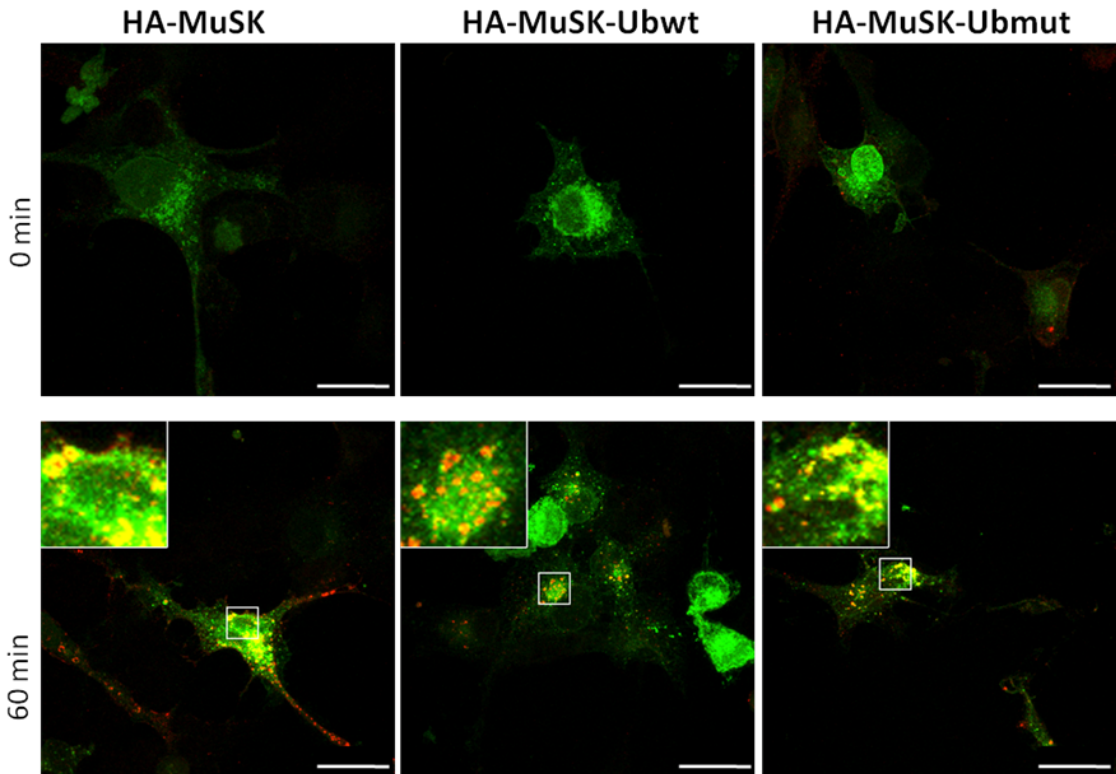


Figure 23| Internalization of HA-MuSK, HA-MuSK-Ubwt and HA-MuSK-Ubmut and Co-localization with Rab7 Rab7-EGFP was co-expressed with HA-MuSK, HA-MuSK-Ubwt or HA-MuSK-Ubmut in COS-7 cells. Surface MuSK was labeled by incubating the cells with anti-HA at 4°C. Then the cells were either directly stripped (0 min) or MuSK internalization was permitted by incubation at 37°C for 60 min. Scale bars, 25 µm.

4 Conclusion and Outlook

An inducible, heterologous model system for MuSK activation would be a useful tool for the investigation of MuSK internalization. But as reported, the establishment of such a system has been and might also in the future be hampered by several factors: First of all, heterologous expression of MuSK generally results in overexpression of the protein and strong basal autophosphorylation. It can be concluded from the performed experiments that transient transfection is for this reason inapt for the reconstitution of MuSK stimulation. Alternatively, MuSK and associated proteins could be stably expressed in non-muscle cells at a physiological expression level. However, the number of proteins that can be (stably) transfected into a cell is limited. Stable cell lines expressing e.g. MuSK, LRP4 and Dok7 as created by the group of S. Burden (Bergamin et al.) might allow studying the interplay of the three proteins. But it is unclear whether such cells are suitable for studying agrin-stimulated MuSK endocytosis. Possibly several additional muscle-specific proteins are needed for a functional MuSK internalization model system. In this case, the complexity of the agrin/ LRP4/MuSK-signaling cascade might exceed the possibilities of a heterologous cell system. But if MuSK, LRP4 and Dok7 combined with only a few other proteins were found to render MuSK responsive to agrin in non-muscle cells it would greatly enhance our understanding of the agrin signaling cascade.

Lacking a working model system, the results described in this thesis were gained by transfection of non-muscle cells with mutant MuSK and associated proteins. Kinase-inactive and kinase-active MuSK variants were used to determine the effects of MuSK phosphorylation on its endocytosis. Zhu et al. reported that stimulation of MuSK with agrin induces rapid internalization of the kinase, which is required for AChR clustering. However, constitutively active and inactive MuSK mutants were found to exhibit no differences in the extent or speed of internalization upon heterologous expression in COS-7 cells. This implies that regulation of MuSK internalization is independent of its kinase activity. Increased endocytosis in response to agrin might be a consequence of MuSK clustering by LRP4. This process cannot be reconstituted in heterologous cells so far. Thus, it would have to be assessed in muscle cells whether internalization of kinase-inactive MuSK changes upon agrin stimulation. The experiments described in this thesis were performed in COS-7 cells and thus do not exclude the possibility that phosphorylation regulates MuSK internalization in muscle cells. Such a scenario would suggest the existence of a muscle-specific regulator of internalization that interacts with phosphorylated MuSK. MuSK mutants carrying point mutations at individual phosphorylation target sites might help identifying such downstream signaling.

The second project discussed in this thesis concentrated on MuSK ubiquitination. As reported by Lu et al., MuSK expression on the muscle cell surface is regulated by ubiquitination in response to agrin-stimulation (Lu et al., 2007b). To further characterize the influence of ubiquitination on MuSK targeting MuSK-Ub chimeras comprising wild-type (HA-MuSK-Ubwt) or mutant Ub (HA-MuSK-Ubmut) were used. Whereas the HA-MuSK-Ubwt was predominantly polyubiquitinated, HA-MuSK-Ubmut occurred to the biggest part in bona fide monoubiquitinated or di-ubiquitinated forms. As reported, experiments concentrated on the internalization of the two chimeras in comparison to wild-type MuSK in COS-7 cells. It was found that both chimeras were internalized and degraded in a similar way as wild-type MuSK in spite of the deletion of the cytoplasmic MuSK domain and the different ubiquitination levels. The findings could not be supported with inhibitor experiments due to methodical problems. However, there was no indication that posttranslational modification by ubiquitin determines by which pathway MuSK is degraded. It has been suggested that activation-dependent ubiquitination of EGFR decreases clathrin-dependent EGFR endocytosis and thus EGFR

recycling and enhances clathrin-independent endocytosis and degradation of the receptor. The created MuSK-Ub chimeras provide a good tool to investigate whether recycling of MuSK is regulated accordingly. The internalization assay established in this thesis could be adapted for the purpose. However, it can be hypothesized that correct targeting of ubiquitinated MuSK (and of MuSK in general) is dependent on muscle-specific mechanisms. Regulation of MuSK breakdown in COS-7 did apparently not depend on the intracellular domain of MuSK, which was absent in MuSK-Ub chimeras. Therefore, HA-MuSK-Ubwt and HA-MuSK-Ubmut should be tested in muscle cells. This has not been done so far but might reveal differences in MuSK targeting that were not observed in heterologous cells.

5 Materials and Methods

5.1 Materials

Table 1 | Cell Culture Dishes

Cell Culture Dish	Supplier
10 cm	IWAKI
6 cm	NUNC
3.5 cm	IWAKI
6 well	IWAKI
12 well	NUNC
24 well	IWAKI
Cultube sterile culture tube with cap, polypropylene, 4 mL	Simport

5.2 Plasmids

Table 2 | Non-Commercial Plasmids

Plasmids	Gene	Vector	Source	Reference
C-Ag 4.8	C-terminal half of agrin, N-terminus deleted	pCMV	C. Fuhrer	(Ferns et al., 1993)
CMV/ HA-MuSK	N-terminally tagged MuSK	unknown, Amp+, CMV-promoter	R. Herbst	unpublished data
GFP-Rab7 wt	Rab7 wt	pEGFP-C1	C. Bucci	(Bucci et al., 2000)
pBabe/ TK Dok7-HA	C-terminally tagged Dok7	pBabe, TK promoter	S. Burden	(Kim et al., 2008)
pBabe/c-Fos Dok7-HA	C-terminally tagged Dok7	pBabe, c-Fos promoter	S. Burden	(Kim et al., 2008)
pBluescript/MuSK-Ubmut	MuSK-Ubmut (human Ub)	pcDNA3	R. Herbst	unpublished data
pcDNA3/ HAMUbmut	HA-MuSK-Ubiquitin-mut	pcDNA3	M. Schlauf	*
pcDNA3/ HAMUbwt	HA-MuSK-Ubiquitin-wt	pcDNA3	M. Schlauf	*
pcDNA3/ MuSK-HA	C-terminally tagged MuSK	pcDNA3	D. Hantai	(Chevessier et al., 2004)
pcDNA3/ SBP-MuSK	SBP(2x)-MuSK	pcDNA3	R. Herbst	unpublished data
pcDNA3/SBP-MuSK-K608A	SBP(2x)-MuSK-K608A	pcDNA3	M. Schlauf	*
pcDNA3/SBP-MuSK-LS745/746MT	SBP(2x)-MuSK-LS745/746MT	pcDNA3	M. Schlauf	*
pLitmus 29/MuSK-Ubwt	MuSK-Ubwt (sint Ub)	pcDNA3	R. Herbst	unpublished data
RSV/ Myc-MuSK	MuSK with Myc-tag near N-terminus	unknown, Amp+, RSV-promoter	R. Herbst	(Herbst and Burden, 2000)
RSV/ SBP-MuSK-K608A	SBP(4x)-MuSK-K608A	unknown, Amp+, RSV-promoter	S. Luiskandl	unpublished data
RSV/ SBP-MuSK-LS745/746MT	SBP(4x)-MuSK-LS745/746MT	unknown, Amp+, RSV-promoter	S. Luiskandl	unpublished data

* for details see Section 5.6.9

Table 3 | Commercial Plasmids

Vector	Source
pcDNA3	Invitrogen
pEGFP-N2	Clontech

5.3 Chemicals and Reagents

Table 4 | DNA Purification and Extraction Kits

Reagents	Supplier
GeneJET™ Plasmid Miniprep Kit	Fermentas Life Sciences
Pure Link™, HiPure Plasmid Midiprep Kit	invitrogen
GeneJET™ Gel Extraction Kit	Fermentas Life Sciences

Table 5 | Antibodies - Immunocytochemistry

Antibody	Supplier
Anti-HA antibody produced in rabbit	Sigma-Aldrich Co., Sigma
Anti-Rabbit IgG (of Donkey) Cy3 conjugated Affini Pure	Jackson ImmunoResearch Laboratories, Inc.
Anti-Rabbit IgG (of Donkey) DyLight488	Jackson ImmunoResearch Laboratories, Inc.
DYKDDDK Tag Antibody (anti-FLAG) (Biotinylated)	Cell Signaling Technology, Inc.
DyLight488-conjugated Streptavidin	Jackson ImmunoResearch Laboratories, Inc.
DyLight649-conjugated Streptavidin	Jackson ImmunoResearch Laboratories, Inc.
Monoclonal ANTI-c-MYC clone 9E10	Sigma-Aldrich Co., Sigma
Phosphotyrosin Mouse mAb (P-Tyr-100)	Cell Signaling Technology, Inc.
Ubiquitin (P4D1) Mouse mAb	Cell Signaling Technology, Inc.

Table 6 | Antibodies – Immunoblotting

Antibody	Supplier
Anti-Mouse IgG (of Goat), Peroxidase-conjugated	Jackson ImmunoResearch Laboratories, Inc.
Anti-Rabbit IgG (of Goat), Peroxidase-conjugated	Jackson ImmunoResearch Laboratories, Inc.
GFP (B-2)	Santa Cruz Biotechnology, Inc.
HA-Tag (6E2) Mouse mAb	Cell Signaling Technology, Inc.
Monoclonal ANTI-c-MYC clone 9E10	Sigma-Aldrich Co., Sigma
Monoclonal ANTI-FLAG M2, Clone M2 (ms)	Sigma-Aldrich Co., Sigma
MuSK-Antibody (Rb α MuSK) polyclonal	C. Fuhrer, Ph.D., Zürich
Phosphotyrosin Mouse mAb (P-Tyr-100) *	Cell Signaling Technology, Inc.
p-Tyr (PY99) *	Santa Cruz Biotechnology, Inc.
Purified Mouse Anti-Actin Ab-5	BD Transduction Laboratories
Ubiquitin (P4D1) Mouse mAb	Cell Signaling Technology, Inc.

* to detect pTyr in immunoblotting a mix of PY99 and P-Tyr-100 diluted in 5 % BSA/ TBS-T was used

Table 7 | List of Chemicals and Reagents

Reagent	Supplier
Acetic acid glacial (100%)	Carl Roth GmbH + Co. KG
Aprotinin	Carl Roth GmbH + Co. KG
BES	Carl Roth GmbH + Co. KG
Bromphenol Blue	Carl Roth GmbH + Co. KG
Chloroquine	AppliChem GmbH
Cycloheximide	Sigma-Aldrich Co., Fluka Analytical
DMEM with 4.5g/L-Glucose	Lonza Group Ltd
EGTA	Carl Roth GmbH + Co.
FBS	PAA Laboratories GmbH
Glycerol	Carl Roth GmbH + Co.
Glycine	Carl Roth GmbH + Co. KG
HEPES	Carl Roth GmbH + Co. KG
Igepal CA 630 (NP-40)	Sigma-Aldrich Co., Fluka Analytical
KCl	Carl Roth GmbH + Co. KG
KH ₂ PO ₄	Carl Roth GmbH + Co. KG
Leupeptin	Roche Diagnostics GmbH
Milk powder	Carl Roth GmbH + Co. KG
Mowiol 4-88	Carl Roth GmbH + Co. KG
Na ₂ HPO ₄	Carl Roth GmbH + Co. KG
Na ₂ HPO ₄ ·2H ₂ O	Carl Roth GmbH + Co. KG
NaCl	Carl Roth GmbH + Co. KG
Na-Desoxycholat	Sigma-Aldrich Co., Fluka Analytical
NaF	Sigma-Aldrich Co.
NaOH	Carl Roth GmbH + Co. KG
OptDMEM I + GlutaMAX -I (1 x)	Life Technologies, Invitrogen, GIBCO
Page Ruler Prestained Protein Ladder #SM0671	Fermentas GmbH
Penicillin/ Streptomycin	PAA Laboratories GmbH
Pepstatin A	US biological
PFA	Sigma-Aldrich Co., Fluka Analytical
Phenylmethylsulfonylfluorid (PMSF)	Carl Roth GmbH + Co. KG
Protein A agarose beads	Roche Diagnostics GmbH
Protein G agarose beads	Roche Diagnostics GmbH
Puromycin	Sigma-Aldrich Co.
Restriction Enzymes	Fermentas Life Sciences
Rotiphorese Gel 40 (40% acrylamide)	Carl Roth GmbH + Co KG
Shrimp Alkaline Phosphatase, 1u/μL	Fermentas GmbH
Sodium dodecyl sulfate (SDS)	SERVA Electrophoresis GmbH
Sodium Orthovanadate	Sigma-Aldrich Co.
β-mercaptoethanol	Carl Roth GmbH + Co. KG
Streptavidin Agarose	Merck KGaA, Novagen
T4 ligase, 1000u, 5u/μL	Fermentas GmbH
TEA	Sigma-Aldrich Co., Fluka Analytical

Reagent	Supplier
Tris-(hydroxymethyl)-aminomethan (Tris)	Carl Roth GmbH + Co. KG
Tris-(hydroxymethyl)-aminomethanhydrochlorid (Tris-HCl)	Carl Roth GmbH + Co. KG
Triton X-100	Carl Roth GmbH + Co. KG
Trypsin-EDTA	PAA Laboratories GmbH
Turbofect in vitro Transfection Reagent	Fermentas GmbH
Tween 20	Carl Roth GmbH + Co. KG
Z-Leu-Leu-Leu-al (MG132)	Sigma-Aldrich Co.

5.4 Solutions and Buffers

Table 8 | 10 x PBS

Reagent	Concentration
NaCl	1.37 M
KCl	27 M
Na ₂ HPO ₄ ·2 H ₂ O	43 M
KH ₂ PO ₄	14 M

To yield a 1 x PBS working solution the 10 x PBS stock solution was diluted 1:10. The working solution had a pH of about 7.3.

Table 9 | 4% PFA/ PBS

Reagent	Amount	Concentration
PFA	0.8 g	4 %
1 x PBS	20 mL	
0.5 M NaOH	50 µL	1.25 mM

0.8 g PFA were dissolved in 20mL 1 x PBS and 50 µL 0.5 M NaOH were added. The solution was heated to 50-100°C and stirred until the PFA had completely dissolved, then filtered with a folded filter (ROTH Art. CA16.1, Rotilabo[®]-Faltenfilter, qualitativ) and stored at 4°C. The solution had to be pH-neutral, which was checked with pH-indicator strips. 4 % PFA/PBS wasn't used for longer than two weeks after preparation.

Table 10 | 4 x SDS Loading Buffer

Reagent	Amount	Concentration
1 M Tris-Cl, pH 6.8	2.4 mL	240 mM
100 % β-mercaptoethanol	1 mL	8 %
20 % SDS	2 mL	8 %
100 % glycerol	4 mL	40 %
ddH ₂ O	0.6 mL	
bromphenol blue	a few grains	

Table 11| 50 x TAE

Reagent	M _w (g/mol)	Amount
Tris	121.14 g/mol	242 g
Acetic Acid glacial (100 %)		57.1 mL
0.5M EDTA (pH 8.0)		100 mL
dH ₂ O		adjusted to 1 L

5.5 Cell Culture

5.5.1 Cell Culture Conditions

Table 12| HEK293T Growth Medium

Reagent	Concentration
DMEM	
FBS	10 %
Pen/Strep	1 x

Table 13| Cell Types and Culture Conditions

Cell Type	Culture Conditions
HEK293T	HEK293T growth medium, 37°C, 5 % CO ₂
COS-7	HEK293T growth medium, 37°C, 5 % CO ₂
HeLa	HEK293T growth medium, 37°C, 5 % CO ₂
Phoenix	HEK293T growth medium, 37°C, 5 % CO ₂
Phoenix A	HEK293T growth medium, 37°C, 5 % CO ₂
COS-7 TK Dok7-HA	HEK293T growth medium + 1µg/mL puromycine, 37°C, 5 % CO ₂
COS-7 c-Fos Dok7-HA	HEK293T growth medium + 1µg/mL puromycine, 37°C, 5 % CO ₂
HeLa TK Dok7-HA	HEK293T growth medium + 0.5µg/mL puromycine, 37°C, 5 % CO ₂
HeLa c-Fos Dok7-HA	HEK293T growth medium + 0.5µg/mL puromycine, 37°C, 5 % CO ₂

5.5.2 Preparation of Agrin/ OptiMEM

Agrin/ OptiMEM was not prepared for this diploma thesis but was already available. The following protocol has the purpose to inform the reader on the nature of the agrin solution that was used. Details concerning e.g. the cultivation of myotubes, which were employed to test the agrin solution, will not be explained in this thesis, as neither muscle cells nor muscle cell precursors were used for any other experiments.

Protocol:

One day before transfection HEK293T cells were plated in a 10 cm dish at a density of 1×10^6 cells/ 10 cm dish. The cells were transfected with C-Ag 4.8 (= an expression vector coding for the C-terminal half of agrin) as explained in Section 5.5.5.1 for 15 h. To stop the transfection, the medium containing the transfection mix was aspirated, the cells were washed with PBS once and OptiMEM + 1 x Pen/ Strep + 5 % FBS was added (7 mL/ 10 cm dish). The cells were incubated at 37°C to allow synthesis of agrin and its secretion into the growth medium. 48h after medium change the growth medium was taken off and cells and cell debris were removed from the medium (herein after referred to as 'agrin/ OptiMEM') by centrifugation at 389 rcf for 5 min. To determine the concentration of agrin/ OptiMEM that was required for MuSK-activation experiments, myotubes

were treated with increasing concentrations of the agrin solution and MuSK phosphorylation levels were assessed biochemically (see Section 5.6.7). The lowest concentration, at which maximal MuSK activation was detected, was used in all further experiments.

5.5.3 Freezing Cells

Cells were trypsinized and pelleted by centrifugation at 389 rcf for 4 min. The supernatant was aspirated and the cells were resuspended in freezing medium containing DMSO (Table 14), quickly transferred to cryotubes (1-1.5 mL/ tube) and frozen at -80°C. If the cells were supposed to be stored for a longer period of time they were transferred to liquid N₂ tanks 24 h after initial freezing. Otherwise they were kept at -80°C until further use.

Reagent	Concentration
DMEM	
FBS	20 %
Pen/Strep	1 x
DMSO	10 %

5.5.4 Thawing Cells

If fresh cells were needed a cryotube containing a frozen cell suspension was incubated in a water bath at 37°C to ensure quick thawing. As soon as the suspension was nearly completely thawed the tube was transferred into the sterile laminar airflow work bench and the cell suspension (approx. 1-1.5 mL) was quickly pipetted into 5-6 mL fresh growth medium. To remove DMSO the cells were pelleted by centrifugation at 389 rcf for 4 min, the supernatant was removed and the cells were resuspended in fresh growth medium and plated in an appropriate concentration.

5.5.5 Transient Transfection

5.5.5.1 CaCl₂/ BBS–Transfection

Reagents:

Stock solutions were prepared, autoclaved or filter-sterilized according to Table 15 and stored at RT.

Solution	Concentration
CaCl ₂ (autoclaved or filter-sterilized)	2.5 M
NaCl (autoclaved)	5 M
BES	1 M
Na ₂ HPO ₄	1 M

The stock solutions were used to prepare working solutions 0.25 M CaCl₂ and 2 x BBS (Table 16 and Table 17). Usually 100 mL of each working solution were prepared, filter-sterilized in a sterile laminar airflow work bench, aliquoted (10 x 10 mL) and stored at -20°C.

Table 16| Preparation of 0.25 M CaCl₂

Solution	Volume
2.5 M CaCl ₂	10 mL
ddH ₂ O (autoclaved)	90 mL

Table 17| Preparation of 2 x BBS

Solution	Volume
ddH ₂ O (autoclaved)	80 mL
5 M NaCl	5.6 mL
1 M BES	5 mL
1 M Na ₂ HPO ₄	150 µL
The pH-value of the working solution was adjusted to 6.95 ± 0.02 with HCl.	
ddH ₂ O	adjusted to 100 mL

15-30 min before use aliquots of the working solutions were thawed in a water bath at RT.

Protocol:

For the number of plated cells, volumes of 0.25 M CaCl₂, 2 x BBS and growth medium and amounts of DNA required for individual dish sizes see Table 18.

Preparation of cells: One day before transfection cells were trypsinized and plated in defined cell number in normal growth medium. The volume of growth medium in the culture dish was adjusted depending on the dish size.

Transfection: DNA was pipetted into a 4mL sterile culture tube. 0.25 M CaCl₂ was added drop wise and the solution was mixed by snipping against the tube. 2 x BBS was added drop wise under vortexing and the mix was incubated at RT for 13-15 min to allow DNA/ Ca₃(PO₄)₂ precipitates to form. Following incubation the transfection mix was pipetted drop wise into the growth medium and the cells were incubated at 37°C, 5 % CO₂ for 8 h (over day-transfection) or 15 h (over night-transfection). Finally the supernatant (growth medium + DNA/ CaCl₂/ BBS) was aspirated from the dish, fresh growth medium was added and the cells were incubated at 37°C, 5 % CO₂ for 24 h.

(In case that more than one transfection was performed in parallel, first DNA was pipetted into all tubes. Then CaCl₂ was added to all tubes. A timer was started and 2 x BBS was added to the tubes one after the other in equal time intervals of e.g. 30 sec. Addition of the mixtures to the plates was performed 13 min after addition of 2 x BBS to the first tube in the same time intervals.)

Table 18| CaCl₂/ BBS-Transfection: Volumes and Amounts of Reagents Required for Distinct Dish Sizes

Dish Size	Cell Number	Growth Medium	DNA	0,25 M CaCl ₂	2 x BBS
10 cm	0.8 - 1.0 x 10 ⁶	10 mL	20 µg	875 µL	875 µL
6 cm	0.4 - 0.5 x 10 ⁶	5 mL	10 µg	437.5 µL	437.5 µL
1 well (6-well plate)	0.7 - 1.0 x 10 ⁵	2 mL	4 µg	175 µL	175 µL
1 well (12-well plate)	cells were plated on coverslips in a 10cm dish (0.8 - 1.0 x 10 ⁶ / 10 cm dish, ~12 coverslips/ 10 cm dish)	1.7 mL	3 µg	145 µL	145 µL

5.5.5.2 Turbofect-Transfection

Reagents:

Table 19| Reagents for Turbofect-Transfection

Reagent	Supplier
Turbofect™ in vitro Transfection Reagent *	Fermentas
OPTI-MEM I + GlutaMAX™-I (1 x)**	GIBCO invitrogen
DMEM with 4.5 g/L Glucose with L-Glutamine	LONZA

* further called Turbofect, ** further called OPTI-MEM

Protocol:

For the the number of plated cells, the volumes of DMEM, Opti-MEM and Turbofect and the amounts of DNA required for individual dish sizes see Table 20.

Preparation of cells: One day before transfection cells were trypsinized and plated in defined number in normal growth medium. Shortly before transfection, growth medium was aspirated, cells were washed with PBS once and the appropriate volume of DMEM was added.

Transfection: DNA was pipetted into a 4mL sterile culture tube. OPTI-MEM was added drop wise and the solution was mixed briefly by snipping against the tube. Turbofect was added and the mixture was again mixed thoroughly. The transfection mix was incubated at RT for 17.5 min and then added to the cell culture dish drop wise. The cells were incubated at 37°C, 5 % CO₂ for 3h to allow uptake of DNA. (If the transfection efficiency was found to be low and the cells were not too sensitive to Turbofect-treatment the incubation time was prolonged.) Following incubation, the supernatant (DMEM + DNA/ OPTI-MEM /Turbofect) was aspirated from the dish, the cells were washed with growth medium once and then incubated in fresh growth medium at 37°C, 5 % CO₂ for 20-24 h (herein after referred to as 'medium change').

Table 20| Turbofect-Transfection: Volumes and Amounts of Reagents Required for Distinct Dish Sizes

Dish Size	Cell Number	DMEM	DNA	OPTI-MEM	Turbofect
6 cm	0.4 - 0.5 x 10 ⁶	6 mL	10 µg	900 µL	7.5 µL
1 well (6-well plate)	0.7 - 1.0 x 10 ⁵	4 mL	6 µg	600 µL	5 µL
1 well (12-well plate)	cells were plated on coverslips in a 10cm dish (0.8 - 1.0 x 10 ⁶ / 10 cm dish, ~12 coverslips/ 10 cm dish)	2 mL	3 µg	300 µL	2.5 µL

5.5.6 Stable Transfection

Stable transfections of COS-7 and HeLa cells were performed. Phoenix A cells were used as virus particle producer cells. The target cells were infected twice to increase the transfection efficiency. To create negative controls Phoenix A cells were transfected with CaCl₂/ BBS-mix without DNA. Hence, these Phoenix A cells shouldn't be able to produce virus particles. The supernatant of the cells was used for the 'infection' of negative control cells. Negative controls should therefore not be resistant to selection reagent.

Preparation of producer cells (Day 0): One day before transfection Phoenix A cells were split and plated in 10cm dishes, 1.1 x 10⁶ cells/ 10 cm dish.

Transfection of producer cells (Day 1 & 2): Phoenix A cells were transfected with plasmid via CaCl₂/ BBS-Transfection o/n for 15 h as explained in Section 5.5.5.1. On Day 2 the medium of the transfected Phoenix A cells was aspirated and the cells were incubated in fresh growth medium (7 mL/ 10 cm dish).

Preparation of target cells (Day 2): Target cells for stable transfections (COS-7, HeLa) were plated in 6-well plates, 0,7 x 10⁵ cells/ well.

Harvest of virus particles and first infection of target cells (Day 3):

Harvest: 24 h after medium change the supernatant containing virus particles was aspirated from the producer cells and transferred to a 15 mL Falcon tube. Fresh growth medium was added to producer cells and cells were incubated at 37°C, 5 % CO₂ for further 24 h. To remove cell debris the harvested supernatant was centrifuged at 1559 rcf for 10 min and transferred to a fresh Falcon tube.

Infection: The growth medium of the target cells was aspirated and the supernatant harvested from the producer cells (1.5 mL/ well of a 6- well plate) mixed with polybrene (5 µg/mL) were added. Cells were centrifuged at 18 rcf, 32°C for 1 h, and incubated at 37°C, 5 % CO₂ for further 5 h. Then the supernatant was removed, the cells were washed with PBS once and incubated in normal growth medium, 37°C, 5 % CO₂ o/n (herein after referred to as 'medium change').

Harvest of virus particles and second infection of target cells (Day 4): Harvest and Infection were repeated as explained for Day 3. Phoenix A producer cells were discarded after the second harvest.

Start of selection (Day 5 & 6): More than 24 h after the last medium change the infected target cells were split to 10 cm dishes and incubated in growth medium containing the selection reagent puromycin (starting concentrations: COS-7: 2 µg/mL, HeLa: 1 µg/mL).

Cultivation (After Day 6): Control cells stopped growing two to three days after the start of puromycin treatment if puromycin treatment was selective enough. After several days of selection the puromycin concentration was decreased to reduce cellular stress (COS-7: 1.0 µg/mL, HeLa: 0.5 µg/mL).

5.5.7 Agrin-Stimulation

Normal growth medium was removed and the cells were washed with PBS once. In order to deprive the cells of nutrients and make them more sensitive to agrin, the cells were incubated in a defined volume of DMEM (Table 21) at 37°C, 5 %CO₂ for 3 h. Following this 'starvation', agrin/ OptiMEM was added in the tested concentration (see Section 5.5.2) and the cells were incubated at 37°C, 5 % CO₂ for another 30 min to 1 h.

Table 21| Starvation: Volume of DMEM required for different dish sizes

Dish size	DMEM
10 cm	4 mL
6 cm	2 mL

Starvation of transiently transfected cells was started 20 h - 20.5 h after medium change to allow lysis of cells 24 h after medium change.

5.5.8 Antibody-Mediated Stimulation of MuSK

Cells were transfected with an N-terminally tagged MuSK construct (HA-MuSK, Myc-MuSK) as explained in Section 5.5.5.1 over day for 8 h. The cells were starved as explained for agrin-stimulation in 5.5.7 for 3 h, starting 20 - 20.5 h after medium change. 3 mL instead of 4 mL DMEM was added per 10 cm dish to reduce the amount of required antibody in the next step. In order to activate MuSK 50-100 nM antibody (= 7.5 - 15 µg/mL) specific for the N-terminal tag of the used MuSK variant (anti-HA, anti-c-Myc) was added and cells were incubated at 37°C, 5 % CO₂ for 30 min - 1 h. Cells were lysed as explained in Section 5.6.1 24 h after medium change.

5.5.9 Immunocytochemistry

5.5.9.1 Conventional Immunocytochemistry

(Transfection: For detection of heterologously expressed proteins cells were transfected with the protein(s) of interest via CaCl₂/ BBS- or Turbofect-transfection as explained in Section 5.5.5 and immunocytochemical stainings were performed 20 - 24 h after medium change.)

Washing: Growth medium was aspirated and the cells were carefully washed with cold PBS 3 times (3 x).

Fixation: To fix the cells they were incubated in 4 % PFA at RT for 10 min.

Permeabilization: Permeabilization was achieved by incubation of the cells in 0.1 % Triton/PBS at RT for 5 min. (This step was skipped, if only surface protein should be stained.)

Washing: The cells were washed 3 x by incubation in PBS (RT) for 5 min.

Blocking: To block unspecific binding sites, the permeabilized or unpermeabilized cells were incubated in 10 % FBS/ PBS at RT for 20 min.

Primary antibody: The protein of interest was detected by incubating the cells in primary antibody dilution at RT for 1 h. For this purpose, the coverslips were put upside down on droplets of 20 μ L of antibody-dilution. Subsequently the coverslips were washed by dipping into PBS 3 x.

Secondary antibody: Bound primary antibody was detected by incubating the cells in secondary antibody dilution (anti-rbt-Cy3, 1:800 in 10 % FBS/PBS) as explained for the primary antibody incubation at RT for 45 min. Subsequently the coverslips were washed by dipping into PBS 3 x.

Mounting: The coverslips were mounted on glass slides and the surplus of mounting medium was carefully aspirated (avoiding moving of the coverslip) to ensure that the coverslips were pressed tightly onto the glass slide. Mowiol was used as mounting medium. The mounted coverslips were kept at RT in the dark for 1 h to allow the mounting medium to harden. Afterwards the glass slides were stored at 4°C in the dark to be analyzed via fluorescence or confocal fluorescence microscopy.

5.5.9.2 Surface Protein Internalization Assay (Streptavidin)

Streptavidin incubation: Living cells were starved by incubation in cold DMEM at 4°C for 30 min and then incubated with fluorophore-coupled streptavidin diluted 1:1000 in DMEM without supplements (cold!) at 4°C for further 30 min (280 μ L/ well of 12-well plate). The cells were washed once - with cold PBS if the cells were immediately used for fixation or in normal GM if internalization was allowed in the next step. (For this purpose, the coverslips were transferred from the 12-well plate to pre-chilled 3.5 mm dishes containing cold PBS or cold, normal GM. The 12-well plate and the 3.5 mm dishes were kept on ice during the whole procedure. PBS or GM was aspirated from the 3.5 mm dishes and replaced depending on the next step. If the cells should exhibit no internalization – in the case of time point 0min and stripping positive and negative controls– the cells were directly subject to fixation after this step.)

Internalization: After washing, the cells were incubated in normal GM at 37°C to allow internalization of surface proteins. The internalization was stopped at defined time points by putting the dishes on ice and washing them with cold PBS 3 x. (Commonly tested durations of internalization were 5, 15, 30, 60 and 120 min.)

Fixation, permeabilization and further stainings were performed as explained in Section 5.5.9.1.

5.5.9.3 Surface Protein Internalization Assay (Antibody)

(The protocol was adapted from (Sharma et al., ; Tanowitz and von Zastrow, 2003) and (Cao et al., 1999).)

Primary antibody incubation (Step #1): Living cells were incubated with anti-HA (rbt, Sigma) diluted 1:100 in DMEM without supplements (cold!) at 4°C for 20min (280 μ L/ well of 12-well plate). The

cells were washed once - with cold PBS if the cells were immediately used for stripping and fixation or in normal GM if internalization was allowed in the next step. (For this purpose, the coverslips were transferred from the 12-well plate to pre-chilled 3.5 mm dishes containing cold PBS or cold, normal GM. The 12-well plate and the 3.5 mm dishes were kept on ice during the whole procedure. PBS or GM was aspirated from the 3.5 mm dishes and replaced depending on the next step. If the cells should exhibit no internalization – in the case of time point 0 min and stripping positive and negative controls– the cells were directly subject to stripping (Step #3) after this step.)

Internalization (Step #2): After washing, the cells were incubated in normal GM at 37°C to allow internalization of surface proteins. The internalization was stopped at defined time points by putting the dishes on ice and washing them with cold PBS once. (Commonly tested durations of internalization for the proteins HA-MuSK, HA-MuSK-Ubwt and HA-MuSK-Ubmut were 5, 15, 30, 60 and 120 min.)

Antibody Stripping (Step #3): To detach primary antibody from surface protein not internalized in the previous step, the cells were incubated in cold PBS (pH 2.5) (stripping buffer) on a shaker, shaking at moderate speed, 2 x for 4 min. The stripping buffer was changed after the first 4 min. After stripping, the cells were washed with cold PBS 3 x to remove the stripping buffer.

(If stripping wasn't desired – in case of "stripping negative control" for example – the cells were treated with PBS (pH-neutral) instead of PBS (pH 2.5) for 2 x 4 min.)

Fixation (Step #4): To fix the cells, they were incubated in 4 % PFA at RT for 10 min.(The following step was skipped, if permeabilization wasn't intended at this stage – e.g. in the case of stripping positive and negative control.)

Permeabilization & Blocking (Step #5): Permeabilization was achieved by incubation of the cells in 0,1% Triton/ PBS at RT for 5min. Afterwards the cells were washed with PBS (RT) 3 x for 5min. To block unspecific binding sites permeabilized cells were incubated in 10% FBS/ PBS at RT for 20min.

Secondary antibody (Step #6): Anti-HA antibody bound to internalized protein was stained by incubating cells in secondary antibody dilution (anti-rbt-Cy3, 1:800 in 10 % FBS/ PBS) at RT for 45 min. For this, coverslips were put upside down on droplets of 20 µL of antibody-dilution. Subsequently coverslips were washed by dipping into PBS 3 x.

Permeabilization and Blocking (Step #1a): see Step#5

Primary antibody (Step #2a): Total protein of interest was detected by incubating cells in primary antibody dilution (anti-HA (rbt), 1:100 in 10 % FBS/PBS) as explained in Step#6 but for 1h.

Secondary antibody (Step #3a): Anti-HA antibody bound to total protein of interest was stained by incubating cells in different 2nd antibody dilution than in Step#6 (anti-rbt-488, 1:500 in 10 % FBS/ PBS) as explained in Step #6 .

Mounting (Step #7): Coverslips were mounted on glass slides and surplus of mounting medium was carefully aspirated (avoiding moving of coverslip) to ensure that coverslips were pressed tightly onto the glass slide. Mowiol was used as mounting medium. Mounted coverslips were kept at RT in the

dark for 1 h to allow the mounting medium to harden. Then glass slides were stored at 4°C in the dark to be analyzed via fluorescence or confocal fluorescence microscopy.

Table 22 | Scheme 1 for sample antibody internalization-experiment

Coverslip #	Name	Description
1	stripping neg. control	cells transfected with protein of interest and treated with primary antibody after 0 min of internalization (no internalization), <u>not</u> subject to antibody stripping, not permeabilized
2	stripping pos. control	cells transfected with protein of interest and treated with primary antibody after 0 min of internalization (no internalization), subject to antibody stripping, not permeabilized
3	timepoint 0 min	cells transfected with protein of interest and treated with primary antibody after 0 min of internalization (no internalization)
4	timepoint 0 min	cells transfected with protein of interest and treated with primary antibody after 5 min of internalization
5	timepoint 0 min	cells transfected with protein of interest and treated with primary antibody after 15 min of internalization
6	timepoint 0 min	cells transfected with protein of interest and treated with primary antibody after 30 min of internalization
7	timepoint 0 min	cells transfected with protein of interest and treated with primary antibody after 60 min of internalization
8	timepoint 0 min	cells transfected with protein of interest and treated with primary antibody after 120 min of internalization
9	negative control	untransfected cells treated with secondary but not with primary antibody, duration of internalization step not relevant, as no antibody can be internalized

Table 23 | Scheme 2 for sample antibody internalization-experiment

coverslip#\step	(transfection with protein of interest)	#1 antibody incubation	#2 internalization	#3 antibody stripping	#4 fixation	#5 permeabilization & blocking	#6 secondary antibody
1	+	+	-	-	+	-	+
2	+	+	-	+	+	-	+
3	+	+	-	+	+	+	+
4	+	+	5min	+	+	+	+
5	+	+	15min	+	+	+	+
6	+	+	30min	+	+	+	+
7	+	+	60min	+	+	+	+
8	+	+	120min	+	+	+	+
9	-	-	optional	+	+	+	+

Coverslips ‘stripping negative control’ and ‘stripping positive control’ should demonstrate the efficiency of antibody stripping. The cells on the two coverslips were not permeabilized. After incubation of the living cells on the coverslips in primary antibody, ‘stripping positive control’ was subject to Step #3, antibody stripping, by which all bound antibody should be detached from the target protein on the cell surface. ‘Stripping negative control’ was treated with PBS 2 x for 4 min instead of stripping reagent. The primary antibody should remain bound to surface target protein. After fixation, the cells were not permeabilized. Therefore only surface-bound primary antibody should be stained in the subsequent staining with fluorophore 1-coupled secondary antibody (, in this case anti-rbt-Cy3). However, target protein-positive but successfully stripped cells would now not be possible to discriminate from untransfected cells anymore. As a consequence it was necessary to identify target protein-positive cells in a second round of staining. Following the surface staining,

cells were therefore permeabilized, blocked and treated with the same primary antibody as in the first round of staining (anti-HA (rbt)). This time the antibody should bind all free epitopes on the cell surface as well as intracellular target protein. Incubation with secondary antibody carrying a different fluorophore 2 (in this case anti-rbt-488) should bind this primary antibody and should make it possible to discriminate between anti-HA antibody bound in the first and second round of staining. If stripping has been successful, on the 'stripping positive control' HA-tag-positive cells identified in the second staining should exhibit no specific fluorophore 1-staining originating from the first staining round. Contrarily, HA-tag-positive cells on the 'stripping negative control' should show clear surface staining for fluorophore 1.

5.6 Molecular Biology

5.6.1 Cell Lysis

Cells were placed on ice and washed with cold PBS three times. Then appropriate volume (see Table 26) of lysis buffer containing protease inhibitors, RIPA-buffer + inhibitors or NP-40-buffer + inhibitors, was added. (As protease inhibitors are not stable after dilution in lysis buffer, the inhibitors were added only shortly (~10 min) before washing of the cells was started. For this purpose, the required volume of lysis buffer was aliquoted and inhibitors were added according to their recommended dilution factor as listed in Table 27. PMSF was added last, the mixture was vortexed immediately afterwards and put on ice until use.) The dishes were incubated on a shaker at moderate speed, at 4°C, for 25 - 30 min. Following incubation, the cells were scraped from the dish with a rubber scraper and the lysate was transferred to a prechilled 1.5 mL Eppendorff tube. Cell debris was pelleted by centrifugation at 16,100 rcf for 10 min. The supernatant (=lysate) was transferred to a fresh tube and was used directly for immunoblotting, subject to immunoprecipitation (Section 5.6.3) or pull-down (5.6.4) or frozen in liquid N₂ and stored at -20 or -80°C.

Table 24 | RIPA-Buffer

Reagent	Concentration
Tris-HCl (pH 7,5)	50 mM
NaCl	150 mM
NP-40	1 % (v/v)
Na-Desoxycholat	0,5 % (w/v)
NaF	50 mM

Table 25 | NP-40-Buffer

Reagent	Concentration
NP40	1 %
EGTA	5 mM
NaCl	50 mM
TEA pH 7.5	30 mM
NaF	50 mM

Table 26 | Volume of lysis buffer required for individual dish sizes

Dish size	Volume
10 cm dish	600 µL
6 cm dish	250-300 µL

Table 27 | Proteinase Inhibitors – Stock Solutions and Dilution Factor for Use in Cell Lysis

Inhibitor	M _w (g/mol)	Stock Concentration	diluted in	Dilution Factor for Working Concentration
Pepstatin		0.5 mg/mL	EtOH*	1:500
Leupeptin		1 mg/mL	dH ₂ O	1:1000
Aprotinin		1 mg/mL	dH ₂ O	1:1000
Sodium Orthovanadate	183.9	200 mM	dH ₂ O**	1:200
PMSF		100 mM	EtOH	1:500

* Inhibitor was dissolved o/n on a shaker. The flask was covered with aluminum foil as the compound is light sensitive.

** 1.47 g powder was dissolved in 30 mL dH₂O first and the pH was adjusted with HCl (diluted 1:2 in dH₂O) to pH 10. (→ Then the solution turned yellow.) The solution was boiled until it turned clear again. It was aliquoted and aliquots were frozen at -80°C.

5.6.2 Preparation of Total Aliquots for Immunoblotting

If cell lysates (as prepared according to Section 5.6.1) should be analyzed directly via SDS-PAGE and immunoblotting 4 x SDS loading dye was added 1:4 to a defined volume of lysate. Commonly 40 µL total aliquot sample (30 µL lysate + 10 µL 4 x SDS loading dye) were sufficient to yield strong signals in immunodetection. For weakly expressed proteins up to 70 µL of total aliquot sample were loaded. (The volume of 70 µL was chosen as it represented the maximum volume that could be conveniently pipetted into one slot of a 1.5 mm PAGel with 10 slots.)

5.6.3 (Co-)Immunoprecipitation

Background Information:

Immunoprecipitation yields at concentrating a specific protein from a cell lysate. For this purpose the lysate is incubated with a protein-specific antibody. The resulting protein-antibody complexes are precipitated with agarose beads, which bind antibodies independently from their specificity. For untagged proteins antibodies against protein-intrinsic epitopes were applied. Tagged proteins were in general immunoprecipitated by the use of tag-specific antibodies.

Co-immunoprecipitation is performed in a similar way as immunoprecipitation but with the goal not only to purify a single protein but complexes of two or more proteins. In order to avoid dissociation of complexes it can be necessary to reduce stringency (salt or detergent concentration) in the procedure by adaptation of lysis buffers.

Protocol:

Cells were lysed as explained in Section 5.6.1. Antibody was added according to Table 28 and the lysate/ Ab-mix was incubated at 4°C, end-to-end rotating, o/n to allow the antibody to bind its target protein. The next day, protein A or protein G agarose beads were added and the lysates were incubated for an additional hour at 4°C, end-to-end rotating during which agarose beads was allowed to bind the antibody.

To remove unbound protein from agarose beads, the beads were washed with lysis buffer. (In the case of normal immunoprecipitation the same lysis buffer, RIPA-buffer + inhibitors, was used for lysis and washing. For co-immunoprecipitation NP-40-buffer + inhibitors, 50 mM NaCl, was used during lysis. For washing of beads the same buffer was used, but the concentration of NaCl was increased to 150 mM.) Lysate containing beads was centrifuged at 16,100 rcf for 2 min. The supernatant was taken off except for approximately 100 μ L. 1mL lysis buffer + inhibitors was added and tube was inverted 5 - 10 x. The beads were again pelleted by centrifugation at 16,100 rcf for 2 min. This step was repeated twice. After the third washing, the beads were pelleted and the supernatant was taken off so that only approximately 30 μ L buffer were left in the tube. 10 μ L 4 x SDS loading dye were added, sample was mixed and used directly for immunoblotting or stored at -20 or -80°C.

Table 28| Antibodies for (Co-)IP

Antibody	Dilution Factor
Anti-HA antibody produced in rabbit	1:200
Monoclonal ANTI-c-MYC clone 9E10	1:1000

5.6.4 (Co-)Pull-Down

Background Information:

Pull-down (PD) and co-pull-down (Co-IP) are also methods aiming at purifying a protein (PD) or protein complexes (Co-PD) from a total cell lysate. However, in contrast to IP or Co-IP, in PD and Co-PD one takes advantage of the strong natural interaction between streptavidin-binding protein (SBP) and streptavidin. Upon co-incubation the two proteins form a strong complex. This makes it possible to purify SBP-tagged proteins from cell lysates with streptavidin-coupled agarose beads. No tag- or protein-specific antibody is required.

Protocol:

Cells were lysed as explained in Section 5.6.1. 20 μ L streptavidin agarose beads were added per sample and the mix was incubated at 4°C, end-to-end rotating, o/n to allow streptavidin and the SBP-tag to interact and bind.

The next day the beads were washed with lysis buffer to remove unbound proteins. Washing was performed as explained for immuno- and co-immunoprecipitation (Section 5.6.3) . After the third washing, the beads were pelleted and the supernatant was taken off so that only approximately 30 μ L buffer were left in the tube. 10 μ L 4 x SDS loading dye were added, the sample was mixed and used directly for immunoblotting or stored at -20 or -80°C.

5.6.5 SDS-PAGE and Immunoblotting

Resolving gels with a concentration of acrylamide/bisacrylamide according to the size of the analyzed protein were prepared. They were overlaid with 5 % stacking gels

4 x SDS PAGE sample buffer was added to the samples (in a dilution of 1:4). To denature and linearize the proteins the samples were incubated at 95°C for 5 min.

The samples were loaded onto PAGels next to 5 μL of protein size standard. As size standard Page Ruler Prestained Protein Ladder #SM0671 (Fermentas) was used. Gel electrophoresis was performed at 70-130mV in Running Buffer using the Mini Protein III gel electrophoresis system (BioRad).

After electrophoresis, the gels were blotted onto a PVDF membrane at 50 mA/ 1 gel ($\sim 1.01 \text{ mA/cm}^2$) for 85 min in transfer buffer using the Trans-Blot[®] SD Semi-Dry Transfer Cell blotting system (BioRad).

If a blot needed to be cut vertically between lanes, it was in general stained reversibly with Ponceau solution to visualize protein bands and thus lanes. For this purpose, the membrane was incubated in Ponceau solution for 2 - 3 min and washed with dH_2O until the lanes were clearly visible. The membrane was cut and destained in TBS-T.

To prevent unspecific binding of antibody the blots were incubated in 5 % milk powder/TBS-T for 1 h or in 5 % BSA/TBS-T for 2 h or o/n. After blocking with milk, the blots were washed 3 x for 10 min in order not to contaminate the primary antibody solution with milk. Blots blocked in BSA were not washed as primary antibodies were in general diluted in 5% BSA. The blots were transferred to primary antibody solution and incubated at 4°C, shaking, o/n. The next day, the immunoblots were washed with TBS-T 3 x for 10 min and incubated in HRP-coupled secondary antibody (anti-rbt-HRP or anti-ms-HRP diluted 1:5000 in 5 % Milk/ TBS-T for 1 h at RT. (For each staining fresh secondary antibody-dilution was prepared.) Following incubation, the blots were washed with TBS-T 3 x for 10 min, dipped dry and placed on a glass plate. They were covered with Lumi-Light Western Blotting Substrate (Roche) (about 1.0 mL per membrane, $\sim 51 \text{ cm}^2$) and incubated for 5 min. Then the solution was poured off and the blots were put into a transparency and developed in a Fluor-S Multiimager (BioRad) using Quantity One 4.4.1 detection software (BioRad).

Table 29| Running Gel Buffer (pH $\sim 8.8^*$)

Reagent	Concentration
Tris	1.5M
HCl	0.25M

*pH-value wasn't adjusted but checked

Table 30| Stacking Gel Buffer (pH $\sim 6.8^*$)

Reagent	Concentration
Tris	0.02M
Tris-Cl	0.48M

*pH-value wasn't adjusted but checked

Table 31| Running Gel (1 Gel, 1.5 mm Thickness)

Reagent	Concentration [Acrylamide]		
	7.5 %	10 %	12.5 %
40 % acrylamide mix	1.88 mL	2.5 mL	3.1 mL
1.5 M Tris / 0.25M HCl	2.5 mL	2.5 mL	2.5 mL
dH_2O	5.4 mL	4.8 mL	4.2 mL
10 % SDS (w/v)	100 μL	100 μL	100 μL
10 % APS (w/v)	50 μL	50 μL	50 μL
TEMED	10 μL	10 μL	10 μL

Table 32| Stacking Gel (1 Gel, 1.5 mm thickness)

Reagent	Concentration 5 %
40 % acrylamide mix	0.625 mL
1.5 M Tris / 0.25 M HCl	1.25 mL
dH ₂ O	3.025 mL
10 % SDS (w/v)	50 µL
10 % APS (w/v)	50 µL
TEMED	5 µL

Table 33| 5 x Running Buffer Stock Solution

Reagent	Amount	Concentration
Tris	15.05 g	0.12 M
Glycine	72 g	0.96 M
SDS	5 g	0.017 M
dH ₂ O	adjusted to 1 L	

To prepare a 1 x working solution the 5 x running buffer stock solution was diluted 1:5 in dH₂O.

Table 34| 10 x Transfer Buffer Stock Solution

Reagent	Amount	Concentration
Tris	58 g	0.48 M
Glycine	29 g	0.39 M
SDS	5 g	0.017 M
dH ₂ O	adjusted to 1 L	

To prepare a 1 x working solution the 10 x stock solution was diluted 1:10 in 10% Methanol / dH₂O.

Table 35| 10 x TBS-Tween Stock Solution

Reagent	Concentration 10 x / 1 x
1 M Tris-Cl pH 8	100 mM / 10 mM
NaCl	1.5 M / 0.15 M
Tween	0.5 % / 0.05 %

To prepare a 1 x working solution the 10 x stock solution was diluted 1:10 in dH₂O.

5.6.6 Stripping of an Immunoblot after Development

To remove remaining immunoblotting substrate solution after development, the membrane was washed by shaking in dH₂O for 5 min. Secondary antibodies were stripped from the blot by shaking in 0.2 M NaOH/dH₂O for 5 min and the blot was washed in dH₂O for further 5 min. Following this 'stripping' the blot was stored in TBS-T at 4°C or used directly for another round of detection. In this case the blot was again blocked in 5 % BSA/ TBS-T or 5 % Milk/ TBS-T previous to incubation in primary antibody.

5.6.7 Biochemical Quantification of MuSK Tyrosine Phosphorylation

IP or PD samples containing MuSK were resolved via SDS-PAGE and transferred onto a PVDF membrane as described in Section 5.6.5. After blocking of the membrane with 5 % BSA/TBS-T for 2 h at RT the blot was incubated in anti-pTyr at 4°C, shaking, o/n and developed the following day. Then

the blot was stripped with NaOH (Section 5.6.6), again blocked with 5 % BSA/TBS-T and probed for MuSK with an antibody against MuSK (anti-MuSK C.F) or against the tag of the respective construct used in this experiment (e.g. anti-HA for MuSK-HA). Chemiluminescence of pTyr-signals corresponding in molecular mass with MuSK (pTyr (MuSK)) and specific MuSK-signals (MuSK) were quantified for all individual samples and pTyr (MuSK)/MuSK ratios were calculated.

5.6.8 Analysis of Protein Stability in COS-7 Cells

Reagents:

Cycloheximide stock solution: 10mg/mL

To prepare the stock solution, 15 mg cycloheximide were diluted in 1.5 mL sterile ddH₂O. The solution was aliquoted and the aliquots were stored at 4°C.

Protocol:

COS-7 cells were transfected via CaCl₂/ BBS-transfection with the gene of interest and a vector coding for EGFP-N2, which was used as internal standard. The transfection was performed over day for 8 h as explained in Section 5.5.5.1. Cells were lysed with RIPA-buffer with inhibitors 23 - 24 h after medium change as explained in Section 5.6.1. To analyze the protein half-life transfected cells were treated with 50 µg/mL cycloheximide for certain periods of times before lysis. The reagent blocks ribosomal protein synthesis and therefore prevents new protein from being produced whilst the pool of protein already present in the cells at the beginning of inhibition is degraded according to its stability. The degradation process can be assessed by quantification of the amount of the protein of interest relative to the amount of a standard protein of longer half-life than the duration of cycloheximide treatment. EGFP-N2 was chosen as internal standard for its high stability of more than 24 h ((Barrow et al., 2005)).

$$f(x) = \frac{\left[\frac{ha(t_x)}{gfp(t_x)} \right]}{\left[\frac{ha(t_0)}{gfp(t_0)} \right]} \times 100$$

5.6.9 Cloning

5.6.9.1 Enzymatic Restriction

For enzymatic restriction of purified DNA Fermentas restriction enzymes and corresponding buffers were used. If double digests were required a restriction enzyme buffer yielding 50-100 % activity for either of the two restriction enzymes was chosen. If none such buffer was available the restriction was performed in two subsequent steps. In between either step the buffer concentration was adapted (e.g. from 2 x Tango buffer to 1 x Tango).

5.6.9.2 DNA Purification after Enzymatic Restriction

Digested DNA was resolved on an agarose-gel of an agarose concentration that yielded optimal separation of desired restriction fragments. (Commonly 0.8 % agarose gels were used for fragments ranging from 100 - 6000 bp. Larger fragments were separated on gels of 0.6 - 0.7 % agarose

concentration.) DNA bands of interest were cut out and DNA was eluted from the agarose gel blocks with GeneJET Gel Extraction Kit (Fermentas) according to the corresponding protocol.

5.6.9.3 DNA Ligation

Purified vector and insert DNA, ligase buffer and ligase were mixed according to Table 36.

Reagent	Amount
vector	50 ng
insert	x ng
T4 ligase buffer (10 x)	2 μ L
T4 ligase	1 μ L
ddH ₂ O	adapted to 20 μ L
total volume	20 μ L

The required amount of insert DNA was calculated as follows:

$$ng(insert) = \frac{ng(vector) \times bp(insert) \times 3}{bp(vector)} = \frac{50ng \times bp(insert) \times 3}{bp(vector)}$$

The ligation mix was incubated for 1 - 2 h at RT and then directly used for the transformation of competent bacteria or stored at -20°C.

5.6.9.4 Cloning of SBP-MuSK-K608A and SBP-MuSK-LS745/746MT

Kinase-active and kinase-inactive MuSK phosphorylation mutants had been kindly provided by S. Burden and had been used by S. Luiskandl to clone variants with fourfold SBP-tags (unpublished data). These plasmids were used to create similar constructs with double SBP-tags (Figure 24).

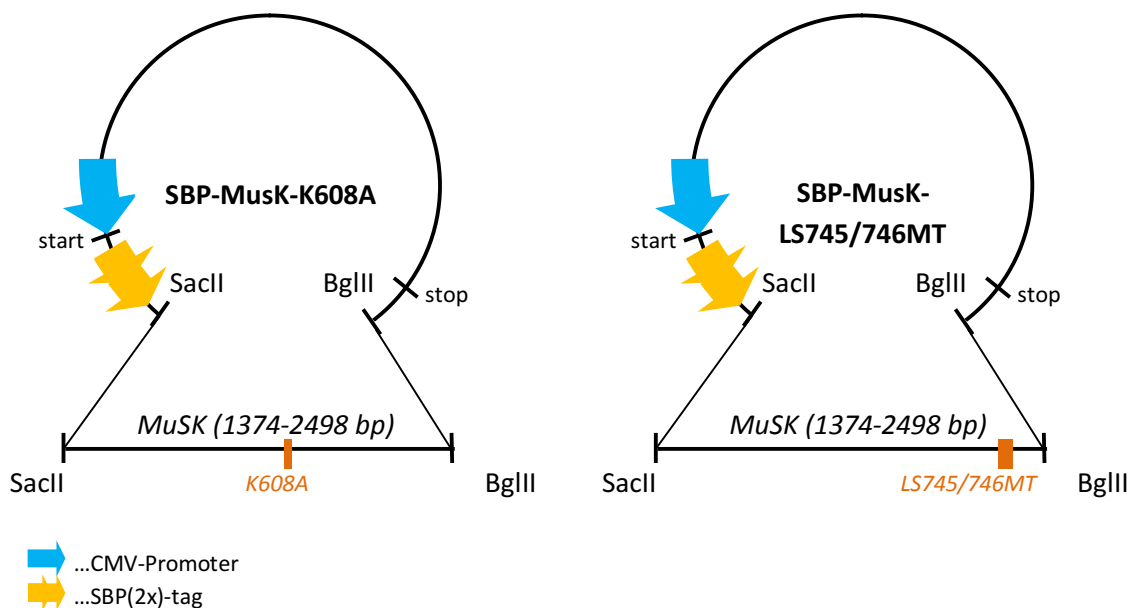


Figure 24| Cloning of SBP-MuSK Mutants The SBP-MuSK (wt) expression vector was enzymatically restricted 3' to the SBP coding sequence in the MuSK gene and 5'-terminal to the MuSK stop codon. The coding sequence in between was excised and replaced by the corresponding portion of MuSK-K608A or MuSK-LS745/746MT respectively. SBP(2x)-tag ... double SBP-tag

5.6.9.5 Cloning of HA-MuSK-Ubwt and HA-MuSK-Ubmut

MuSK-Ubwt and MuSK-Ubmut chimeras created by R. Herbst (unpublished data) were cloned into a eukaryotic expression vector and provided with an N-terminal HA-tag.

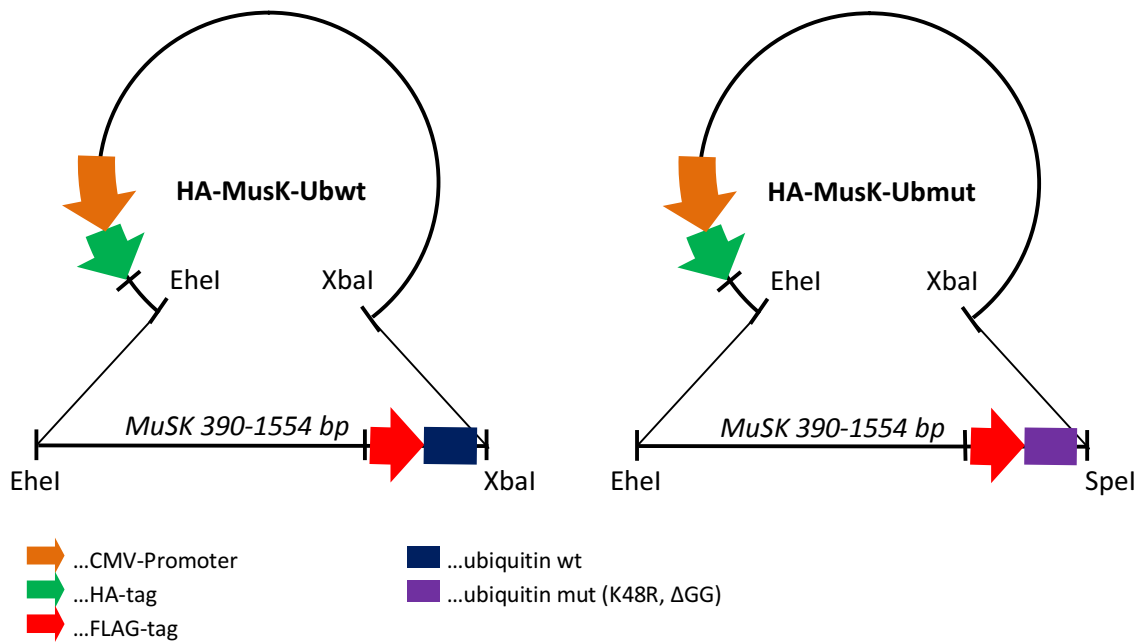


Figure 25| Cloning of HA-MuSK-Ub chimeras HA-MuSK-Ubwt & HA-MuSK-Ubmut CMV/HA-MuSK was enzymatically restricted after the 3'-terminus of the MuSK coding sequence and within the sequence coding for the extracellular part of MuSK. The resulting fragment was removed and replaced with fragments excised from vectors pLitmus 29/ MuSK-Ubwt and pBluescript/MuSK-Ubmut (R. Herbst, unpublished data). These fragments reconstituted the coding sequence of MuSK extracellular and transmembrane domain. Instead of MuSK intracellular domain they comprised coding sequences for a FLAG-tag and wild-type or mutant ubiquitin.

5.6.10 Transformation of Competent Bacteria

Background Information:

Bacteria were transformed in order to select and amplify successfully ligated plasmids after cloning or to gain fresh cells for amplification of already purified plasmid. In the first case competent bacteria were transfected with the ligation mix, which in general contained functional plasmids in a rather low concentration. Therefore it was important to yield optimal transformation efficiency. For transformation with already purified plasmid plasmid solutions of high concentration were used. Thus transformation efficiency was less essential and individual incubation times were shortened and steps were left out as indicated.

Protocol:

Competent E.coli were thawed on ice. 100 µL competent bacteria and 20 µL 5 x KCM were mixed in an Eppendorf tube. If bacteria were transformed with freshly ligated plasmid the total volume of ligation mix was added. If bacteria were transfected with purified plasmid in order to gain fresh cells for

plasmid amplification, ~300 ng - 2 µg DNA of plasmid preparation were added. The transfection mixture was adjusted to 200µL with sterile ddH₂O, gently mixed and incubated on ice for 30 min. (15 min of incubation were sufficient for purified plasmid). E.coli were heat-shocked by incubation at 42°C for 2 min and put back on ice briefly. 900 µL LB-medium w/o selective antibiotics were added and the cells were allowed to regenerate at 37°C for 30 min (15 min for purified plasmid). In case the transformation was performed with a ligation mix the bacteria were pelleted via centrifugation at 16,100 rcf in a table-top centrifuge, LB-medium was removed apart from ~100 µL, in which bacteria were resuspended. This suspension was plated on LB-plates containing the selective antibiotic corresponding to the resistance conferred by the transfected plasmid. If purified plasmid was transfected bacteria were not pelleted. 100 - 200 µL of transfection mix diluted in non-selective LB-medium were directly plated on selective LB dishes after 15 min of regeneration.

Table 37 | 5 x KCM Buffer

Reagent	Concentration
KCl	0.5 M
CaCl ₂	0.15 M
MgCl ₂	0.25 M

6 Abbreviations

AA	acrylamide
aa	amino acid(s)
Ab	antibody
Ach	acetylcholine
AchR	acetylcholine receptor
AchR α	AchR subunit α
AchR β	AchR subunit β
AchR γ	AchR subunit γ
AchR δ	AchR subunit δ
AChR ϵ	AChR subunit ϵ
ADP	adenosine diphosphate
ARF6	ADP-ribosylation factor 6
Asn	asparagine
ATP	adenosine triphosphate
BBS	BES-buffered saline
BES	N,N-Bis(2-hydroxyethyl)taurine N,N-Bis(2-hydroxyethyl)-2-aminoethanesulfonic acid
BSA	bovine serum albumine
Cdc42	cell division control protein 42
CME	clathrin-mediated endocytosis
CMS	congenital myasthenic syndrome(s)
D-box	destruction-box
ddH ₂ O	double-distilled water
dH ₂ O	distilled water
Dok7	docking protein-7
DUB	de-ubiquitinating enzyme
E#	embryonic day #
E1	ubiquitin activating enzyme
E2	ubiquitin-conjugating enzyme
E3	ubiquitin ligase
EGF	epidermal growth factor
EGFP	enhanced green fluorescent protein
EGFR	epidermal growth factor receptor
GAP	GTPase-activating protein
GDP	guanosine diphosphate
GEF	GDP/ GTP exchange factor
GTP	guanosine triphosphate
h	hour(s)
IB	immunoblot
Ig	immunoglobulin
IgG	immunoglobulin G
IP	immunoprecipitation
IRK	insulin receptor kinase
JM	juxtamembrane
K	lysine

kDa	kiloDalton
LDLR	low-density lipoprotein receptor
LRP4	low-density lipoprotein receptor - related protein 4
<i>lrp4</i>	<i>lrp4</i> gene
Lys	lysine
MG	myasthenia gravis
MG132	Z-Leu-Leu-Leu-al, Cbz-leu-leu-leucinal
min	minute(s)
ms	mouse
MuSK	muscle-specific kinase
<i>MuSK</i>	<i>MuSK</i> gene
MVBs	multivesicular bodies
NMJ	neuromuscular junction
NMS	neuromuscular synapse
NPXY	Asn-Pro-X-Tyr
NSF	N-ethylmaleimide sensitive fusion protein
o/n	over night
P#	postnatal day #
PAGE	polyacrylamide gel electrophoresis
PBS	phosphate-buffered saline
PCR	polymerase chain reaction
PD	pull-down
PDGF	platelet-derived growth factor
PDGFR	platelet-derived growth factor receptor
PDZRN3	PDZ domain containing RING finger 3
PEST sequences	proline-glutamate-serine-threonine-rich sequences
PFA	paraformaldehyde
PH	pleckstrin-homology
PPi	inorganic diphosphate
Pro	proline
PTB	phosphotyrosine-binding
pTyr	phosphorylated tyrosine
Rab	Ras-related in brain
RATL	rapsyn-associated transmembrane linker protein
RIPA buffer	radioimmunoprecipitation assay buffer
rbt	rabbit
RTK	receptor tyrosine kinase
SBP	streptavidin-binding protein
SDS	sodium dodecyl sulfate
sec	second(s)
SH2	Src homology 2
Stim	stimulation
TBS-T	Tris-buffered saline + Tween
TF	transfection
TK	tyrosine kinase
TM	transmembrane
Tyr	tyrosine

Ub	ubiquitin
UBD	ubiquitin binding domain
UIM	ubiquitin-interaction motif
UT	untransfected
X	optional amino acid residue
x	times

7 References

- Acconcia, F., Sigismund, S., and Polo, S. (2009). Ubiquitin in trafficking: the network at work. *Exp Cell Res* 315, 1610-1618.
- Adams, J. (2004). The proteasome: a suitable antineoplastic target. *Nat Rev Cancer* 4, 349-360.
- Alwan, H. A., van Zoelen, E. J., and van Leeuwen, J. E. (2003). Ligand-induced lysosomal epidermal growth factor receptor (EGFR) degradation is preceded by proteasome-dependent EGFR de-ubiquitination. *J Biol Chem* 278, 35781-35790.
- Apel, E. D., Glass, D. J., Moscoso, L. M., Yancopoulos, G. D., and Sanes, J. R. (1997). Rapsyn is required for MuSK signaling and recruits synaptic components to a MuSK-containing scaffold. *Neuron* 18, 623-635.
- Arevalo, J. C., Waite, J., Rajagopal, R., Beyna, M., Chen, Z. Y., Lee, F. S., and Chao, M. V. (2006). Cell survival through Trk neurotrophin receptors is differentially regulated by ubiquitination. *Neuron* 50, 549-559.
- Bache, K. G., Slagsvold, T., and Stenmark, H. (2004). Defective downregulation of receptor tyrosine kinases in cancer. *Embo J* 23, 2707-2712.
- Barrow, J., Bernardo, A. S., Hay, C. W., Blaylock, M., Duncan, L., Mackenzie, A., McCreath, K., Kind, A. J., Schnieke, A. E., Colman, A., *et al.* (2005). Purification and Characterization of a Population of EGFP-Expressing Cells from the Developing Pancreas of a Neurogenin3/EGFP Transgenic Mouse. *Organogenesis* 2, 22-27.
- Beeson, D., Higuchi, O., Palace, J., Cossins, J., Spearman, H., Maxwell, S., Newsom-Davis, J., Burke, G., Fawcett, P., Motomura, M., *et al.* (2006). Dok-7 mutations underlie a neuromuscular junction synaptopathy. *Science* 313, 1975-1978.
- Berg, D. K., Kelly, R. B., Sargent, P. B., Williamson, P., and Hall, Z. W. (1972). Binding of -bungarotoxin to acetylcholine receptors in mammalian muscle (snake venom-denervated muscle-neonatal muscle-rat diaphragm-SDS-polyacrylamide gel electrophoresis). *Proc Natl Acad Sci U S A* 69, 147-151.
- Bergamin, E., Hallock, P. T., Burden, S. J., and Hubbard, S. R. The cytoplasmic adaptor protein Dok7 activates the receptor tyrosine kinase MuSK via dimerization. *Mol Cell* 39, 100-109.
- Bevan, S., and Steinbach, J. H. (1977). The distribution of alpha-bungarotoxin binding sites of mammalian skeletal muscle developing in vivo. *J Physiol* 267, 195-213.
- Bezakova, G., and Lomo, T. (2001). Muscle activity and muscle agrin regulate the organization of cytoskeletal proteins and attached acetylcholine receptor (AChR) aggregates in skeletal muscle fibers. *J Cell Biol* 153, 1453-1463.
- Bright, N. A., Gratian, M. J., and Luzio, J. P. (2005). Endocytic delivery to lysosomes mediated by concurrent fusion and kissing events in living cells. *Curr Biol* 15, 360-365.
- Bucci, C., Lutcke, A., Steele-Mortimer, O., Olkkonen, V. M., Dupree, P., Chiariello, M., Bruni, C. B., Simons, K., and Zerial, M. (1995). Co-operative regulation of endocytosis by three Rab5 isoforms. *FEBS Lett* 366, 65-71.
- Bucci, C., Thomsen, P., Nicoziani, P., McCarthy, J., and van Deurs, B. (2000). Rab7: a key to lysosome biogenesis. *Mol Biol Cell* 11, 467-480.
- Burden, S. J. SnapShot: Neuromuscular Junction. *Cell* 144, 826-826 e821.
- Burgess, R. W., Nguyen, Q. T., Son, Y. J., Lichtman, J. W., and Sanes, J. R. (1999). Alternatively spliced isoforms of nerve- and muscle-derived agrin: their roles at the neuromuscular junction. *Neuron* 23, 33-44.

- Campagna, J. A., Ruegg, M. A., and Bixby, J. L. (1995). Agrin is a differentiation-inducing "stop signal" for motoneurons in vitro. *Neuron* 15, 1365-1374.
- Cao, T. T., Deacon, H. W., Reczek, D., Bretscher, A., and von Zastrow, M. (1999). A kinase-regulated PDZ-domain interaction controls endocytic sorting of the beta2-adrenergic receptor. *Nature* 401, 286-290.
- Cartaud, J., Cartaud, A., Kordeli, E., Ludosky, M. A., Marchand, S., and Stetzkowski-Marden, F. (2000). The torpedo electrocyte: a model system to study membrane-cytoskeleton interactions at the postsynaptic membrane. *Microsc Res Tech* 49, 73-83.
- Ceresa, B. P., and Schmid, S. L. (2000). Regulation of signal transduction by endocytosis. *Curr Opin Cell Biol* 12, 204-210.
- Chevessier, F., Faraut, B., Ravel-Chapuis, A., Richard, P., Gaudon, K., Bauche, S., Prioleau, C., Herbst, R., Goillot, E., Loos, C., *et al.* (2004). MUSK, a new target for mutations causing congenital myasthenic syndrome. *Hum Mol Genet* 13, 3229-3240.
- Ciechanover, A. (1994). The ubiquitin-proteasome proteolytic pathway. *Cell* 79, 13-21.
- Ciechanover, A. (2006). Intracellular protein degradation: from a vague idea thru the lysosome and the ubiquitin-proteasome system and onto human diseases and drug targeting. *Hematology Am Soc Hematol Educ Program*, 1-12, 505-506.
- Cohen, I., Rimer, M., Lomo, T., and McMahan, U. J. (1997). Agrin-induced postsynaptic-like apparatus in skeletal muscle fibers in vivo. *Mol Cell Neurosci* 9, 237-253.
- Cole, R. N., Ghazanfari, N., Ngo, S. T., Gervasio, O. L., Reddel, S. W., and Phillips, W. D. Patient autoantibodies deplete postsynaptic muscle-specific kinase leading to disassembly of the ACh receptor scaffold and myasthenia gravis in mice. *J Physiol* 588, 3217-3229.
- Coux, O., Tanaka, K., and Goldberg, A. L. (1996). Structure and functions of the 20S and 26S proteasomes. *Annu Rev Biochem* 65, 801-847.
- Dai, Z., Luo, X., Xie, H., and Peng, H. B. (2000). The actin-driven movement and formation of acetylcholine receptor clusters. *J Cell Biol* 150, 1321-1334.
- De Duve, C., Gianetto, R., Appelmans, F., and Wattiaux, R. (1953). Enzymic content of the mitochondria fraction. *Nature* 172, 1143-1144.
- DeChiara, T. M., Bowen, D. C., Valenzuela, D. M., Simmons, M. V., Poueymirou, W. T., Thomas, S., Kinetz, E., Compton, D. L., Rojas, E., Park, J. S., *et al.* (1996). The receptor tyrosine kinase MuSK is required for neuromuscular junction formation in vivo. *Cell* 85, 501-512.
- Di Guglielmo, G. M., Drake, P. G., Baass, P. C., Authier, F., Posner, B. I., and Bergeron, J. J. (1998). Insulin receptor internalization and signalling. *Mol Cell Biochem* 182, 59-63.
- Dimitropoulou, A., and Bixby, J. L. (2005). Motor neurite outgrowth is selectively inhibited by cell surface MuSK and agrin. *Mol Cell Neurosci* 28, 292-302.
- Duan, L., Miura, Y., Dimri, M., Majumder, B., Dodge, I. L., Reddi, A. L., Ghosh, A., Fernandes, N., Zhou, P., Mullane-Robinson, K., *et al.* (2003). Cbl-mediated ubiquitylation is required for lysosomal sorting of epidermal growth factor receptor but is dispensable for endocytosis. *J Biol Chem* 278, 28950-28960.
- Duclert, A., and Changeux, J. P. (1995). Acetylcholine receptor gene expression at the developing neuromuscular junction. *Physiol Rev* 75, 339-368.
- Engel, A. G., Ohno, K., and Sine, S. M. (2003). Sleuthing molecular targets for neurological diseases at the neuromuscular junction. *Nat Rev Neurosci* 4, 339-352.
- Engel, A. G., Shen, X. M., Selcen, D., and Sine, S. M. What have we learned from the congenital myasthenic syndromes. *J Mol Neurosci* 40, 143-153.

- Feng, Y., Press, B., and Wandinger-Ness, A. (1995). Rab 7: an important regulator of late endocytic membrane traffic. *J Cell Biol* 131, 1435-1452.
- Ferns, M. J., Campanelli, J. T., Hoch, W., Scheller, R. H., and Hall, Z. (1993). The ability of agrin to cluster AChRs depends on alternative splicing and on cell surface proteoglycans. *Neuron* 11, 491-502.
- Froehner, S. C., Luetje, C. W., Scotland, P. B., and Patrick, J. (1990). The postsynaptic 43K protein clusters muscle nicotinic acetylcholine receptors in *Xenopus* oocytes. *Neuron* 5, 403-410.
- Galan, J. M., and Haguener-Tsapis, R. (1997). Ubiquitin lys63 is involved in ubiquitination of a yeast plasma membrane protein. *Embo J* 16, 5847-5854.
- Gautam, M., Noakes, P. G., Moscoso, L., Rupp, F., Scheller, R. H., Merlie, J. P., and Sanes, J. R. (1996). Defective neuromuscular synaptogenesis in agrin-deficient mutant mice. *Cell* 85, 525-535.
- Gautam, M., Noakes, P. G., Mudd, J., Nichol, M., Chu, G. C., Sanes, J. R., and Merlie, J. P. (1995). Failure of postsynaptic specialization to develop at neuromuscular junctions of rapsyn-deficient mice. *Nature* 377, 232-236.
- Geetha, T., Jiang, J., and Wooten, M. W. (2005). Lysine 63 polyubiquitination of the nerve growth factor receptor TrkA directs internalization and signaling. *Mol Cell* 20, 301-312.
- Gesemann, M., Denzer, A. J., and Ruegg, M. A. (1995). Acetylcholine receptor-aggregating activity of agrin isoforms and mapping of the active site. *J Cell Biol* 128, 625-636.
- Ghazanfari, N., Fernandez, K. J., Murata, Y., Morsch, M., Ngo, S. T., Reddel, S. W., Noakes, P. G., and Phillips, W. D. Muscle specific kinase: organiser of synaptic membrane domains. *Int J Biochem Cell Biol* 43, 295-298.
- Gianetto, R., and De Duve, C. (1955). Tissue fractionation studies. 4. Comparative study of the binding of acid phosphatase, beta-glucuronidase and cathepsin by rat-liver particles. *Biochem J* 59, 433-438.
- Glass, D. J., Apel, E. D., Shah, S., Bowen, D. C., DeChiara, T. M., Stitt, T. N., Sanes, J. R., and Yancopoulos, G. D. (1997). Kinase domain of the muscle-specific receptor tyrosine kinase (MuSK) is sufficient for phosphorylation but not clustering of acetylcholine receptors: required role for the MuSK ectodomain? *Proc Natl Acad Sci U S A* 94, 8848-8853.
- Glass, D. J., Bowen, D. C., Stitt, T. N., Radziejewski, C., Bruno, J., Ryan, T. E., Gies, D. R., Shah, S., Mattsson, K., Burden, S. J., *et al.* (1996). Agrin acts via a MuSK receptor complex. *Cell* 85, 513-523.
- Glotzer, M., Murray, A. W., and Kirschner, M. W. (1991). Cyclin is degraded by the ubiquitin pathway. *Nature* 349, 132-138.
- Goldberg, A. L. (1995). Functions of the proteasome: the lysis at the end of the tunnel. *Science* 268, 522-523.
- Gronostajski, R. M., Pardee, A. B., and Goldberg, A. L. (1985). The ATP dependence of the degradation of short- and long-lived proteins in growing fibroblasts. *J Biol Chem* 260, 3344-3349.
- Haglund, K., Sigismund, S., Polo, S., Szymkiewicz, I., Di Fiore, P. P., and Dikic, I. (2003). Multiple monoubiquitination of RTKs is sufficient for their endocytosis and degradation. *Nat Cell Biol* 5, 461-466.
- Hamuro, J., Higuchi, O., Okada, K., Ueno, M., Iemura, S., Natsume, T., Spearman, H., Beeson, D., and Yamanashi, Y. (2008). Mutations causing DOK7 congenital myasthenia ablate functional motifs in Dok-7. *J Biol Chem* 283, 5518-5524.
- Herbst, R., and Burden, S. J. (2000). The juxtamembrane region of MuSK has a critical role in agrin-mediated signaling. *Embo J* 19, 67-77.
- Hershko, A., and Ciechanover, A. (1998). The ubiquitin system. *Annu Rev Biochem* 67, 425-479.

- Hicke, L. (1999). Gettin' down with ubiquitin: turning off cell-surface receptors, transporters and channels. *Trends Cell Biol* 9, 107-112.
- Hicke, L., Schubert, H. L., and Hill, C. P. (2005). Ubiquitin-binding domains. *Nat Rev Mol Cell Biol* 6, 610-621.
- Hopf, C., and Hoch, W. (1998). Dimerization of the muscle-specific kinase induces tyrosine phosphorylation of acetylcholine receptors and their aggregation on the surface of myotubes. *J Biol Chem* 273, 6467-6473.
- <http://faculty.ucr.edu/~karine/research.html>, available: 2011-02-21, 4.00 p.m..
- Huang, F., Goh, L. K., and Sorkin, A. (2007). EGF receptor ubiquitination is not necessary for its internalization. *Proc Natl Acad Sci U S A* 104, 16904-16909.
- Huang, F., Kirkpatrick, D., Jiang, X., Gygi, S., and Sorkin, A. (2006). Differential regulation of EGF receptor internalization and degradation by multiubiquitination within the kinase domain. *Mol Cell* 21, 737-748.
- Hubbard, S. R., and Till, J. H. (2000). Protein tyrosine kinase structure and function. *Annu Rev Biochem* 69, 373-398.
- Huebsch, K. A., and Maimone, M. M. (2003). Rapsyn-mediated clustering of acetylcholine receptor subunits requires the major cytoplasmic loop of the receptor subunits. *J Neurobiol* 54, 486-501.
- Hurley, J. H., Lee, S., and Prag, G. (2006). Ubiquitin-binding domains. *Biochem J* 399, 361-372.
- Inoue, A., Setoguchi, K., Matsubara, Y., Okada, K., Sato, N., Iwakura, Y., Higuchi, O., and Yamanashi, Y. (2009). Dok-7 activates the muscle receptor kinase MuSK and shapes synapse formation. *Sci Signal* 2, ra7.
- Jadhav, T., and Wooten, M. W. (2009). Defining an Embedded Code for Protein Ubiquitination. *J Proteomics Bioinform* 2, 316.
- Jennings, C. G., Dyer, S. M., and Burden, S. J. (1993). Muscle-specific trk-related receptor with a kringle domain defines a distinct class of receptor tyrosine kinases. *Proc Natl Acad Sci U S A* 90, 2895-2899.
- Jing, L., Lefebvre, J. L., Gordon, L. R., and Granato, M. (2009). Wnt signals organize synaptic prepattern and axon guidance through the zebrafish unplugged/MuSK receptor. *Neuron* 61, 721-733.
- Joazeiro, C. A., Wing, S. S., Huang, H., Levenson, J. D., Hunter, T., and Liu, Y. C. (1999). The tyrosine kinase negative regulator c-Cbl as a RING-type, E2-dependent ubiquitin-protein ligase. *Science* 286, 309-312.
- Johnson, E. B., Hammer, R. E., and Herz, J. (2005). Abnormal development of the apical ectodermal ridge and polysyndactyly in Megf7-deficient mice. *Hum Mol Genet* 14, 3523-3538.
- Kim, N., Stiegler, A. L., Cameron, T. O., Hallock, P. T., Gomez, A. M., Huang, J. H., Hubbard, S. R., Dustin, M. L., and Burden, S. J. (2008). Lrp4 is a receptor for Agrin and forms a complex with MuSK. *Cell* 135, 334-342.
- Kummer, T. T., Misgeld, T., Lichtman, J. W., and Sanes, J. R. (2004). Nerve-independent formation of a topologically complex postsynaptic apparatus. *J Cell Biol* 164, 1077-1087.
- Kuriyan, J., and Cowburn, D. (1997). Modular peptide recognition domains in eukaryotic signaling. *Annu Rev Biophys Biomol Struct* 26, 259-288.
- Lamarque, N., Tapon, N., Stowers, L., Burbelo, P. D., Aspenstrom, P., Bridges, T., Chant, J., and Hall, A. (1996). Rac and Cdc42 induce actin polymerization and G1 cell cycle progression independently of p65PAK and the JNK/SAPK MAP kinase cascade. *Cell* 87, 519-529.

- Lanker, S., Valdivieso, M. H., and Wittenberg, C. (1996). Rapid degradation of the G1 cyclin Cln2 induced by CDK-dependent phosphorylation. *Science* *271*, 1597-1601.
- LaRochelle, W. J., and Froehner, S. C. (1986). Determination of the tissue distributions and relative concentrations of the postsynaptic 43-kDa protein and the acetylcholine receptor in Torpedo. *J Biol Chem* *261*, 5270-5274.
- Lee, D. H., and Goldberg, A. L. (1996). Selective inhibitors of the proteasome-dependent and vacuolar pathways of protein degradation in *Saccharomyces cerevisiae*. *J Biol Chem* *271*, 27280-27284.
- Lee, D. H., and Goldberg, A. L. (1998). Proteasome inhibitors: valuable new tools for cell biologists. *Trends Cell Biol* *8*, 397-403.
- Lichtman, J. W., and Colman, H. (2000). Synapse elimination and indelible memory. *Neuron* *25*, 269-278.
- Lin, W., Burgess, R. W., Dominguez, B., Pfaff, S. L., Sanes, J. R., and Lee, K. F. (2001). Distinct roles of nerve and muscle in postsynaptic differentiation of the neuromuscular synapse. *Nature* *410*, 1057-1064.
- Linnoila, J., Wang, Y., Yao, Y., and Wang, Z. Z. (2008). A mammalian homolog of *Drosophila* tumorous imaginal discs, *Tid1*, mediates agrin signaling at the neuromuscular junction. *Neuron* *60*, 625-641.
- Longva, K. E., Blystad, F. D., Stang, E., Larsen, A. M., Johannessen, L. E., and Madshus, I. H. (2002). Ubiquitination and proteasomal activity is required for transport of the EGF receptor to inner membranes of multivesicular bodies. *J Cell Biol* *156*, 843-854.
- Lu, Y., Tian, Q. B., Endo, S., and Suzuki, T. (2007a). A role for LRP4 in neuronal cell viability is related to apoE-binding. *Brain Res* *1177*, 19-28.
- Lu, Z., Je, H. S., Young, P., Gross, J., Lu, B., and Feng, G. (2007b). Regulation of synaptic growth and maturation by a synapse-associated E3 ubiquitin ligase at the neuromuscular junction. *J Cell Biol* *177*, 1077-1089.
- Luzio, J. P., Gray, S. R., and Bright, N. A. Endosome-lysosome fusion. *Biochem Soc Trans* *38*, 1413-1416.
- Luzio, J. P., Pryor, P. R., and Bright, N. A. (2007). Lysosomes: fusion and function. *Nat Rev Mol Cell Biol* *8*, 622-632.
- Maimone, M. M., and Merlie, J. P. (1993). Interaction of the 43 kd postsynaptic protein with all subunits of the muscle nicotinic acetylcholine receptor. *Neuron* *11*, 53-66.
- McMahan, U. J. (1990). The agrin hypothesis. *Cold Spring Harb Symp Quant Biol* *55*, 407-418.
- Meier, T., Hauser, D. M., Chiquet, M., Landmann, L., Ruegg, M. A., and Brenner, H. R. (1997). Neural agrin induces ectopic postsynaptic specializations in innervated muscle fibers. *J Neurosci* *17*, 6534-6544.
- Mercer, J., Schelhaas, M., and Helenius, A. Virus entry by endocytosis. *Annu Rev Biochem* *79*, 803-833.
- Meriggioli, M. N. (2009). Myasthenia gravis with anti-acetylcholine receptor antibodies. *Front Neurol Neurosci* *26*, 94-108.
- Meriggioli, M. N., and Sanders, D. B. (2009). Autoimmune myasthenia gravis: emerging clinical and biological heterogeneity. *Lancet Neurol* *8*, 475-490.
- Mishina, M., Takai, T., Imoto, K., Noda, M., Takahashi, T., Numa, S., Methfessel, C., and Sakmann, B. (1986). Molecular distinction between fetal and adult forms of muscle acetylcholine receptor. *Nature* *321*, 406-411.

- Missias, A. C., Mudd, J., Cunningham, J. M., Steinbach, J. H., Merlie, J. P., and Sanes, J. R. (1997). Deficient development and maintenance of postsynaptic specializations in mutant mice lacking an 'adult' acetylcholine receptor subunit. *Development* *124*, 5075-5086.
- Mukhopadhyay, D., and Riezman, H. (2007). Proteasome-independent functions of ubiquitin in endocytosis and signaling. *Science* *315*, 201-205.
- Muller, J. S., Herczegfalvi, A., Vilchez, J. J., Colomer, J., Bachinski, L. L., Mihaylova, V., Santos, M., Schara, U., Deschauer, M., Shevell, M., *et al.* (2007). Phenotypical spectrum of DOK7 mutations in congenital myasthenic syndromes. *Brain* *130*, 1497-1506.
- Noakes, P. G., Phillips, W. D., Hanley, T. A., Sanes, J. R., and Merlie, J. P. (1993). 43K protein and acetylcholine receptors colocalize during the initial stages of neuromuscular synapse formation in vivo. *Dev Biol* *155*, 275-280.
- Okada, K., Inoue, A., Okada, M., Murata, Y., Kakuta, S., Jigami, T., Kubo, S., Shiraishi, H., Eguchi, K., Motomura, M., *et al.* (2006). The muscle protein Dok-7 is essential for neuromuscular synaptogenesis. *Science* *312*, 1802-1805.
- Ontell, M., and Kozeka, K. (1984). Organogenesis of the mouse extensor digitorum logus muscle: a quantitative study. *Am J Anat* *171*, 149-161.
- Peng, J., Schwartz, D., Elias, J. E., Thoreen, C. C., Cheng, D., Marsischky, G., Roelofs, J., Finley, D., and Gygi, S. P. (2003). A proteomics approach to understanding protein ubiquitination. *Nat Biotechnol* *21*, 921-926.
- Peters, P. J., Hsu, V. W., Ooi, C. E., Finazzi, D., Teal, S. B., Oorschot, V., Donaldson, J. G., and Klausner, R. D. (1995). Overexpression of wild-type and mutant ARF1 and ARF6: distinct perturbations of nonoverlapping membrane compartments. *J Cell Biol* *128*, 1003-1017.
- Pickart, C. M. (2001). Mechanisms underlying ubiquitination. *Annu Rev Biochem* *70*, 503-533.
- Pickart, C. M., and Fushman, D. (2004). Polyubiquitin chains: polymeric protein signals. *Curr Opin Chem Biol* *8*, 610-616.
- Rink, J., Ghigo, E., Kalaidzidis, Y., and Zerial, M. (2005). Rab conversion as a mechanism of progression from early to late endosomes. *Cell* *122*, 735-749.
- Rock, K. L., Gramm, C., Rothstein, L., Clark, K., Stein, R., Dick, L., Hwang, D., and Goldberg, A. L. (1994). Inhibitors of the proteasome block the degradation of most cell proteins and the generation of peptides presented on MHC class I molecules. *Cell* *78*, 761-771.
- Rogers, S., Wells, R., and Rechsteiner, M. (1986). Amino acid sequences common to rapidly degraded proteins: the PEST hypothesis. *Science* *234*, 364-368.
- Saeki, Y., Kudo, T., Sone, T., Kikuchi, Y., Yokosawa, H., Toh-e, A., and Tanaka, K. (2009). Lysine 63-linked polyubiquitin chain may serve as a targeting signal for the 26S proteasome. *Embo J* *28*, 359-371.
- Sanes, J. R., and Lichtman, J. W. (2001). Induction, assembly, maturation and maintenance of a postsynaptic apparatus, Vol 2).
- Schlesinger, M. J., and Bond, U. (1987). Ubiquitin genes. *Oxf Surv Eukaryot Genes* *4*, 77-91.
- Schlessinger, J., and Ullrich, A. (1992). Growth factor signaling by receptor tyrosine kinases. *Neuron* *9*, 383-391.
- Seibenhener, M. L., Babu, J. R., Geetha, T., Wong, H. C., Krishna, N. R., and Wooten, M. W. (2004). Sequestosome 1/p62 is a polyubiquitin chain binding protein involved in ubiquitin proteasome degradation. *Mol Cell Biol* *24*, 8055-8068.
- Sharma, N., Deppmann, C. D., Harrington, A. W., St Hillaire, C., Chen, Z. Y., Lee, F. S., and Ginty, D. D. Long-distance control of synapse assembly by target-derived NGF. *Neuron* *67*, 422-434.

- Shih, S. C., Prag, G., Francis, S. A., Sutanto, M. A., Hurley, J. H., and Hicke, L. (2003). A ubiquitin-binding motif required for intramolecular monoubiquitylation, the CUE domain. *Embo J* 22, 1273-1281.
- Sigismund, S., Argenzio, E., Tosoni, D., Cavallaro, E., Polo, S., and Di Fiore, P. P. (2008). Clathrin-mediated internalization is essential for sustained EGFR signaling but dispensable for degradation. *Dev Cell* 15, 209-219.
- Sigismund, S., Woelk, T., Puri, C., Maspero, E., Tacchetti, C., Transidico, P., Di Fiore, P. P., and Polo, S. (2005). Clathrin-independent endocytosis of ubiquitinated cargos. *Proc Natl Acad Sci U S A* 102, 2760-2765.
- Sine, S. M., and Engel, A. G. (2006). Recent advances in Cys-loop receptor structure and function. *Nature* 440, 448-455.
- Stenmark, H., and Olkkonen, V. M. (2001). The Rab GTPase family. *Genome Biol* 2, REVIEWS3007.
- Stiegler, A. L., Burden, S. J., and Hubbard, S. R. (2006). Crystal structure of the agrin-responsive immunoglobulin-like domains 1 and 2 of the receptor tyrosine kinase MuSK. *J Mol Biol* 364, 424-433.
- Sun, L., and Chen, Z. J. (2004). The novel functions of ubiquitination in signaling. *Curr Opin Cell Biol* 16, 119-126.
- Takahashi, M., Kubo, T., Mizoguchi, A., Carlson, C. G., Endo, K., and Ohnishi, K. (2002). Spontaneous muscle action potentials fail to develop without fetal-type acetylcholine receptors. *EMBO Rep* 3, 674-681.
- Tanaka, R. D., Li, A. C., Fogelman, A. M., and Edwards, P. A. (1986). Inhibition of lysosomal protein degradation inhibits the basal degradation of 3-hydroxy-3-methylglutaryl coenzyme A reductase. *J Lipid Res* 27, 261-273.
- Tang, H., Veldman, M. B., and Goldman, D. (2006). Characterization of a muscle-specific enhancer in human MuSK promoter reveals the essential role of myogenin in controlling activity-dependent gene regulation. *J Biol Chem* 281, 3943-3953.
- Tanowitz, M., and von Zastrow, M. (2003). A novel endocytic recycling signal that distinguishes the membrane trafficking of naturally occurring opioid receptors. *J Biol Chem* 278, 45978-45986.
- Tian, Q. B., Suzuki, T., Yamauchi, T., Sakagami, H., Yoshimura, Y., Miyazawa, S., Nakayama, K., Saitoh, F., Zhang, J. P., Lu, Y., *et al.* (2006). Interaction of LDL receptor-related protein 4 (LRP4) with postsynaptic scaffold proteins via its C-terminal PDZ domain-binding motif, and its regulation by Ca/calmodulin-dependent protein kinase II. *Eur J Neurosci* 23, 2864-2876.
- Till, J. H., Becerra, M., Watty, A., Lu, Y., Ma, Y., Neubert, T. A., Burden, S. J., and Hubbard, S. R. (2002). Crystal structure of the MuSK tyrosine kinase: insights into receptor autoregulation. *Structure* 10, 1187-1196.
- Touchot, N., Chardin, P., and Tavitian, A. (1987). Four additional members of the ras gene superfamily isolated by an oligonucleotide strategy: molecular cloning of YPT-related cDNAs from a rat brain library. *Proc Natl Acad Sci U S A* 84, 8210-8214.
- Valenzuela, D. M., Stitt, T. N., DiStefano, P. S., Rojas, E., Mattsson, K., Compton, D. L., Nunez, L., Park, J. S., Stark, J. L., Gies, D. R., and *et al.* (1995). Receptor tyrosine kinase specific for the skeletal muscle lineage: expression in embryonic muscle, at the neuromuscular junction, and after injury. *Neuron* 15, 573-584.
- Van Der Sluijs, P., Hull, M., Zahraoui, A., Tavitian, A., Goud, B., and Mellman, I. (1991). The small GTP-binding protein rab4 is associated with early endosomes. *Proc Natl Acad Sci U S A* 88, 6313-6317.
- Vincent, A., Leite, M. I., Farrugia, M. E., Jacob, S., Viegas, S., Shiraishi, H., Benveniste, O., Morgan, B. P., Hilton-Jones, D., Newsom-Davis, J., *et al.* (2008). Myasthenia gravis seronegative for acetylcholine receptor antibodies. *Ann N Y Acad Sci* 1132, 84-92.

Vock, V. M., Ponomareva, O. N., and Rimer, M. (2008). Evidence for muscle-dependent neuromuscular synaptic site determination in mammals. *J Neurosci* 28, 3123-3130.

Wallace, B. G. (1989). Agrin-induced specializations contain cytoplasmic, membrane, and extracellular matrix-associated components of the postsynaptic apparatus. *J Neurosci* 9, 1294-1302.

Watty, A., Neubauer, G., Dreger, M., Zimmer, M., Wilm, M., and Burden, S. J. (2000). The in vitro and in vivo phosphotyrosine map of activated MuSK. *Proc Natl Acad Sci U S A* 97, 4585-4590.

Weatherbee, S. D., Anderson, K. V., and Niswander, L. A. (2006). LDL-receptor-related protein 4 is crucial for formation of the neuromuscular junction. *Development* 133, 4993-5000.

Weston, C., Yee, B., Hod, E., and Prives, J. (2000). Agrin-induced acetylcholine receptor clustering is mediated by the small guanosine triphosphatases Rac and Cdc42. *J Cell Biol* 150, 205-212.

Willems, A. R., Lanker, S., Patton, E. E., Craig, K. L., Nason, T. F., Mathias, N., Kobayashi, R., Wittenberg, C., and Tyers, M. (1996). Cdc53 targets phosphorylated G1 cyclins for degradation by the ubiquitin proteolytic pathway. *Cell* 86, 453-463.

Witzemann, V. (2006). Development of the neuromuscular junction. *Cell Tissue Res* 326, 263-271.

Witzemann, V., Schwarz, H., Koenen, M., Berberich, C., Villarroel, A., Wernig, A., Brenner, H. R., and Sakmann, B. (1996). Acetylcholine receptor epsilon-subunit deletion causes muscle weakness and atrophy in juvenile and adult mice. *Proc Natl Acad Sci U S A* 93, 13286-13291.

Woelk, T., Oldrini, B., Maspero, E., Confalonieri, S., Cavallaro, E., Di Fiore, P. P., and Polo, S. (2006). Molecular mechanisms of coupled monoubiquitination. *Nat Cell Biol* 8, 1246-1254.

Won, K. A., and Reed, S. I. (1996). Activation of cyclin E/CDK2 is coupled to site-specific autophosphorylation and ubiquitin-dependent degradation of cyclin E. *Embo J* 15, 4182-4193.

Wu, H., Xiong, W. C., and Mei, L. To build a synapse: signaling pathways in neuromuscular junction assembly. *Development* 137, 1017-1033.

Xie, M. H., Yuan, J., Adams, C., and Gurney, A. (1997). Direct demonstration of MuSK involvement in acetylcholine receptor clustering through identification of agonist ScFv. *Nat Biotechnol* 15, 768-771.

Xu, P., Duong, D. M., Seyfried, N. T., Cheng, D., Xie, Y., Robert, J., Rush, J., Hochstrasser, M., Finley, D., and Peng, J. (2009). Quantitative proteomics reveals the function of unconventional ubiquitin chains in proteasomal degradation. *Cell* 137, 133-145.

Yaglom, J., Linskens, M. H., Sadis, S., Rubin, D. M., Futcher, B., and Finley, D. (1995). p34Cdc28-mediated control of Cln3 cyclin degradation. *Mol Cell Biol* 15, 731-741.

Yamaguchi, Y. L., Tanaka, S. S., Kasa, M., Yasuda, K., Tam, P. P., and Matsui, Y. (2006). Expression of low density lipoprotein receptor-related protein 4 (Lrp4) gene in the mouse germ cells. *Gene Expr Patterns* 6, 607-612.

Yang, X., Arber, S., William, C., Li, L., Tanabe, Y., Jessell, T. M., Birchmeier, C., and Burden, S. J. (2001). Patterning of muscle acetylcholine receptor gene expression in the absence of motor innervation. *Neuron* 30, 399-410.

Yang, X., Li, W., Prescott, E. D., Burden, S. J., and Wang, J. C. (2000). DNA topoisomerase IIbeta and neural development. *Science* 287, 131-134.

Zerial, M., and McBride, H. (2001). Rab proteins as membrane organizers. *Nat Rev Mol Cell Biol* 2, 107-117.

Zhang, B., Luo, S., Wang, Q., Suzuki, T., Xiong, W. C., and Mei, L. (2008). LRP4 serves as a coreceptor of agrin. *Neuron* 60, 285-297.

Zhang, J., Lefebvre, J. L., Zhao, S., and Granato, M. (2004). Zebrafish unplugged reveals a role for muscle-specific kinase homologs in axonal pathway choice. *Nat Neurosci* 7, 1303-1309.

Zhou, H., Glass, D. J., Yancopoulos, G. D., and Sanes, J. R. (1999). Distinct domains of MuSK mediate its abilities to induce and to associate with postsynaptic specializations. *J Cell Biol* 146, 1133-1146.

Zhu, D., Yang, Z., Luo, Z., Luo, S., Xiong, W. C., and Mei, L. (2008). Muscle-specific receptor tyrosine kinase endocytosis in acetylcholine receptor clustering in response to agrin. *J Neurosci* 28, 1688-1696.

8 Appendix

8.1 Acknowledgements

First of all, I want to thank Dr. Ruth Herbst for providing this interesting project and for allowing me to work independently. Special thanks go to Susan Luiskandl. I really enjoyed our collaboration! I wish to thank all my other colleagues for the great working atmosphere and particularly Barbara Woller for answering even the most stupid questions.

Many thanks also go to the group of Prof. Dr. Werner Sieghart for sharing knowledge and equipment with us.

Finally, I wish to thank my family for supporting and encouraging me throughout my studies.

8.2 Zusammenfassung

Die Rezeptor-Tyrosin-Kinase MuSK (muscle-specific kinase) ist ein Muskel-spezifisches Transmembranprotein und essentiell für die Bildung der Neuromuskulären Synapse an der Kontaktstelle von Motorneuron und Muskel.

MuSK wird durch das Proteoglykan Agrin aktiviert, ein Protein, das an Nervenendigungen sekretiert wird. Aktiviertes MuSK auto-phosphoryliert und stimuliert die Aggregation von Acetylcholin-Rezeptoren (AChRs) in dem der Nervenendigung gegenüberliegenden Bereich der Muskelzell-Membran. Dies führt zur Ausbildung eines postsynaptischen Apparates. Um diese Prozesse zu koordinieren sind komplexe Signalmechanismen erforderlich, welche in den vergangenen Jahrzehnten intensiv studiert wurden. Zahlreiche weitere Proteine, die an der Bildung der Neuromuskulären Synapse beteiligt sind, wie LRP4, Dok7 und Tid1, wurden mittlerweile identifiziert und ihre Interaktion mit MuSK wurde erforscht. Dennoch sind die Kenntnisse über die Agrin-MuSK-Signalkaskade unvollständig.

Es wurde berichtet, das Aktivierungs-abhängige Endozytose von MuSK für die Aggregation von AChR erforderlich ist. Darauf folgende Modifikation von MuSK durch Ubiquitylierung könnte den intrazellulären Transport der Kinase regulieren. Diese Diplomarbeit konzentrierte sich auf darauf, nicht-Muskel Zellsysteme zu etablieren, in welchen die beiden Prozesse, MuSK Endozytose und MuSK Ubiquitylierung, untersucht werden können. Heterologe Zellsysteme sind einfacher zu handhaben als Muskelzellsysteme und erlauben es, bestimmte Komponenten der Agrin-MuSK Signalkaskade unabhängig von anderen Muskel-spezifischen Proteinen zu exprimieren und zu untersuchen.

Ein Ziel dieser Arbeit war, ein Modellsystem zu erschaffen, in welchem heterolog-exprimiertes MuSK zu einem definierten Zeitpunkt aktiviert werden kann. Es wurde getestet, ob die Kinase durch Dimerisierung mittels Antikörpern zu stimulieren ist. Ebenso wurde versucht, MuSK mit dem Agrin-Rezeptor LRP4 zu ko-exprimieren und mit Agrin zu aktivieren. Leider erzielten beide beschriebenen Methoden keine detektierbare Aktivierung. Daher wurde eine konstitutiv inaktive, unphosphorylierte und eine konstitutiv aktive, phosphorylierte MuSK-Mutante entsprechend der experimentellen Anforderungen modifiziert. Internalisierungsstudien mit diesen zwei Mutanten legten nahe, dass der Phosphorylierungszustand von MuSK keine Auswirkung auf deren Endozytose und den intrazellulären Transport hat.

Um den Effekt von MuSK-Ubiquitynierung auf die Internalisierung der Kinase zu untersuchen, wurden HA-markierte MuSK-Ubiquitin Chimären HA-MuSK-Ubwt und HA-MuSK-Ubmut kloniert. Es wurde gezeigt, dass HA-MuSK-Ubwt, welches die extrazelluläre und die Transmembrandomäne fusioniert an Wildtyp-Ubiquitin enthält, in COS-7 Zellen polyubiquityniert wird. HA-MuSK-Ubmut, welches zwei Mutationen im Ubiquitin-Teil enthält, wird größtenteils mittels Anhängen eines einzelnen Ubiquitin-Moleküls modifiziert oder bleibt unmodifiziert. Es wurde festgestellt, dass MuSK-Ubiquitynierung, ähnlich wie der Phosphorylierungszustand, keinen signifikanten Einfluss auf seine Internalisierung und den Transport innerhalb der Zelle hat.

8.3 Abstract

The receptor tyrosine kinase MuSK (muscle-specific kinase) is a muscle-specific, transmembrane protein that is essential for the formation of the neuromuscular junction at the site of contact of motor neuron and muscle.

MuSK is activated via the proteoglycan agrin, a soluble protein secreted by nerve terminals. Activated MuSK autophosphorylates and stimulates aggregation of acetylcholine receptors (AChRs) in the area of the muscle cell membrane that opposes the nerve terminal. Consequently a postsynaptic apparatus is established. To coordinate these processes complex signaling mechanisms are required, which have been studied extensively in the past decades. Numerous additional proteins involved in neuromuscular junction formation like LRP4, Dok7 and Tid1 have been identified and their interaction with MuSK has been investigated. However, the knowledge about agrin-MuSK-signaling is still incomplete.

Activation-dependent endocytosis of MuSK has been reported to be required for AChR clustering. Subsequent modification of MuSK by ubiquitination might control intracellular trafficking of the kinase. This diploma thesis focused on the establishment of non-muscle cell systems for the investigation of the two processes, MuSK endocytosis and MuSK ubiquitination. Heterologous cell systems are easier to handle than muscle cell systems and allow the selective expression and characterization of distinct components of the agrin-MuSK-signaling cascade independent from other muscle-specific proteins.

Initially, the goal was to create a model system, in which heterologously expressed MuSK could be activated at a defined time point. Stimulation by clustering with antibodies was tested. It was also tried to co-express MuSK with the agrin-receptor LRP4 and activate it with agrin. Unfortunately the respective methods did not result in detectable induction. Hence, constitutively inactive, unphosphorylated and active, phosphorylated MuSK mutants were modified according to the experimental requirements. Internalization studies with these two mutants suggested that the phosphorylation level of MuSK has no effect on its endocytosis and intracellular trafficking.

To study the effect of ubiquitination on MuSK internalization, HA-tagged MuSK-ubiquitin chimeras HA-MuSK-Ubwt and HA-MuSK-Ubmut were created. HA-MuSK-Ubwt comprising the extracellular and transmembrane domain of MuSK fused to wild-type ubiquitin, was shown to be polyubiquitinated upon expression in COS-7 cells. HA-MuSK-Ubmut contains two mutations in the ubiquitin portion and is rather modified by addition of a single ubiquitin molecule or not modified at all. But similar to phosphorylation levels, the extent of ubiquitination was found not to significantly influence internalization and protein targeting.

8.4 Lebenslauf

Persönliche Daten:

Name: Marlies Schlauf
Adresse: Rielgasse 41, 1230 Wien
Telefon: 0664/ 7313 0905
E-mail: Schlauf@gmx.at

Geburtsdatum: 11.06.1987
Geburtsort: Wien
Nationalität: Österreich
Familienstand: ledig



Schulbildung:

Jänner 2010 – Jänner 2011 Diplomarbeit in der Arbeitsgruppe von Priv.-Doz. Dr. Ruth Herbst, Zentrum für Hirnforschung, Medizinische Universität Wien
Fokus: Endozytose der Rezeptor-Tyrosin-Kinase MuSK und deren Einfluss auf die Entwicklung der neuromuskulären Synapse

Dezember 2009 einmonatiges Praktikum in der Arbeitsgruppe von Prof. Dr. Javier Martinez, IMBA, Wien
Fokus: RNAi Biologie

August – Oktober 2009 Dreimonatiges Praktikum in der Arbeitsgruppe von Prof. Dr. Hartmut Beug, IMP, Wien
Fokus: Analyse der Eigenschaften des lysosomalen Proteins CREG und seiner Rolle in EMT

Februar 2009 einmonatiges Praktikum in der Arbeitsgruppe von Prof. Dr. Roland Foisner, Max F. Perutz Laboratories Biozentrum Bohrgasse, Universität Wien
Fokus: Bestimmung der Expressionslevel des Zellkern-lokalisiereten Proteins LAP2alpha in verschiedenen Maus-Geweben und Organen

September 2008 einmonatiges Ferialpraktikum in der Arbeitsgruppe von Prof. Dr. Ferdinand Steinböck, Institut für Krebsforschung, Medizinische Universität Wien
Fokus: Analyse der schützenden Eigenschaften einer Substanz gegen chemische Mutagenese in Hefe

August 2007 einmonatiger Ferialjob in der Geschäftsleitung der Novartis Pharma GmbH in Wien

Juli 2006 einmonatiges Ferialpraktikum in einem Labor der Böhlinger Ingelheim Austria GmbH in Wien
Fokus: Klonierung und Plasmid-Präparation

seit Okt. 2005 Studium an der Universität Wien, Studiengang Molekulare Biologie

Juni 2005 AHS-Matura (mit ausgezeichnetem Erfolg) am Bundesgymnasium Diefenbachgasse

1997-2005: Bundesgymnasium Diefenbachgasse, Wien XV, Zweig: Sprachliches Gymnasium

1993-1997: Volksschule Maurer Lange Gasse, Wien XXIII

Sprachen:

Englisch: Sehr gut
2004: Schulsprachreise nach Dublin/ Irland

Französisch: Gut
2003: 2-wöchiger Sprachkurs in Cannes/ Frankreich

Spanisch: Grundkenntnisse

Sonstiges:

EDV: erfolgreiche Absolvierung des Europäischen Computer-Führerscheines (ECDL)

Hobbies: Musik
Zeichnen & Grafik
Sport (Ski, Snowboard, Eislaufen, Tennis, Radfahren, u. a.)
Sprachen

8.5 Curriculum Vitae

Personal Data:

Name: Marlies Schlauf
Address: Rielgasse 41, 1230 Vienna
Mobile Phone: 0664/7313 0905
E-mail: Schlauf@gmx.at

Birthday: June 11th 1987
Birthplace: Vienna
Citizenship: Austria
Marital Status: single



Education:

January 2010 – January 2011 diploma thesis in the group of Ruth Herbst, Section of Synapse Formation, Center for Brain Research, Medical University of Vienna
focus: endocytosis of muscle-specific kinase and its role in neuromuscular junction formation

December 2009 practical training of one month in the group of Javier Martinez, IMBA, Vienna
focus: RNAi biology

August-October 2009 practical training of three months in the group of Hartmut Beug, IMP, Vienna
focus: properties of the lysosomal protein CREG and its role in EMT

February 2009 practical training of one month in the group of Roland Foisner, Biocenter Bohrgasse, University of Vienna
focus: expression levels of cell nucleus-localized protein LAP2alpha in mouse tissues and organs

September 2008 practical training of one month in the group of Ferdinand Steinböck, Cancer Research Institute, Medical University of Vienna
focus: analysis of the protective effects of a substance against chemical mutagenesis in yeast

July 2006 practical training of one month in a laboratory of Boehringer Ingelheim Austria GmbH, Vienna

since Oct. 2005 studies at the University of Vienna, branch: Molecular Biology

June 2005 final exams at grammar school Diefenbachgasse, Vienna XV

1997-2005: grammar school Diefenbachgasse, Vienna XV; branch: Sprachliches Gymnasium (6 years French, 4 years Latin)

Languages:

English: very good
2004: language course (1 week) in Dublin/ Ireland

French: good
2003: language course (2 weeks) in Cannes/ France

Spanish: basic knowledge

Other:

EDV: ECDL (European Computer Driving License)

Hobbies: music
drawing & graphic design
sports (ski, snowboard, ice skating, tennis, cycling, etc.)
languages